

DISSERTATION

THE ROLE OF RETROVIRAL CYCLIN IN THE DEVELOPMENT OF WALLEYE  
DERMAL SARCOMA

Submitted by

Claire Birkenheuer

Department of Microbiology, Immunology, and Pathology

In partial fulfillment of the requirements

For the Degree of Doctor of Philosophy

Colorado State University

Fort Collins, Colorado

Spring 2015

Doctoral Committee:

Advisor: Joel Rovnak

Co-Advisor: Sandra L. Quackenbush

Jennifer Nyborg

Susan VandeWoude

Jeff Wilusz

Copyright by Claire Halley Birkenheuer 2015

All Rights Reserved

## ABSTRACT

### THE ROLE OF RETROVIRAL CYCLIN IN THE DEVELOPMENT OF WALLEYE DERMAL SARCOMA

The retroviral cyclin (RV-cyclin) is an accessory protein encoded by walleye dermal sarcoma virus (WDSV). This virus causes the formation of walleye dermal sarcoma, and requires the tumor tissue to replicate. RV-cyclin is one of only two proteins expressed by the virus during tumor development before production of the WDSV virion, and the mechanism by which RV-cyclin causes tumor formation was explored and is presented here.

RV-cyclin interacts with TAF9 and CDK8, which are cellular proteins that regulate RNA Pol II transcription. RV-cyclin's influence on transcription was explored by analyzing transcript levels of *CCND1*, *CDKN2D*, *FOS*, *EGR1*, and *JUN*. All of these genes are important oncogenes in human cancers, and were hypothesized to contribute to development of walleye dermal sarcoma (WDS). Quantitative reverse transcription PCR analysis of these genes in HeLa and HCT116 cell lines expressing wt or mutant RV-cyclin, or over-expressing cyclin C was carried out. These analyses showed that wt RV-cyclin enhances expression of all genes tested and that the interactions with TAF9 and with CDK8 contribute to this enhancement.

Western blot analysis of phosphorylated Elk1 and SRF, two transcription factors that initiate RNA Pol II transcription, revealed that RV-cyclin's mechanism of gene activation is downstream of transcription factor phosphorylation. Messenger RNA (mRNA) decay assays demonstrated that RV-cyclin does not alter the rate of mRNA decay, framing RV-cyclin's mechanism of activation to the level of RNA Pol II transcription. Nuclear run-on and chromatin

immunoprecipitation analysis of *EGR1* with an RNA Pol II antibody support a role for RV-cyclin in transcription elongation and re-initiation. ChIP analysis of the mutant RV-cyclin cells and cells over-expressing cyclin C demonstrated that RV-cyclin requires both a functional CDK8 and TAF9 interaction for efficient activation and extension of the *EGR1* serum response. CDK8 ChIPs demonstrated that the RV-cyclin enhances CDK8 occupancy at the *EGR1* gene locus, and HA-ChIPs show that CDK8 and RV-cyclin occupancy correlate with each other on the locus.

At this point, it was hypothesized that RV-cyclin functions to enhance CDK8 kinase activity in addition to bringing more CDK8 to select oncogenic loci *in vivo*. For this reason kinase assays using recombinant, baculovirus-produced CDK8/RV-cyclin or CDK8/cyclin C constructs were attempted. CDK8 bound to RV-cyclin was able to autophosphorylate to similar levels as CDK8 bound to cyclin C. Other CDK8 substrates remain to be tested.

RV-cyclin's function in transcription requires activation of the MAPK pathway, suggesting RV-cyclin needs an outside signal like serum stimulation for efficient WDS formation. This signal likely comes from the presence of the Orf b protein, the other WDSV accessory protein expressed during tumor development. The protein Orf b causes phosphorylation and activation of the p90RSK complex. This event likely causes aberrant phosphorylation of SRF and Elk-1 giving RV-cyclin the activated transcription factors required for its function on specific proto-oncogenes. Taken together, the Orf b protein and RV-cyclin illustrate a previously un-described, *trans*-acting mechanism of retroviral-induced oncogenesis.

## ACKNOWLEDGMENTS

The research presented in this dissertation was a result of collaboration and mentorship, and without this it would have not been possible. The two people that helped the most in this endeavor were my wonderful mentors, Joel Rovnak and Sandra Quackenbush. I would like to thank them for the countless hours spent critiquing my experiments and helping me push through the obstacles of this project. They provided an excellent working environment, and the support that I needed to complete my PhD. I could not have wished, hoped or asked for a better experience.

I would also like to thank Connie Brewster, Stephanie Moon and Ryan Troyer. Connie not only helped with the research but also gave moral support along the way, and became a lasting friend. Stephanie Moon was invaluable for her help on the mRNA decay assays, and Ryan Troyer gave me the graphing software and showed me how to use it so I could prepare the Figures.

Finally my close friends and family provided the support I needed to push through and finish this project. Daniel Galindo, my parents—Daniel and Nancy Birkenheuer, and my extended family members—Mary Jean Martin, Gloria Martin, Sarah Place, and Rebecca Johnson gave countless words of support and much needed love and encouragement. I am so thankful to have such wonderful, supportive people in my life.

## TABLE OF CONTENTS

ABSTRACT.....	ii
ACKNOWLEDGMENTS .....	iv
LIST OF KEYWORDS .....	vi
CHAPTER 1: INTRODUCTION.....	1
CHAPTER 2: AIM 1—DETERMINE THE EFFECT OF RV-CYCLIN ON SERUM RESPONSE GENE EXPRESSION.....	26
CHAPTER 3: AIM 2—DETERMINE IF GENE ACTIVATION BY RV-CYCLIN IS DUE TO ENHANCED TRANSCRIPTIONAL PROCESSIVITY .....	49
CHAPTER 4: AIM 3—DETERMINE IF RV-CYCLIN ENHANCES THE KINETICS OF CDK8 PHOSPHORYLATION <i>IN VITRO</i> .....	81
CHAPTER 5: CONCLUDING REMARKS AND FUTURE DIRECTIONS .....	96
REFERENCES .....	99

## LIST OF KEYWORDS

WDSV, Retroviral-cyclin, RV-cyclin, CDK8, TAF9, RNA Pol II, Chromatin immunoprecipitation, ChIP, *CCND1*, *CDKN2D*, *EGR1*, *FOS*, *JUN*, Nuclear Run-On, Transcriptional shut-off, qRTPCR, Serum response, Baculovirus expression system, Kinase assay

## CHAPTER 1-INTRODUCTION

Retroviruses have been a known cause of cancer in animals since Peyton Rous first described the ability of a sarcoma to be transmitted from chicken to chicken using a cell-free filtrate [1-3]. Since this initial discovery, retroviruses have been associated with a number of different cancers in both animals and humans (Table 1) [3, 4]. The study of these cancers is important as they can and have had a great impact on economic activity, animal health and human health issues, as well as our understanding of basic cellular mechanisms [3].

Table 1 An example of some of the many retroviruses that cause cancer.

<b>Virus</b>	<b>Cancer type</b>	<b>Host organism</b>
<u>Alpharetrovirus</u>		
Rous Sarcoma Virus (RSV)	Sarcoma	Chickens
<u>Betaretrovirus</u>		
Jaagsiekte Sheep Retrovirus (JSRV)	Adenocarcinoma	Sheep
<u>Deltaretrovirus</u>		
Human T-Cell Lymphoma virus (HTLV-1 and HTLV-2)	Lymphoma	Humans
<u>Gammaretrovirus</u>		
Feline leukemia virus	Leukemia	Cats
<u>Epsilonretrovirus</u>		
Walleye dermal sarcoma virus (WDSV)	Sarcoma	Walleye fish

Adapted from Rosenberg N, 2011 Overview of retrovirology in *Retroviruses and insights into cancer* Dudley, J ed. Springer Science and Business Media [3], and Pederson and Sorensen, Pathogenesis of oncoviral infections in retroviruses 2010 Kurth and Bannert ed. Caister Academic Press [4]

### **Retroviral Replication**

Retroviruses infect a wide variety of cells using different receptors. Upon infection, the cleaved envelope glycoproteins, surface (SU), and trans-membrane (TM) of the virus bind to receptors on the host cell and induce fusion of the host and viral membranes [5]. This results in viral entry, and, depending on the virus, this occurs either through direct fusion of the viral envelope with the plasma membrane or through endocytosis of the viral particle [5, 6]. Once

inside the host cell, viral reverse transcriptase converts the RNA genome into double stranded DNA [7].

Reverse transcriptase has four distinct enzymatic activities and two functional domains. The enzymatic activities include RNA and DNA dependent polymerase activity, helicase activity, and RNase H activity. The reverse transcriptase binds the viral RNA through recognition of the tRNA primer bound to the primer binding site (PBS) at the 5' end of the genome, WDSV, for example uses the histidyl tRNA as its primer. As the RNA template is copied using the polymerase and helicase activity, it is degraded by the RNase H activity in the reverse transcriptase [7]. The polypurine tract (PPT) is resistant to RNase H degradation. The residual RNA of the PPT stays bound to the single stranded DNA copy, and serves as the primer for the second round of DNA replication (plus-strand synthesis). Due to the placement of the PBS sequence and the PPT sequence in the genome, in relation to the 5' untranslated region (U5), the repeat region (R), and the 3' untranslated region (U3), the linear double stranded DNA copy of the genome has two long terminal repeats (LTRs), which flank each side of the genome [7].

After reverse transcription the viral, double-stranded, linear DNA molecule is ready for integration into the cellular genomic DNA in the nucleus [8]. Before this occurs, the linear molecule is converted into a non-covalently closed, circular intermediate which is called the pre-integration complex (PIC). The PIC is transported into the nucleus, in a process that varies for individual retroviruses [8].

Inside the nucleus, the integrase protein (IN) inserts the DNA copy of the retroviral genome into the host DNA sequence [8]. The host's DNA damage machinery then repairs the breaks in the host genomic DNA [8]. The LTRs of the provirus act as regulatory regions for

RNA Pol II mediated transcription [9]. They contain both enhancer and promoter sequences for cellular transcription factor binding, and control of retroviral gene expression and genomic replication. The orientation of the 3'LTR provides RNA Pol II access to the needed transcription termination and polyadenylation signals [9].

Since RNA Pol II is responsible for gene expression and genomic replication of the retrovirus, the transcripts produced from the provirus are subjected to the co-transcriptional processing that occurs with cellular transcripts. The retroviral RNAs are capped, polyadenylated, and can be spliced [9]. The ratio of spliced mRNA to un-spliced, genomic RNA is important for regulating transcription and viral assembly of the new viral particles. Once capped, spliced (if needed), and polyadenylated, the retroviral mRNAs are exported out of the nucleus [9]. They are translated by free and endoplasmic reticulum (ER) bound ribosomes [10]. The ER-translated proteins travel through the Golgi apparatus, where multiple post-translational modifications are added. The nascent proteins and full length genomic RNAs are targeted to the plasma membrane by a myristol group in the Gag polyprotein. At the membrane the new viral particles are assembled. During this assembly, the polyproteins are cleaved by the protease, allowing formation of mature viral particles [10]. The Env poly-protein is cut to form the SU and the TM domains, and the Gag-poly protein is cleaved to form the matrix protein and the capsid protein [10]. Once assembly is complete, the viral particles exit the cell through budding [3, 10].

### **Retroviral Tumor Development**

Many viral induced tumors are an unforeseen consequence of the virus infection. The tumors are a result of the virus stimulating different cellular pathways that control cell growth. This aberrant stimulation can contribute to tumor development. Some viruses that cause tumors

in this manner are: papillomaviruses, polyomaviruses, herpesviruses, and transforming retroviruses [11]. Unlike these viruses, WDSV seems to require tumor formation for viral replication as tumor formation precedes viral particle formation and release [12-15]. Therefore, understanding the mechanisms of tumor formation and regression in the WDSV model will provide valuable insights into certain mechanisms of human tumor development and insights into possible cancer therapeutics.

There are three types of retroviruses that cause cancer: non-acute transforming retroviruses, acute transforming retroviruses, and *trans*-acting retroviruses [11]. Many simple retroviruses are non-acute transforming retroviruses, and cause cancer by insertional mutagenesis [16, 17]. Insertional mutagenesis occurs when the provirus inserts itself into a region of the host DNA that encodes an oncogene. Because the LTRs of the retroviruses are RNA Pol II promoters, the placement of a 3' LTR upstream or near the beginning of a proto-oncogene can cause its aberrant expression leading to tumor development [16, 18]. This can occur either through promoter insertion or by enhancer activation.

Acute transforming retroviruses cause cancer by acquiring the sequence of a proto-oncogene, and then transferring this oncogene to the next cell upon infection. The presence of the additional oncogenic sequence in the infected cell leads to tumor development. Incorporation of the sequence occurs when RNA Pol II reads through the transcription termination signal in the 3'LTR of the provirus, attaching part of a host sequence to the retroviral genome [18]. If the downstream-host sequence happens to be a proto-oncogene, a tumor can develop as a result of infection. Many times the sequence of these copied genes are altered by base substitutions, deletions, or fusions with viral sequences, altering the protein [17]. The oncogene-containing viral particles are called acute-transforming retroviruses and are usually replication defective.

This means the acute transforming retrovirus must co-infect a cell with a full-length, correctly packaged version of the retrovirus for efficient replication. The exception to this statement is Rous sarcoma virus (RSV), which contains the *SRC* oncogene but remains replication competent [11, 18].

Finally, there are *trans*-acting retroviruses, which cause cancer through viral-host, protein-protein interactions. The host proteins involved usually aid in cell division in some way. Two particular retroviruses that cause cancer in this way are human T-cell lymphotropic virus type 1 (HTLV-1) and Jaagsiekte sheep retrovirus (JSRV) [17, 19, 20].

HTLV-1 infection gives rise to adult T-cell leukemia (ATL) in 2-5% of infected patients, after a latent period of 30 to 60 years [20, 21]. HTLV-1, like bovine leukemia virus, causes cancer due to the induced clonal expansion required for viral replication [21]. This means that there is little cell-to-cell virus spread. Once integrated into a T-cell genome, the provirus is replicated by the clonal expansion of the T-cell. It has been found that all HTLV-1-induced ATL originate from one of these surviving T-cell clones [21, 22]. The HTLV-1 Tax protein is encoded by one of the eight accessory genes in the HTLV-1 genome [21]. Tax expression alone can immortalize T-cells and cause transformation of rodent and human cells [21]. It does this by deregulating the CREB, NF $\kappa$ B, SRF, and AP-1 transcriptional response [23, 24].

One direct way Tax stimulates transcription is through the CREB transcriptional pathway. Tax directly binds DNA, and this is directed by cyclic AMP response elements (CRE) in the promoters of the target genes [25]. The cyclin D1 (*CCND1*) and HTLV-1 promoters are two targets of Tax. Once bound, Tax recruits active, CREB (pCREB) and facilitates the formation of a complex containing pCREB and the transcriptional activators CBP/p300, and TORC [23, 26, 27]. Through this mechanism, and many others, Tax promotes expression of the

HTLV-1 proviral genome, and it up-regulates expression of important genes required for replication through clonal expansion which can lead to transformation. These genes include proto-oncogenes and cytokines. Tax aids the cell in bypassing inhibitory cell-cycle signals from the DNA damage response, and inactivates tumor suppressors like p53 [24]. The Tax protein contributes to the transforming events required to initiate HTLV-1 induced ATL, but then its expression is lost in the transformed cells over time and is only found in ~30% of human ATL cases [20, 26]. After the transforming events by Tax, another HTLV-1-encoded protein, the HBZ protein, is thought to help maintain the tumor cells [20, 21, 26]. In general, the Tax protein is an excellent example of a *trans*-acting mechanism of retroviral-induced oncogenesis.

JSRV causes ovine pulmonary adenocarcinoma, and this virus is one of a very few whose envelope protein is sufficient to induce tumors. It does this in cell culture systems, in mice as well as in sheep [28-35]. In this aspect JSRV transformation is different than transformation by HTLV-1 Tax, as Tax is an accessory protein and not a structural protein. JSRV is similar to three other known retroviruses that have Env proteins responsible for tumorigenesis: enzootic nasal tumor virus (ENTV), avian hemangioma retrovirus (AHV), and Friend spleen focus-forming virus (SFFV) [30].

Initial experiments demonstrated that the JSRV cytoplasmic tail of the TM domain of the cleaved Env protein was sufficient to induce transformation in rodent cells and chicken cells [31-33]. This domain was of interest because it contained the amino acid motif, YXXM, which, if phosphorylated, could be a potential binding site for phosphatidyl-inositol 3 kinase (PI3K). PI3K activates the RAC-alpha serine/threonine-protein kinase (AKT) signaling pathway, which causes gene activation leading to cell division. Indeed if the tyrosine or the methionine was mutated, the NIH3T3 cells were not transformed [30, 32]. Later studies showed that in other cell

lines the YXXM motif was not necessary for transformation, even though the PI3K/AKT pathway was activated and required for transformation [30, 33, 36]. The cytoplasmic tail of the TM domain was indispensable for transformation; however, more recent analysis shows other portions of the JSRV Env, like the SU domain, and the membrane spanning region and ectodomain of TM are also important [30, 37]. This correlates with data showing the activation of the Hyal2 pathway and the mitogen activated associated protein kinase (MAPK) pathway are also required for JSRV Env transformation [30, 36].

Clearly, the study of the numerous non-acute transforming retroviruses, acute transforming retroviruses, and the *trans*-acting retroviruses has contributed greatly to both science and medicine. Not only have they allowed us to treat human disease better, but the knowledge gained along the way provided a greater understanding of eukaryotic cell biology. In particular, the *trans*-acting retroviruses have the potential to identify previously un-described connections between signaling pathways and between protein complexes. This and the historical aspect of retrovirology highlight the multiple benefits that can and will come from studying mechanisms of retroviral transformation. This lends great significance to future scientific endeavors with other oncogenic retroviruses, like walleye dermal sarcoma virus.

### **Walleye Dermal Sarcoma Virus**

In 1969 at Oneida Lake in New York, walleye fish were found to have two different types of skin tumors, an epidermal hyperplasia and a dermal sarcoma [38]. Type C, retroviral-like particles were observed in the regressing dermal sarcoma tissue in 1976 by Yamamoto and others, and reverse-transcriptase activity was later found in the tumor lysates [13, 39]. The WDSV genome is 12.7kb, and contains the *gag*, *pol* and *env* genes, as well as 3 accessory open reading frames (Fig. 1.1) [12, 14]. Developing tumors contain 1 proviral copy of the WDSV

genome per cell, and regressing tumors have significantly more un-integrated copies of the genome than developing tumors [12, 14, 40-42]. The genomic analysis revealed that WDSV is closely related to two other walleye retroviruses, WEHV-1 and 2, that cause walleye epidermal hyperplasia, which was identified with walleye dermal sarcoma in 1969 [14, 43].

WDSV is in the Epsilonretrovirus subfamily of Retroviridae [42]. It induces tumor formation, and is associated with the annual development and regression of walleye dermal sarcoma—a neoplastic disease affecting walleye fish [42]. Fish develop tumors very rapidly, and experimental transmission studies show that up to 92% of infected fish have visible tumors as soon as 14 weeks post experimental infection [44]. The rapid and efficient development of WDS suggests a mechanism of transformation akin to an acute-transforming retrovirus, but the genome of WDSV, shown in Figure 1.1, does not contain a viral copy of a known host oncogene [14, 15, 45]. This suggests that WDSV uses a *trans*-acting mechanism for tumorigenesis.

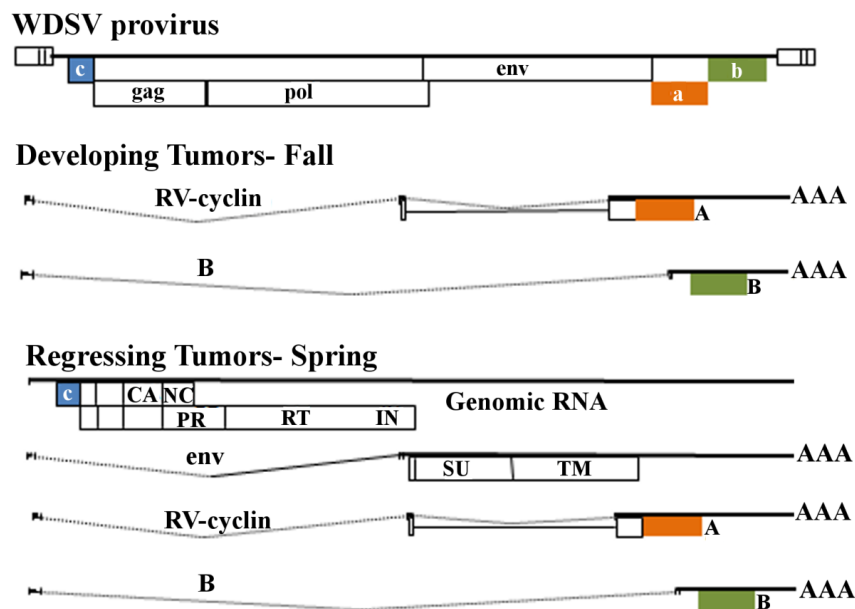


Figure 1.1 The WDSV genome in its proviral state (top panel), and the gene expression profile of the virus during tumor development in the fall (middle panel) and tumor regression in the spring (bottom panel). Adapted from Quackenbush and others 1997 [15].

Un-infected walleye fish are likely exposed to WDSV in the spring during spawning [46]. Newly infected fish are disease-free through the summer months, and develop the dermal sarcomas in the fall. These tumors grow and proliferate in numbers through the winter [47]. During the time of tumor development, there is no production of infectious virus, demonstrated by transmission studies, electron microscopy, and northern blot analysis of WDSV transcripts in tumors [15, 41]. New viral particles are produced during the spring, which coincides with tumor regression and disappearance [15, 47, 48].

### **Accessory Proteins**

The accessory open reading frames (orfs) are called *orf a*, *orf b*, and *orf c*. The full length *orf a* transcript encodes a protein called retroviral cyclin (RV-cyclin), and the other proteins are referred to as the *orf b* protein and the *orf c* protein respectively [12-14, 49]. These accessory proteins function in both tumor development and tumor regression, and their expression is differentially regulated over the course of WDSV infection [15, 42].

The *orf a* and *orf b* transcripts are the only viral transcripts produced during tumor development in the fall and winter (Fig 1.1) [15]. There are multiple splice variants of *orf a*, and this might contribute to the seasonal nature of WDS. The full length *orf a* transcript is the only *orf a* splice variant present during WDS development while the *orf b* transcript remains constant during the entire course of WDSV infection. The proteins from *orf a* and *orf b* continue to be expressed during tumor regression in the spring, however, during the spring full-length genomic RNA is expressed along with the protein encoded by *orf c*, the env protein, and the amino-terminal truncated RV-cyclin proteins from the *orf a* splice variants (Fig 1.1) [12, 13, 15, 41, 42].

In addition to differential expression, the proteins encoded by the accessory orfs localize to different places in the cell [40, 42, 50-52]. The localization patterns of these proteins and

analysis of their functional domains, allowed for the characterization of their role in WDSV infection, which is described below.

#### *The Orf c protein*

The Orf C protein is expressed only in the spring, during the process of tumor regression [15, 53]. The expression of the Orf C protein in tumor cells induces apoptosis, which is thought to contribute to tumor regression in the spring, and tumor shedding during spawning [15, 42, 51, 53, 54]. The Orf C protein is expressed from the full length genomic RNA (Fig 1.1). Once the protein is translated it localizes to the mitochondrial membrane, but can also be found in the nucleus and in the cytoplasm as well [15, 42, 51, 53, 54]. At the mitochondrial membrane, it disrupts the membrane's electrical potential and this correlates with an observable increase in apoptosis [42, 51]. This could be due to the Orf c protein's interaction with the adenine nucleotide transporter (ANT) and Bcl-2 associated x-protein (Bax), two cellular proteins that control apoptosis [54]. Additionally, MCA-205 cells (a cell line from a mouse sarcoma) showed decreased viability when infected with a recombinant lentivirus expressing the Orf c protein, suggesting the potential for the Orf c protein to be used in oncolytic therapy [54].

#### *The orf b protein*

The protein encoded by *orf b*, the Orf b protein, directly interacts with the receptor for activated C kinase (RACK 1), and functions in a complex with protein kinase  $\alpha$  (PKC $\alpha$ ), phosphatidylinositol-3-kinase (PI3K), SRC, and protein phosphatase 2A (PP2A)[50, 55]. These are all components of signaling pathways involved in the regulation of apoptosis and proliferation [50, 55]. As a result, cells expressing the Orf b protein continue to grow in low serum conditions, and are protected from staurosporine-induced apoptosis. This along with its

pattern of expression during WDSV infection suggests a role for the Orf b protein in walleye dermal sarcoma development [15, 55].

### *RV-cyclin*

Transgenic mice expressing RV-cyclin exhibit epithelial hyperplasia at wound sites after tail clipping, which supports a role for RV-cyclin in the development of WDS [49, 56]. When expressed in cells, RV-cyclin increases their division rate, and allows this division to continue in low serum conditions [57]. These data support a role for RV-cyclin in the development of WDS, and this aspect of RV-cyclin was further explored.

### **RV-cyclin expression and host transcription**

RV-cyclin localizes to the nucleus in naturally infected, explanted tumor cells (Fig 1.2 A), and maintains this localization when expressed in mammalian cells through transient transfection (Fig 1.2 B) [40, 52]. The transfection experiments demonstrate that when in the nucleus, RV-cyclin co-localizes with the splicing machinery in interchromatin-granule clusters (IGCs) (Fig 1.2 B) [52]. These are places of active transcription. Multiple experiments analyzing RV-cyclin's effect on transcription show that it can enhance or inhibit gene expression, depending on the promoter/gene and cell type in question [57-61]. RV-cyclin inhibits transcription from the WDSV promoter, and other promoters dependent on NF $\kappa$ B [59, 60]. This inhibition could be in part responsible for immune evasion during the initial infection, and for the timed production of full length genomic RNA and virion assembly in the spring.

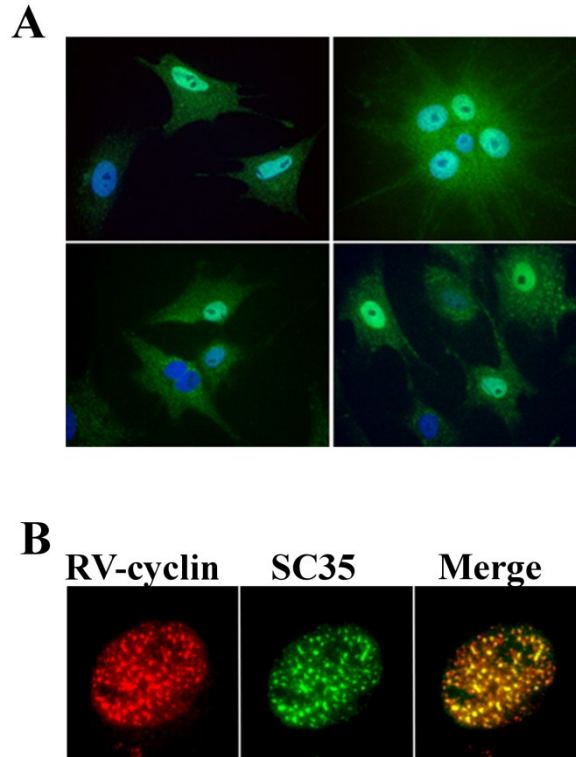


Figure 1.2 RV-cyclin localization in explanted walleye dermal sarcoma cells using a GFP-tagged antibody to label RV-cyclin and DAPI (blue) as a nuclear stain (A) [40]. Isolated Cf2Th nuclei expressing transiently expressed RFP labeled RV-cyclin (red) (B) [52]. Splicing component 35 (green), a marker of active transcription and splicing was labeled with GFP to show co-localization (yellow) with RV-cyclin, indicating RV-cyclin resides in inter-chromatin granule clusters [52].

A role for RV-cyclin in transcription regulation was supported by its co-localization with IGCs and by its association with hyperphosphorylated RNA Pol II in immunoprecipitations [58]. Hyperphosphorylated RNA Pol II is associated with transcription elongation and processing as discussed later on. A cell cycle gene array showed that RV-cyclin up-regulates a number of cell cycle genes (Fig. 1.3) [57]. Two specific genes that were identified in the array, and whose expression is up-regulated by RV-cyclin are *CCND1* and *CDKN2D*. These genes encode the cyclin D and p19INK4d proteins respectively.

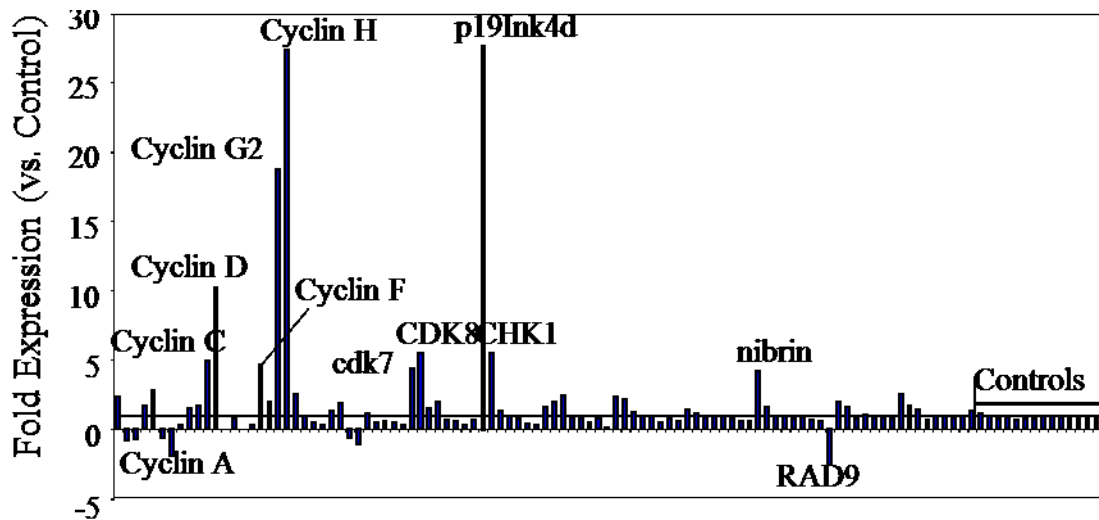


Figure 1.3 Cell cycle gene array showing activation of several cell cycle genes by RV-cyclin. Genes that were significantly up-regulated were cyclin C, cyclin D, cyclin G2, cyclin H, cyclin F, CDK8, p19INK4d, CHK1, and nibrin. The array was performed with HeLa cell RNA collected 32 hours post transfection with RV-cyclin or with an empty vector Brewster CD, Birkenheuer CB, Vogt MB, Quackenbush SL, and Rovnak J, 2010, [57].

Cyclin D1 was originally characterized by Carlo M. Croce, Henry Morris Kronenberg, Andrew Arnold, and others [62-66]. The cyclin D1 protein is encoded by the *CCND1* gene in humans. Expression and retention of cyclin D1 in the nucleus of the cells is dependent on mitogenic signals [62, 67, 68]. When the cell is in an environment that stimulates growth, cyclin D1 is retained in the nucleus where it binds to cyclin dependent kinases 4 and 6 (CDK4 and CDK6 respectively) [62, 67, 69, 70]. When cyclin D1 is bound and the appropriate phosphorylated cip/kip regulatory protein (p21, p27, or p57) is present, the cyclin D1-CDK4/6 complex becomes activated and can phosphorylate different targets [62]. These phosphorylation events drive the transition of the cell from G0 to G1 phase in the cell cycle. Targets of CDK4/6 include retinoblastoma protein (pRb), SMAD1 and SMAD3 [62, 67, 71]. A high level of cyclin D1 is associated with many human cancers, such as breast cancer, melanoma, and lung cancer, and therefore it is thought to be a possible therapeutic drug target for many cancers [71, 72].

Since cyclin D1 expression and stability is altered in many different types of cancer, it is logical that this would be a target of RV-cyclin and play a role during WDS development.

P19INK4d is encoded by *CDKN2D* and was also up-regulated by RV-cyclin in the gene array (Fig 1.3). It is a member of the INK4 family of proteins, which are inhibitors of the CDK4/6 kinase complex. The family consists of p15INK4b, p16INK4a, p18INK4c, and p19INK4d. P19INK4d was the last protein discovered in the family, by H. Hirai and others in C.J. Sherr's lab, and Kun-Lian Guan and others in Yue Xiong's lab in 1995 [73, 74]. It inhibits phosphorylation of pRb by CDK4 and CDK6 [74]. As a result, activated p19INK4d can inhibit cell cycle progression at the G1-phase, and it is thought that this function of the protein is important during developmental processes and differentiation [74-76]. Mice lacking p19INK4d expression do not develop severe cancers, but they do experience progressive hearing loss, and develop testicular atrophy due to un-regulated cell division in the associated tissues [77-79].

In addition to its roles in differentiation, p19INK4d is also activated upon genotoxic stress. Activation of p19INK4d during the DNA damage response inhibits apoptosis in neuroblastoma cells [80]. Additionally, it enhances DNA repair, and cells with knocked-down p19INK4d expression have a reduced ability to perform nucleotide excision repair [81]. Cells over-expressing p19INK4d are more resistant to UV-treatment, suggesting that activation of p19INK4d correlates with enhanced cell survival [81]. Furthermore, p19INK4d's role in the DNA damage response is independent of its role in cell cycle arrest, as treatment of p19INK4d-overexpressing cells with mimosine does not alter the rescuing-effects of p19INK4d expression under UV irradiation [81].

Since cyclin D1 and p19INK4d are both involved in cell division, RV-cyclin's up-regulation of *CCND1* and *CDKN2D* gene expression might be beneficial to WDSV infection.

The ability of RV-cyclin to up-regulate genes associated with cell cycle control and DNA damage could contribute to the development of WDS [57].

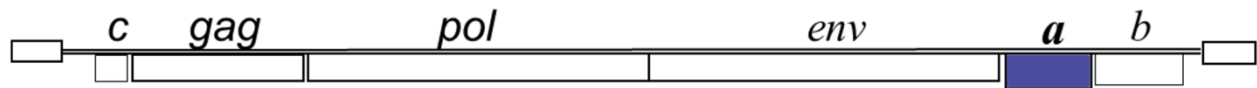
### **Functional domains of RV-cyclin**

As RV-cyclin is expressed during tumor development, it localizes to places of active transcription, and can either activate or inhibit transcription from viral and host genes, it was important to characterize the cellular proteins that RV-cyclin interacts with. The majority of the amino acid sequence of the protein is predicted to fold into a cyclin-box-like motif, which gave the name to the protein [49]. This motif is required for direct interaction between RV-cyclin and the cellular cyclin dependent kinases 3 and 8 (CDK3 and CDK8, respectively) [57]. In addition to the cyclin box motif, RV-cyclin also contains a transcriptional activation domain at the carboxy terminus that interacts with TATA binding protein associated factor 9 (TAF9) [60, 61]. RV-cyclin binds importin  $\beta 2\alpha$  and PP2A as well. These binding partners were identified in a yeast two hybrid screen [82]. A diagram of the functional domains of RV-cyclin is shown in Figure 1.4 [49, 57, 58, 60, 61]. The presence of the cyclin box and activation domain allow RV-cyclin to pull down hyperphosphorylated RNA Pol II, p300/CBP, TATA-binding protein (TBP), and components of the Mediator complex [42, 58, 60, 61]. CDK8 and TAF9 are host proteins that function in RNA Pol II transcription.

### **TAF9**

TAF9 is one of the 13 mammalian Tafs that assemble with TATA-binding protein (TBP) to form the general transcription factor TFIID [83-86]. TFIID is the first general transcription factor recruited to a gene's promoter during formation of the RNA Pol II pre-initiation complex (PIC) [84, 87]. TFIID facilitates the formation of the PIC by recognizing histone marks associated with gene activation.

## WDSV provirus



## RV-cyclin

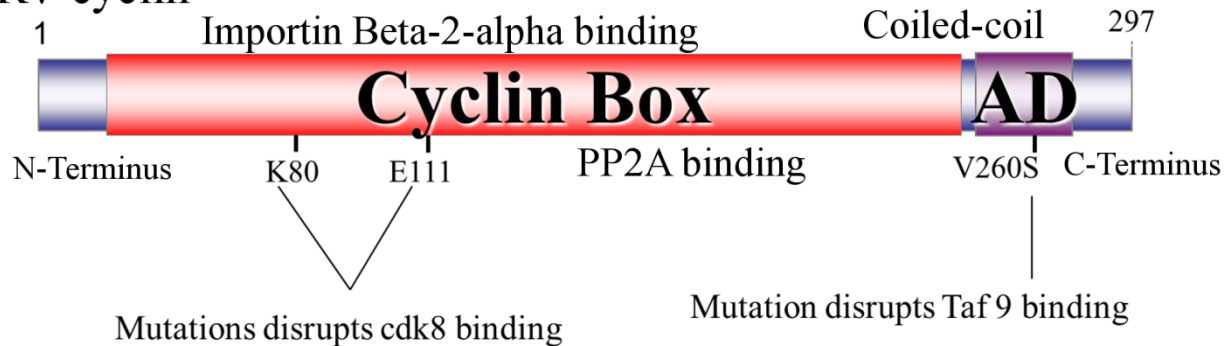


Figure 1.4 Diagram of the functional domains of RV-cyclin, and the RV-cyclin mutations employed in these experiments. The coiled-coil allows RV-cyclin homodimer and homotrimer formation (unpublished data). RV-cyclin binds importin  $\beta 2\alpha$  between amino acids 1 and 95 and PP2A between amino acids 95 and 211. The K80A/E111A double mutation disrupts binding between RV-cyclin and CDK8 and the V260S mutation disrupts binding between RV-cyclin and TAF9 [49, 57, 58, 60, 61].

These marks range from acetylated nucleosomes at the core promoter, to co-activators bound to enhancer regions, and downstream promoter elements [83, 86, 88]. At the promoter, TFIID interacts with TFIIA and TFIIB and this stabilizes this complex for further recruitment of TFIIF, TFIIE, TFIIH, RNA Pol II and the mediator complex [84, 87].

The association of individual Tafs with TFIID is variable, and is promoter dependent [85, 86, 89, 90]. However, TAF9 is always present in the TFIID complex [85, 90]. After formation of the PIC and recruitment and release of RNA Pol II from the promoter, TFIID remains at the promoter [83]. It has been suggested that TFIID does this to form the re-initiation scaffold, however, other studies have shown that efficient re-initiation does not require TFIID [83]. TFIID's retention at promoters might also serve as a marker for an active gene, which a daughter cell can use as a guide to determine which genes to turn on after a cell division event [83, 91].

TAF9 and Taf 6 form a heterodimer that is a core component of TFIID [85, 86]. The conserved C-terminal domain of TAF9 is required for TFIID formation and efficient RNA Pol II transcription at some genes. It is also required for contact between TFIID and the downstream promoter element (DPE) [88, 90]. TAF9 is contacted directly by the activation domains of a number of transcription factors, including p53, NFκB, and the herpes simplex virus transcription factor, VP16, which support its important role in transcription of select genes [89, 92-94].

### **CDK8**

CDK8 and its paralog CDK19 (which exists in vertebrates only) are components of the CDK8 sub-module of the Mediator complex. Mediator is a general transcription factor, which modulates RNA Pol II using a variety of mechanisms [95-98]. The CDK8 sub-module contains mediator subunits Med12, Med13, and cyclin C in addition to CDK8. Association of the CDK8 sub-module with core Mediator is variable, and is regulated by Med13 interaction with Med14 [99, 100]. About 30% of the total CDK8 sub-module exists independently of the complex, and CDK8 target specificity can be determined by sub-module association with Mediator [101, 102]. There are multiple CDK8 substrates, and one of these targets is the carboxy terminal domain (CTD) of the RPB1 subunit in RNA Polymerase II (RNA Pol II).

CDK8 is similar to CDK7 and CDK9 because all three CDKs are active during the entire life of the cell, and they are not restricted to certain points within the cell cycle [103, 104]. Furthermore, they all phosphorylate the CTD of RNA Pol II [103-107]. In human cells, the CTD contains 52 repeats of the heptad consensus sequence YSPTSPS [108]. CDK7, part of the general transcription factor complex TFIIH, phosphorylates Ser5 and Ser7 in the heptad repeat to initiate RNA Pol II transcription after formation of the pre-initiation complex (PIC) at the

promoter [100, 103, 105, 109, 110]. CDK9, which is part of pTefb, phosphorylates Ser2 in the heptad repeat to start RNA Pol II elongation [107, 108, 111, 112].

Ser2 and Ser5 phosphorylation in the heptad repeat are coordinated and allow binding of different mRNA processing complexes as RNA Pol II progresses through the gene during transcription. Phosphorylated Ser5 is a binding site for the mRNA capping enzyme [108, 113]. Additionally, phospho-Ser5 guides SET1, a histone H3 lysine 4 methyltransferase, to actively transcribed regions, maintaining active transcription marks at the gene [108, 114]. As RNA Pol II moves away from the promoter, pTefb-bound CDK9 phosphorylates Ser2 in the heptad repeat, and this provides binding sites for the polyadenylation specificity factor (CPSF) and the cleavage stimulatory factor (CstF) [108, 112, 115]. These components are required for efficient transcription termination [115, 116].

The CDK8 yeast homolog Srb10 and mammalian CDK8 phosphorylate Ser5 and Ser2 in the heptad repeat [99, 103, 105, 106]. Srb10 can both activate and inhibit gene expression in response to changing glucose levels [117-120]. Studies by Liu et al in 2004 demonstrated that yeast CDK7 (yeast Kin28) and Srb 10 both phosphorylate the CTD of RNA Pol II at the promoter, and inhibition of both kinases reduced transcription by 70% in an *in vitro* system using the HIS4 promoter on plasmid constructs [117]. This suggested a gene-specific, transcription activation role for Srb10, which might stabilize a scaffold complex and promote RNA Pol II transcription initiation, elongation, or re-initiation [117].

Mammalian CDK8 activates gene expression in a similar manner to yeast Srb10. This has been demonstrated with *DioI*, a thyroid hormone response gene, with the serum-response genes, and with the hypoxia-induced genes [97, 99, 121]. Phosphorylation of the CTD of RNA Pol II by mammalian CDK8 is required for transcription of the *DioI* gene. Knock down of

CDK8 kinase activity resulted in deficient recruitment of CDK9 to the *DioI* gene, and *DioI* mRNA expression was reduced [99].

A similar CDK8/CDK9 linkage has been shown for genes in the serum response network [121]. CDK8 knockdown in the human colon cancer cell line, HCT116 cells, resulted in a reduction of both Ser5 and Ser2 phosphorylation in the heptad repeat. This correlated with reduced recruitment of CDK7 and CDK9 to the serum response genes. CDK9 depletion was due to decreased bromodomain protein 4 (Brd4) at the serum response genes. Brd4 is a pTefb recruitment protein needed for transcription elongation [121]. Hif1 $\alpha$ -regulated, hypoxia-induced genes are controlled by CDK8 in a similar manner to the serum response genes. *ANKRD37*, which is regulated by Hif1 $\alpha$ , uses CDK8 to recruit pTefb in the super elongation complex for functional transcriptional elongation [97]. Other genes that require CDK8 for efficient transcription include: p53-regulated transcription,  $\beta$ -catenin regulated genes, genes involved in clathrin-mediated endocytosis, and genes under the control of the cytomegalovirus (CMV) immediate early promoter [97, 100, 122-125].

CDK8 also represses transcription. Knock down of CDK8 and its mammalian paralog CDK19 resulted in both activation and repression of gene expression [97, 124]. These studies determined that CDK8 and 19 regulate genes in a pathway-specific manner [97, 124]. The apparent ability of CDK8 to activate or repress gene expression may be attributed in part to the function of CDK19, which has been identified more recently, and is hard to distinguish from CDK8 with the commercially available antibodies [98, 124]. Another reason is the regulated association and disassociation of the CDK8 sub-module and the core mediator complex [101, 126]. The CDK8 sub-module inhibits transcription *in vitro* by associating with the mediator complex and causing conformational changes within the core mediator which are independent of

CDK8 kinase activity [101]. The conformational changes cause the Mediator complex to disassociate from RNA Pol II, which is linked to transcriptional repression [101, 126].

The complexity of identifying CDK8's dual role in transcription is also due to the sheer number of substrates in addition to the CTD of RNA Pol II [127-131]. Phosphorylation of cyclin H in TFIIF by CDK8 results in inhibition of transcription initiation [130], and phosphorylation of SREBP1 by CDK8 leads to SREBP1 degradation resulting in transcriptional shut-down of genes involved in lipogenesis [128]. CDK8 phosphorylation of STAT1 can inhibit or activate transcription of a wide variety of interferon response genes [129], suggesting a role for CDK8 in control of innate immunity. CDK8 influences the adaptive immune response as well, by interacting with the promoter of Notch signaling responsive genes in T-cells [131]. Here, CDK8 phosphorylates ICD in the PEST domain, leading to PEST recruitment and the degradation of ICD [131]. CDK8s mark of ICD for degradation provides the shut-down of transcription required for quick, regulated transcriptional burst [131].

There are CDK8 substrates outside of the CTD of RNA Pol II that have been associated with transcriptional activation. Two of these targets are E2F1 and histone H3 [102, 127, 132]. When CDK8 phosphorylates E2F1, it relieves E2F1 repression of  $\beta$ -catenin regulated genes, which results in the expression of genes related to cell division in colon cancer [127, 132, 133]. Additionally CDK8 is recruited directly to  $\beta$ -catenin regulated genes, which provides another possible mechanism of CDK8-regulated  $\beta$ -catenin transcription [100].

CDK8 phosphorylates serine 10 in the N-terminal tail of histone H3 [102]. Phosphorylation of this histone on this residue has multiple roles, and it's a substrate of many kinases. One of its roles is in cell division. During this process it is an important substrate of Aurora B kinase, and its phosphorylation is a checkpoint for the G2/M transition in cell division

[134]. Ser10 of histone H3 is also phosphorylated by the mitogen and stress-activated protein kinase (MSK) in non-dividing cells for transcription of *FOS* and *JUN* [135]. Histone H3 Ser10 phosphorylation at the *FOS* and *JUN* loci allows efficient transformation of Jb6 cells [136], and is essential for *FOS* and *JUN* activation after arsenite-induction [137]. This mark promotes RNA Pol II release from pausing at heat shock gene loci [138]. CDK8 phosphorylation of histone H3 Ser 10, while not linked to transcription activation at specific genes, is thought to increase GCN5 phosphoacetylation [102, 139]. This maintains transcriptional activity on *in vitro* chromatin templates [102, 139]. Presumably the outcome of Ser10 phosphorylation by CDK8 is similar to that of MSK activity for *FOS* and *JUN* transcription regulation.

These various targets of CDK8 highlight a central role for CDK8 in host transcriptional responses to a variety of different regulatory pathways, and implicate CDK8 function in metabolism (SREBP1), immunological responses to viral and bacterial pathogens (STAT-1 and the Notch ICD), and cancer development (CTD of RNA Pol II). With respect to cancer in particular, CDK8 is an important oncogene in colon cancer, gastric adenocarcinoma, melanoma, and possibly walleye dermal sarcoma [123, 133, 140-142].

### **The RV-cyclin TAF9 interaction**

RV-cyclin interacts with TAF9 through its activation domain (AD) in the carboxy region of the protein (Fig 1.4) [61]. The RV-cyclin AD was identified using RV-cyclin constructs lacking the carboxy-region. These construct were unable to pull down components of the RNA Pol II transcriptional machinery, and the binding partners of this region were investigated [58]. Subsequent analysis demonstrated that the RV-cyclin-AD fused to the Gal4 DNA-binding-domain could replace the Gal4-AD to initiate transcription from the Gal 4 promoter in yeast and mammalian cell culture [60]. Mutational analysis revealed that valine at position 260 was

critical for AD function, and that the AD was required for the inhibition of transcription from the WDSV promoter [60]. The RV-cyclin AD directly binds TAF9, and was able to interfere with TAF9 binding to other host and viral protein activation domains [61]. Additional experiments identified RV-cyclin inhibition of NF $\kappa$ B-regulated transcription, through the activation domain, which could allow for immune evasion by WDSV [59].

### **The RV-cyclin-PP2A interaction**

RV-cyclin binds to the regulatory A subunit of Protein Phosphatase 2 (PP2A) [82]. Originally detected in yeast 2-hybrid screens, this interaction was confirmed by RV-cyclin co-immunoprecipitation with endogenous PP2A and with the co-expressed A subunit. Co-precipitates include the catalytic C subunit, but RV-cyclin interaction precludes the regulatory B subunit from the PP2A complex. The B subunit is the most variable of the PP2A subunits, consisting of a large family of homologous proteins, and it functions as the determinant of PP2A localization in the cell and its substrate specificity [82].

### **The RV-cyclin-CDK8 interaction**

RV-cyclin was first recognized as a cyclin based upon sequence alignments, and its expression was shown to restore cell division in cyclin-deficient yeast strains. These strains included a strain deficient in the yeast homolog of cyclin C (Srb11) [49]. Its specific interaction with metazoan CDK8 was determined by co-precipitation of expressed RV-cyclin with a panel of antibodies to known CDKs [58]. Later recognition of cyclin C binding and activation of CDK3 activity in the regulation of cell division brought to light a specific interaction between RV-cyclin and CDK3 as well [57, 143]. Co-immune precipitation of RV-cyclin with anti-CDK8 antibodies was dependent upon the presence of the entire cyclin box motif [58]. Alignment of RV-cyclin and cyclin C amino acid sequences identified specific residues in RV-cyclin that

correspond to residues in cyclin C. Lysine at position 80 and glutamate at position 111 in the RV-cyclin protein are predicted to directly contact CDK8, and mutation of these residues to alanine (RV-cyclin K80A/E111A) disrupts RV-cyclin-CDK8 binding [57].

RV-cyclin's interaction with CDK8 enhances phosphorylation of at least two of its CDK8's substrates—the CTD of RNA Pol II and Histone H3 [82]. Anti-CDK8 immune precipitates exhibit significantly greater activity toward these substrates *in vitro*. Similar assays with specific anti-CDK19 antibodies demonstrated the opposite effects: apparent inhibition of the kinase activity toward the Pol II CTD and Histone H3 *in vitro* (Fig 1.5 and unpublished data). It remains to be determined whether RV-cyclin alters the kinase activity of CDK8 or CDK19 toward other known substrates or whether it extends the range of substrate specificity for these kinases (Fig. 1.6) [57, 82]. The CDK8 *in vitro* kinase assays also demonstrated that the presence of PP2A can enhance CDK8 kinase activity on the CTD of RNA Pol II. This effect was in addition to the enhancement shown by RV-cyclin, as the presence of PP2A enhanced CDK8 kinase function in control cell IPs which did not contain RV-cyclin [82]. This means PP2A is an important phosphatase needed to regulate CDK8 kinase activity, and RV-cyclin's interaction with PP2A may be directing PP2A's location to specific gene loci [82].

Due to the nature of RV-cyclin's interaction with CDK8, we were interested in proto-oncogenes that are known to be transcriptionally activated by CDK8 or associated with CDK8 targets [57, 82]. Three genes were chosen for analysis—*FOS*, *EGR1*, and *JUN*, because of their demonstrated dependence on CDK8 activity for transcription. CDK8 kinase activity on the CTD of RNA Pol II is required for effective transcription elongation of *FOS*, and *EGR1* [121]. *FOS* and *JUN* also require phosphorylated histone H3 Ser 10 for effective transcription [135, 137]. Additionally, all three genes are important proto-oncogenes in a number of cancers.

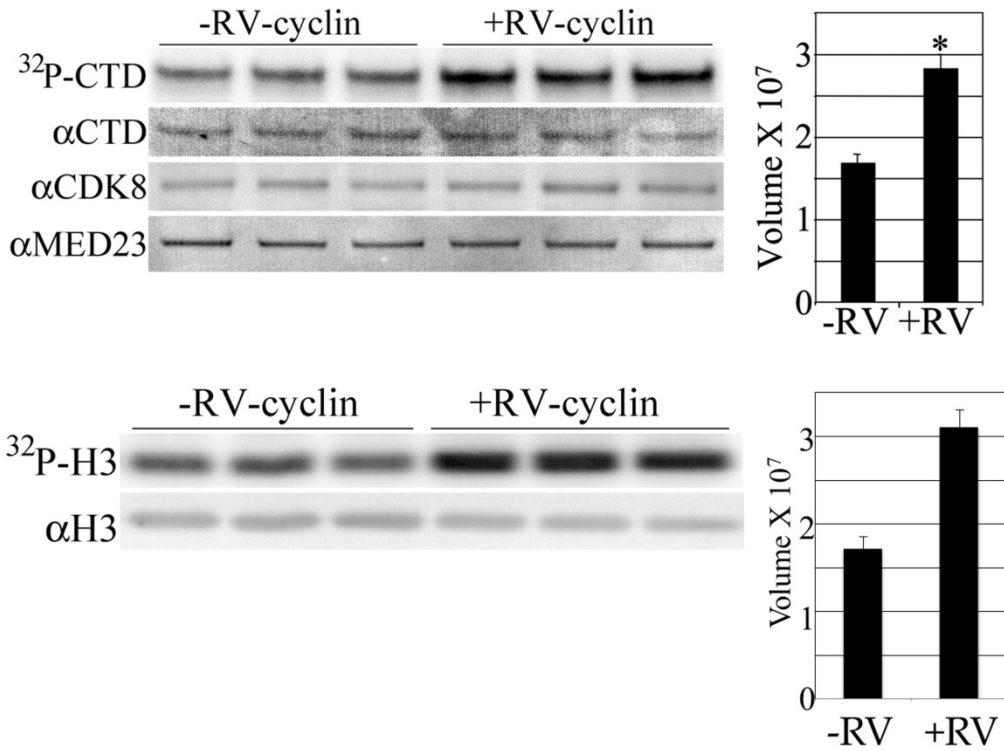


Figure 1.5 *In vitro* kinase assays demonstrating RV-cyclin enhances CDK8 phosphorylation on the CTD of RNA Pol II and CDK19 phosphorylation of histone H3. CDK8 immunoprecipitates from control HeLa cells and HeLa cells expressing RV-cyclin were used for the assay with radio-labeled p32. These radiographs are shown in the left portion of the panel with the RNA Pol II CTD phosphorylation shown in the top portion, and histone H3 phosphorylation shown in the bottom portion. Densitometric analysis, reported in graphical form on the right portion of the panel was performed with two-way ANOVA statistical analysis and a \* indicates a p-value < 0.05. These data was previously published [57, 82].

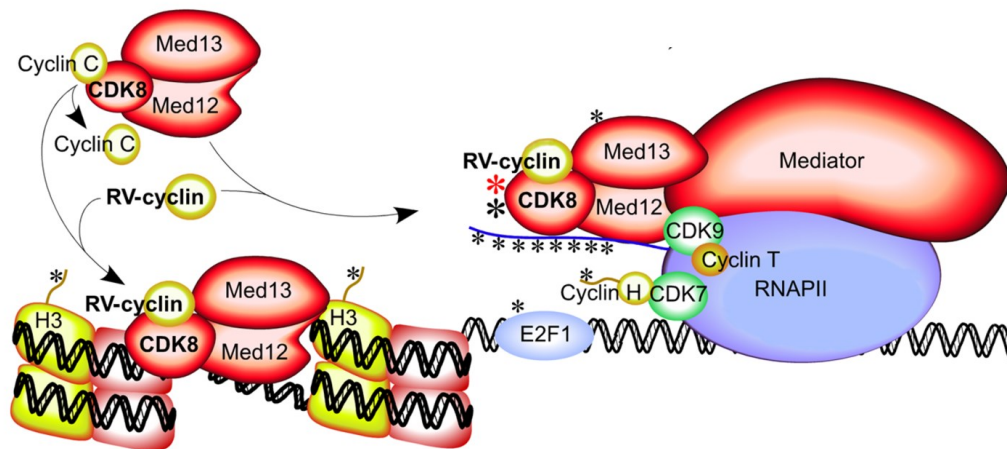


Figure 1.6 Diagram of possible CDK8 substrates whose phosphorylation could be increased by RV-cyclin. Figure modified from Rovnak and others 2012 [57, 82].

*FOS* was first described in its oncogenic, viral form, *v-FOS*, by Tom Curran. Curran found *v-FOS* to be the transforming factor in Finkel-Biskis-Jenkins osteosarcomavirus (a murine virus) [144-147]. The cellular *c-FOS* family is comprised of *c-FOS* (referred to as *FOS* from here on out), *FOSB*, *Fra1*, and *Fra2*. This family, together with the *c-JUN* gene family, form dimers to create different versions of the AP1 transcription factor [148]. The first described member of the *c-JUN* gene family was *v-JUN*, the transforming oncogene in avian sarcoma virus 17 [145, 149]. Since *v-JUN*'s discovery *cJUN* (referred to here as *JUN*), *JUNB*, and *JUND* have been characterized. Both cellular versions of *FOS* and *JUN* are potent proto-oncogenes, and their over expression can easily transform cultured cells [144, 150, 151]. Furthermore AP-1 is oncogenic in a variety of human cancers from melanoma to liver cancer [144, 151, 152].

*EGR1* was identified in a number of different labs and named differently in each. The lab that named *EGR1* for Early Growth Response protein 1 identified it in a cDNA library screen for genes activated in BALB/c 3T3 cells after three hours of stimulation with fetal calf serum [146, 153]. Since its discovery it has proven to be an important oncogene, particularly in prostate cancer, mouse skin carcinomas, and colorectal cancers [154-159].

### **Hypothesis**

Due to the nature of the RV-cyclin/CDK8 interaction, CDK8's involvement in serum-response gene transcription and the role these genes play in tumor development, we hypothesized that RV-cyclin increases CDK8 function to enhance transcriptional processivity of the serum response genes. The three aims developed to test this hypothesis are:

1. Determine the effect of RV-cyclin on serum response gene expression
2. Determine if gene activation by RV-cyclin is due to enhanced transcriptional processivity
3. Determine if RV-cyclin enhances the kinetics of CDK8 phosphorylation *in vitro*

## CHAPTER 2: AIM 1—DETERMINE THE EFFECT OF RV-CYCLIN ON SERUM RESPONSE GENE EXPRESSION

### **Introduction Aim 1**

The qRTPCR assay was used to analyze the effects of RV-cyclin on cell gene expression. Conveniently RV-cyclin's influence on genes identified in the gene array could be used as positive controls (Fig. 1.3). The array was performed using HeLa cell RNA collected 32 hours post transfection with RV-cyclin or control vector (Fig 1.3). This was a significant amount of time post transfection, and long enough for successive rounds of gene expression and downstream induction of expression. For instance, *FOS*, and *JUN* regulate *CCND1* expression, and *EGR1* can activate *CDKN2D* expression in prostate cancer cells [152, 158]. Therefore the *CCND1* activation and possibly the *CDKN2D* activation at 32 hours post transfection could be a result of downstream activation of genes that were directly targeted by RV-cyclin, like *FOS*, *EGR1*, and *JUN*. To analyze the direct effects of RV-cyclin on gene expression, experiments were designed to determine the earliest time point at which RV-cyclin up-regulated transcription of *CCND1* and *CDKN2D*, and to test if RV-cyclin enhanced mRNA levels of the CDK8-regulated genes, *FOS*, *EGR1* and *JUN*.

After determining RV-cyclin's ability to function on these select genes after transient expression, experiments were designed to utilize mutant forms of RV-cyclin with known functional deficits as controls. Validation of RV-cyclin's influence on these genes was also evaluated in other cellular systems: a HeLa tetracycline-inducible system (Tet-Off Cells), where wt and mutant RV-cyclins are under the control of a tetracycline-dependent promoter, and HCT116 cells, the same cells used to identify CDK8's regulation of the serum-response genes

[121]. In the HCT116 cells wt and mutant RV-cyclins are constitutively expressed in clonal lines. HeLa cells are not the ideal cell type for studying the serum-response aspect of transcriptional regulation, because they have lost the ability to shut these genes off in the absence of serum, whereas HCT116 cells maintain the ability to shut-off and turn the serum response genes back on under serum starvation and serum stimulation conditions, respectively. At the beginning of this project, HCT116 cell clones that stably express wt RV-cyclin had been established, but it was necessary to establish HCT116 cell lines stably expressing the mutant RV-cyclins, and tagged human recombinant cyclin C. During the time while HCT116 clones stably expressing the RV-cyclin mutants were being produced, experiments that analyzed mutant RV-cyclins in gene activation in HeLa cells continued with the tetracycline-inducible cell lines.

The experiments with the HeLa inducible cell lines were carried out under low serum conditions and with un-induced controls with tetracycline, induction by removal of tetracycline at 48 hours prior to collection, or with prolonged induction of RV-cyclin (tetracycline was removed 2 weeks prior to the experiment set up). These conditions were determined from time course experiments analyzing RV-cyclin induction after tetracycline removal. Once the stable HCT116 clones were established, serum starvation was used to turn the response gene expression off and test the effects of constitutive RV-cyclins during both shutdown and serum stimulation. These experiments analyzed the effect of wt RV-cyclin on serum response mRNA production, during a genuine serum response. The response was directly compared to control HCT116 cells, stably carrying the expression vector, and cells expressing the mutant RV-cyclins. The results of these experiments demonstrated that RV-cyclin requires an independent activation event, i.e. serum stimulation, prior to its effects on gene expression and both CDK8 and TAF9 binding are

necessary to fully enhance serum response gene expression, but CDK8 binding is critical, and without CDK8 binding RV-cyclin is inhibitory.

### **Hypothesis Aim 1**

Due to the nature of RV-cyclin's activation of *CCND1* and *CDKN2D* in the cell cycle gene array, and CDK8's requirement for efficient transcription of the serum-response genes, it is expected that RV-cyclin expression will enhance transcript levels of *CCND1*, *CDKN2D*, *FOS*, *EGRI*, and *JUN* immediately after expression and nuclear translocation in transfected HeLa cells. Furthermore, the serum-driven expression of *FOS*, *EGRI*, and *JUN* is expected to be increased by RV-cyclin in HCT116 cells during this CDK8-dependent process. This enhancement will be diminished or reduced to control levels when the non-CDK8-binding RV-cyclin mutant, K80A/E111A, is present during the serum response. The function of the RV-cyclin transcription AD in the serum response remains to be determined. The RV-cyclin V260S mutant will yield data necessary to make that determination.

### **Materials and Methods Aim 1**

#### *Cell culture and transient transfection of HeLa cells*

The stock flasks of HeLa cells (ATCC # CCL-2) used for the transient transfection experiments were grown in Dulbecco's modified Eagle's medium (DMEM), with 7% fetal bovine serum and 4mM L-glutamine supplementation with penicillin and streptomycin under 5% CO<sub>2</sub> at 37°C. The cells were split when they reached 70 to 80 percent confluence. One day before the transient transfection experiments, the cells were split from the stock flasks and plated at a density of  $1.5 \times 10^5$  cells/well in a 6-well plate in antibiotic-free media.

Fugene HD transfection reagent from Promega was used in conjunction with either the pKH3 empty vector or the pKH3A vector, encoding RV-cyclin, following the manufacturer's

instructions. After addition of the transfection mixture, the cells were incubated in growth conditions for 2.5, 4, 8, or 10 hours. The cells were washed with cold D-PBS and total RNA was collected.

#### *RNA extraction, reverse transcription and quantitative polymerase chain reaction*

RNA was collected from washed cells using the Trizol reagent (Invitrogen), which was added directly to the plates prior to extraction. The obtained RNA was DNase I-treated using the Turbo DNase I kit from Ambion, and then reverse transcribed (RT) with the Verso cDNA kit (Thermo Scientific) using 1 µg of RNA and random-hexamers as primers. A 3-step quantitative polymerase chain reaction (qPCR) using Sybr green (BioRad) and a CFX96 qPCR machine with a T-1000 thermocycler (BioRad) were used to analyze gene expression. The following protocol was used to amplify the cDNA using validated primers: 95° C for 3 minutes for the initial denaturation, then 40 cycles of 95°C for 10 seconds, 60°C for 10 seconds, and 72°C for 30 seconds, after each cycle there was a plate read for Sybr green fluorescence. After the 40 cycles were complete, the samples were heated to 95°C for 10 seconds before undergoing melt curve analysis. This analysis included a no reverse transcription control to ensure no host DNA contamination, and with a no template control as well. Primer validation was carried out using standard curve dilutions of HeLa cell cDNA, and melt curve analysis to determine only one product was amplified. All primer sets can be found in Table 2, and primer sets that have been referenced previously are indicated. This protocol has been previously published [57].

#### *Cell culture and the HeLa cell lines inducible for RV-cyclin expression*

Dr. Joel Rovnak previously established the HeLa-RV-cyclin-inducible cell lines using the Tet-Off Gene Expression System (BD Biosciences) and G418 selection [57]. The wt RV-cyclin, K80A/E111A, and V260S mutant RV-cyclin clones were maintained in DMEM with 7% FBS.

Un-induced and stably induced cells were passaged in the appropriate tetracycline conditions. Transient induction was carried out by washing the monolayer two times with DPBS and adding media without tetracycline. Gene expression analysis was done by plating un-induced, stably induced, or transiently induced HeLa cells in 6-well cell culture dishes two days prior to collection. The serum and tetracycline concentration was adjusted at the time of plating. Total RNA was collected and subjected to qRTPCR analysis as described.

Table 2 Primer sets used of qRTPCR analysis of gene expression

<b>Primer</b>	<b>Forward Primer</b>	<b>Reverse Primer</b>	<b>Ref.</b>
GAPDH	5' GCCATCAATGACCCCAT 3'	5' CGTCCTGGAAGATGGTG 3'	[57]
$\beta$ -Actin	5' CATGTACGTTGCTATCCAGGC 3'	5' CTCCTTAATGTCACGCACGAT 3'	
CCND1	5' CGGAGGAGAACAACAGA 3'	5' TGAGGCGGTAGTAGGACA 3'	[160]
CDKN2D	5' GCTGCAGGTCATGATGTTG 3'	5' CTGCCAGATGGATTGGAAGT 3'	[161]
FOS	5' AGGAGGGAGCTGACTGATACA 3'	5' GCAGACTTCTCATCTTCTAGTT 3'	[121]
EGR1	5' TACGAGCACCTGACCGCAG 3'	5' CACCAGCACCTTCTCGTTGTT 3'	[121]
JUN	5' CCTCAACGCCTCGTTCCTC 3'	5' TTACTGTAGCCATAAGGTCCGCT 3'	[121]
RV-cyclin	5' CCATCGTTGCTTCTCAACAGA 3'	5' GCCGGACTGGAGTGATAGTC 3'	

#### *HCT116 stable cell line derivation and serum-starvation/stimulation experiments*

The pKH3-RV-cyclin, pKH3-RV-cyclin K80A/E111A, pKH3 RV-cyclin V260S, and pKH3 empty vector were co-transfected with the pMC1neo vector into the human colon carcinoma cell line, HCT116 (ATCC # CCL-247). G418 was used for selection of stable clones. 50 individual colonies of cells were picked for expansion and screening. Positive clones were sub-cloned in two rounds of single-cell dilutions. The cell line transfected with the pKH3 vector and stably selected for G418 resistance was used as the control cell line for all HCT116 experiments. Once selected, the HCT116 cells were used for serum-starvation/serum-stimulation experiments. Cells were plated in 6-well plates two days prior to serum-starvation, at a density of  $2.5 \times 10^5$  cells/well, in DMEM with 10% FBS. After the cells adhered to the plate, they were washed two times with DPBS and incubated in DMEM without any FBS for 24 hours. Serum

was then added to the dishes and total RNA was harvested at the indicated times, following the protocol described in the RNA extraction, reverse transcription and qPCR section above.

#### *Nuclear and Cytoplasmic Extract Preparation and Western Blot Analysis*

Nuclear extracts were prepared directly from cells in the culture dish, using a previously described protocol [57]. Cells were lysed with 0.5% NP-40 diluted in PBS and substituted with protease and phosphatase inhibitors (2 µg/ml leupeptin and aprotinin, 1 µg/ml pepstatin, 0.2 mM phenylmethylsulfonyl fluoride [PMSF], 0.2 mM sodium orthovanadate, 2 mM sodium pyrophosphate, and 1 mM glycerophosphate). The soluble lysate was collected for the cytoplasmic extract, and the isolated nuclei were washed with PBS, and then with Dignam buffer A (10 mM HEPES pH 8.0, 10 mM KCl, 1.5 mM MgCl<sub>2</sub>, 0.5 mM dithiothreitol [DTT]). Nuclear extracts were prepared using Dignam buffer C (10 mM HEPES pH8.0, 420 mM KCl, 20% glycerol, 0.1 mM EDTA, 0.5 mM DTT, protease inhibitors, and phosphatase inhibitors), and then separated by polyacrylamide gel electrophoresis. To do this, 10µg of protein was loaded on a NuPAGE 4-12% Bis-Tris gel (Novex, Life Technologies) and run in 3-(N-morpholino)propanesulfonic acid (MOPS) buffer.

The blots were probed with the following primary antibodies: mouse anti-HA (12CA5 Roche), mouse anti-nucleolin (Active Motif), rabbit anti-SRF, rabbit-phosphorylated SRF (Ser103), and rabbit phosphorylated Elk-1 (Ser383). All rabbit antibodies were purchased from Cell Signaling in Danvers, MA. The appropriate HRP-conjugated antibody was then used to develop and analyze the blots (3, 3', 5, 5'-Tetramethylbenzidine, KPL). Images were obtained with the Visioneer One touch scanner 9420 using a gamma value of 1.0. All contrast adjustments were uniformly applied to each using Adobe Photoshop.

### *Statistical Analysis*

Each gene expression experiment was carried out with at least three independent biological replicates. The data was then averaged and the standard error of the mean calculated. With this data a 2-way ANOVA analysis or a student's T-test was performed depending on the data analyzed. This analysis was done using the Graph Pad Prism 5 software.

### **Results Aim 1**

#### *HeLa cell transient transfection*

To determine the immediate effects of RV-cyclin on gene expression, HeLa cells were transiently transfected with the pKH3A vector encoding HA-tagged RV-cyclin. Total RNA and nuclear extracts were collected at 0, 2.5, 4, and 8 hours post transfection, and qRTPCR and western blot analysis were performed on the samples, respectively. The results are shown in Figure 2.1. RV-cyclin mRNA is detectable in the first sample collected at 2.5 hours and steadily increased in abundance over the time course. HA-tagged RV-cyclin was observed in the nucleus at 4 hours and continued to be present in the nucleus for the duration of the experiment (Fig. 2.1). Both the qRTPCR analysis of RNA expression and the western blot analysis of the presence of HA-tagged protein in the nuclear extracts showed increasing RNA and nuclear protein levels after 2 to 4 hours after transfection. Significant RV-cyclin protein levels were present in the nucleus at 8 hours post transfection, so this time point was selected to test for its immediate effects on gene expression and for the collection of RNA from transfected HeLa cells to analyze this gene expression (Fig. 2.1).

The next transient transfection experiment analyzed levels of *CCND1*, *CDKN2D*, *FOS*, *EGRI*, and *JUN* transcripts close to RV-cyclin's appearance in the nucleus. From the time course analysis shown in Figure 2.1, it was determined the best time to collect total RNA for this

experiment was at 8 and 10 hours post transfection. HeLa cells were transfected with either the empty-vector control or the pH3A vector, and total RNA was collected.

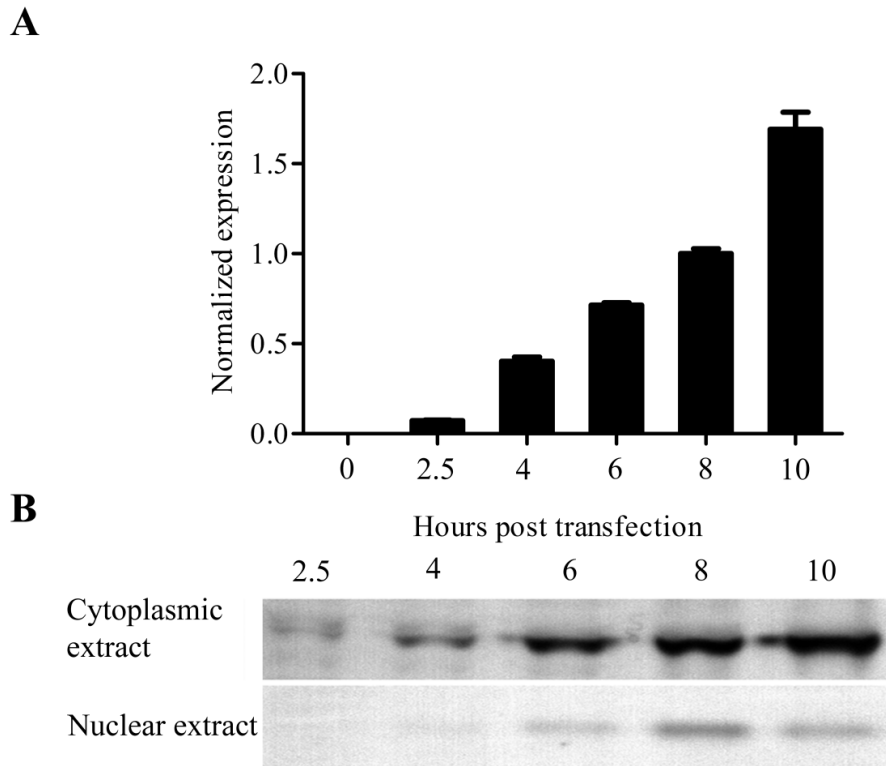


Figure 2.1 (A) qRT-PCR analysis of HA-RV-cyclin mRNA production in HeLa cells following transfection with the pH3A vector, which encodes RV-cyclin. This demonstrates RV-cyclin mRNA is produced shortly after transfection. Normalized fold change was determined using *GAPDH* as the reference gene. (B) SDS-PAGE and western blot analysis of HA-RV-cyclin protein production in nuclear and cytoplasmic extracts from HeLa cells following transfection. This demonstrates production of the RV-cyclin and its translocation to the nucleus, which correlates with mRNA production. Nucleolin was used as a loading control (data not shown).

*CCND1* was significantly up-regulated by the presence of RV-cyclin at both the 8 hour and 10 hour time points, with 5 and 6-fold activation above the control at 8 and 10 hours respectively (Fig. 2.2). *CDKN2D* was also up-regulated by RV-cyclin, but this activation was delayed, and was significant only at the 10 hour time point showing 13-fold above the control. RV-cyclin's influence on the serum response genes at 10 hours is similar to the cell cycle gene array results, which showed greater activation of *CDKN2D* by RV-cyclin than *CCND1* activation

by RV-cyclin (Fig 1.3). RV-cyclin's activation of *CCND1* and *CDKN2D* was not as dramatic as it was for the serum response genes.

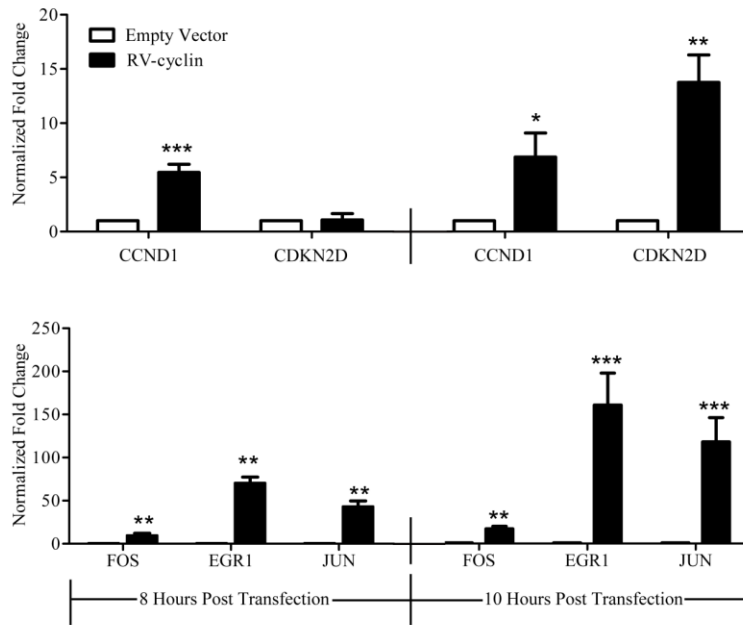


Figure 2.2 qRT-PCR analysis of the fold change in *CCND1* (cyclin C), *CDKN2D* (p19INK4d), *FOS*, *EGR1*, and *JUN* mRNA expression in HeLa cells, at 8 and 10 hours post-transient-transfection with RV-cyclin, showing RV-cyclin significantly activates all genes tested. The empty pKH3 vector was used as a control. \*\* indicates a p-value < 0.01 and \*\*\* indicates a p-value < 0.001 as calculated by a two-way ANOVA analysis of three independent biological replicates.

*FOS*, *EGR1*, and *JUN* were significantly up-regulated in expression by RV-cyclin when compared to the control vector transfection at 8 hours (Fig. 2.2). This up-regulation steadily increased, and the 10 hour time point showed even greater activation of serum response gene expression by RV-cyclin. *FOS* expression was activated 9-fold by RV-cyclin at 8 hours and 17-fold at 10 hours. Similar results were obtained for *EGR1* (60-fold at 8 hours and 70-fold a 10 hours), and for *JUN* (43-fold at 8 hours and 118-fold at 10).

#### *HeLa cells inducible for RV-cyclin expression*

Two genes were chosen for additional analysis with mutant RV-cyclin, *CDKN2D* and *EGR1*. Analysis of *EGR1* was done in the HCT116 cell line and will be described later. For

analysis of *CDKN2D* expression, HeLa cell lines inducible for wt RV-cyclin or either of the mutant RV-cyclins were employed [57]. This approach was taken because it was difficult to achieve consistent RV-cyclin expression between the wt and mutants using transient transfection. The inducible cell lines had the specific RV-cyclin under the control of a tetracycline-responsive promoter, and were created previously by Dr. Joel Rovnak. In this system, expression of *orf a* is under the control of the CMV promoter and an additional, up-stream tetracycline-responsive-element (TRE). When tetracycline is present, it binds to the TRE and blocks transcription of *orf a*, so no RV-cyclin is produced.

*CDKN2D* expression had never been analyzed in the inducible cells, so it was necessary to identify induction times and serum percentages that optimized RV-cyclin's induction of *CDKN2D*. Analysis of *CDKN2D* expression was done in un-induced cells induced for 48 hours, and "stably-induced" cells that had been induced for 2 weeks. Additionally all cell types were exposed to varying levels of serum (1%, 5%, and 10%). This was done in light of RV-cyclin's ability to substitute for serum in HeLa cell growth [57]. Cells in the appropriate induction-state were plated in 6 well plates. One day after plating, the serum concentrations were adjusted. The cells were incubated in their new serum conditions overnight, and total RNA was collected and analyzed by qRTPCR the next day.

The analysis showed that stably induced cells at 1% and 5% serum conditions had significant increases in *CDKN2D* transcription. RV-cyclin cells had 3.44 and 2.8 times above the un-induced levels under these serum conditions respectively (Fig 2.3). The activation of *CDKN2D* by stably induced RV-cyclin did not happen with 10% serum conditions. Furthermore, the 48-hour RV-cyclin-induced cells did not have significantly increased *CDKN2D* levels above the control under any of the serum conditions. The 5% serum conditions suggested

activation of *CDKN2D*, but the error did not lend itself to significance (Fig 2.3). From this experiment, it was determined that the best conditions to look for gene activation by RV-cyclin were 1% serum with stably-induced RV-cyclin.

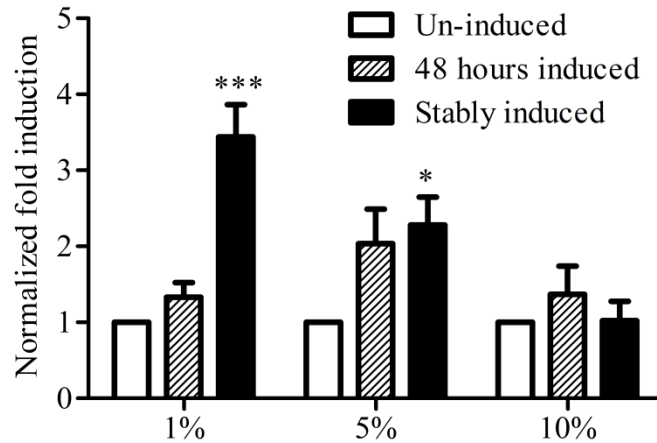


Figure 2.3 Normalized expression of *CDKN2D* in HeLa cells under various stages of induction for RV-cyclin and varying serum concentrations.  $\beta$ -actin was used as a reference gene for the normalization. Statistical analysis was performed using a two-way ANOVA, and \* represents a p-value <0.05 and \*\*\* represents a p-value of <0.001

Once the optimum conditions were determined, the mutants were analyzed for their ability to increase *CDKN2D* expression. We expected that both functional domains were required to enhance *CDKN2D* expression. Before analyzing *CDKN2D* gene expression, the RV-cyclin levels in the stably induced clones were compared. All clones were not expressing RV-cyclin in un-induced conditions, and after the stable induction period, they all were expressing RV-cyclin (Fig 2.4A). The RV-cyclin K80A/E111A clone was expressing 3.8 times less RV-cyclin than the wt or V260S mutant, and this was considered in the analysis of gene expression.

Neither the induced-RV-cyclin K80A/E111A mutant cell line nor the induced-RV-cyclin V260S mutant cell line had *CDKN2D* expression significantly above un-induced levels (Fig 2.4B). This is in contrast to the wt RV-cyclin-induced cells that had significant activation of *CDKN2D*.

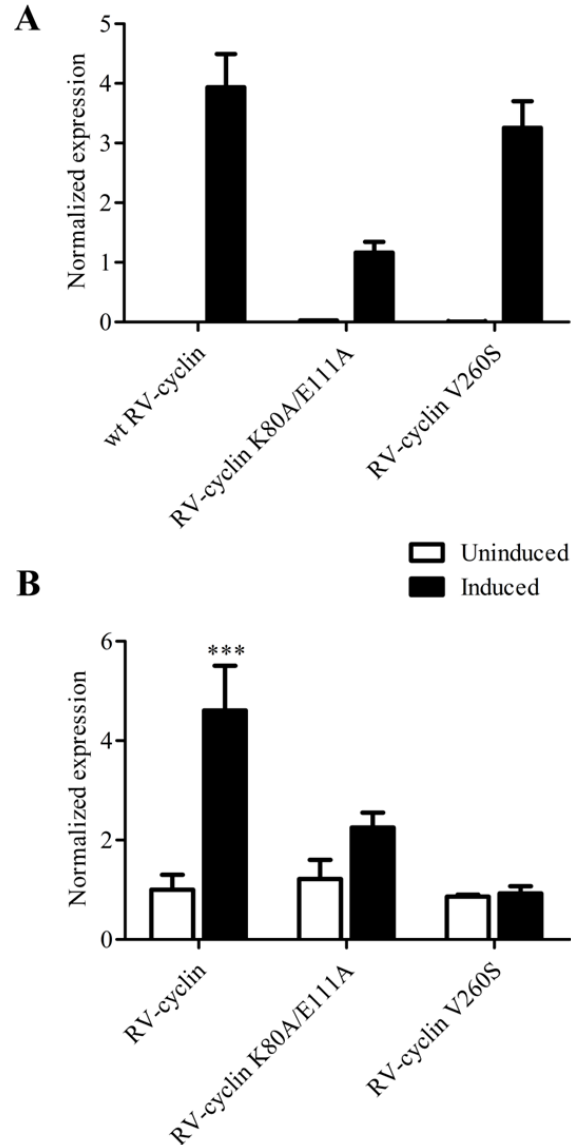


Figure 2.4 Normalized RV-cyclin expression (A) in wt RV-cyclin and mutant RV-cyclin-inducible HeLa cells in un-induced (white bars) and induced (black bars) conditions. Normalized expression of *CDKN2D* in these cells is shown in (B). Statistical analysis was done with a 2-way ANOVA, and \*\*\* represents a p-value<0.001. These data demonstrate RV-cyclin requires a functional cyclin box and activation domain to enhance *CDKN2D* expression.

These cells had 4.6 times greater expression of *CDKN2D* when normalized to  $\beta$ -actin than the un-induced cells (Fig. 2.4B). Additionally, the V260S mutant completely knocked out *CDKN2D* gene activation by RV-cyclin. This suggests a role for the RV-cyclin/TAF9 interaction in the

transcriptional regulation of *CDKN2D*. The RV-cyclin K80A/E111A mutant also didn't activate gene *CDKN2D* gene expression significantly. However, this clone is expressing less RV-cyclin than the wt RV-cyclin clone, so further analysis of mutant RV-cyclin was needed. In general, the inducible cell lines indicate that both functional domains of RV-cyclin are necessary to activate *CDKN2D* expression in HeLa cells.

#### *Serum Starvation and Restoration in HCT116 cells*

To further explore wt and mutant RV-cyclins in serum response gene activation, HCT116 cell lines stably expressing wt and mutant RV-cyclins were established. Control cells, clonal lines harboring an integrated empty vector, were also created. These cell lines were used to analyze RV-cyclin's influence on *FOS*, *EGR1*, and *JUN* during a genuine serum response. Expression of the serum response genes in the HCT116 clones was not altered by RV-cyclin until 30 or 60 minutes post serum stimulation (Fig. 2.5). There was no effect on any of the serum response genes by RV-cyclin under serum-starved conditions, or at 15 minutes post serum stimulation.

*FOS* expression was significantly up-regulated by RV-cyclin expression at 30 minutes post serum stimulation, and *EGR1* and *JUN* levels were not affected by RV-cyclin expression, until 60 minutes post serum stimulation (Fig. 2.5). At 30 minutes, control cells had activated *FOS* expression 52-fold above starved levels, whereas cells expressing wt RV-cyclin activated them to a much greater extent, 94-fold above control. In essence, HCT116 cells expressing RV-cyclin were able to enhance the serum response of *FOS* by 2-fold. By 60 min post serum stimulation, *FOS* activation was shutting down in both cell types, but the RV-cyclin cells still had significantly more transcripts (Fig 2.5). These data are a mean of three independent biological replicates with significance calculated by a two-way ANOVA analysis.

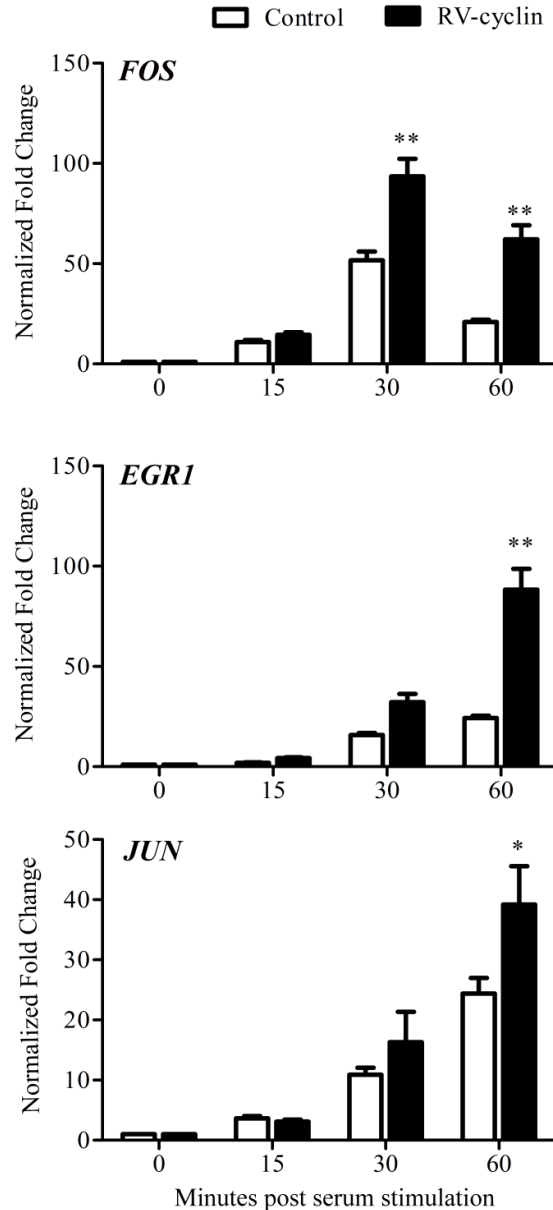


Figure 2.5 *FOS*, *EGRI*, and *JUN* expression in HCT116 control cells (white bars) and HCT116 cells expressing RV-cyclin (black bars) starved for 24 hours (0 minute time point), and then stimulated with serum for 15, 30, or 60 minutes. Total RNA was collected and relative gene expression quantified with qRT-PCR and *GAPDH* as a reference gene. These data demonstrate RV-cyclin enhances serum response gene expression, but only after a serum stimulation event.

*EGRI* and *JUN* were not activated significantly above control levels by RV-cyclin until the 60 min time point. At this time, *EGRI* was activated by RV-cyclin 83-fold above serum starvation levels. The control cells had activated *EGRI* only 24-fold above serum starvation

conditions at this time point, 1/4 of the stimulation observed with RV-cyclin. Similarly, *JUN* was activated 24-fold above starvation levels at 60 minutes, but the RV-cyclin expressing cells had levels 39-fold above starvation, showing RV-cyclin pushed activation of *JUN* 1.5 fold over control.

In order to evaluate the RV-cyclin functional domains required to enhance the expression of the serum response genes, HCT116 cell lines that stably expressed K80A/E111A or V260S mutant RV-cyclin were used (Fig 2.6).

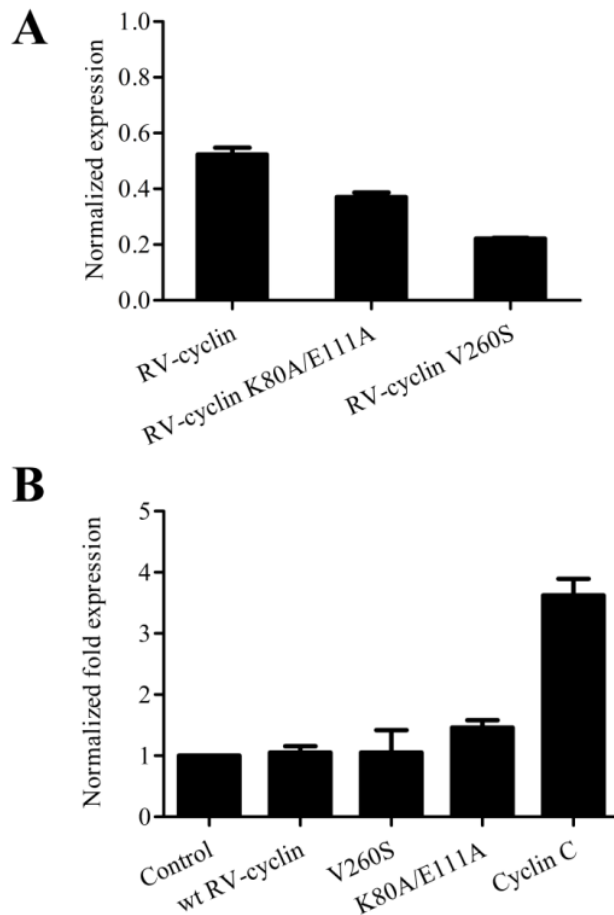


Figure 2.6 Normalized RV-cyclin expression (A) in the HCT116 stable clones, and normalized cyclin C expression (B) in the HCT116 stable clones. These data demonstrate the cell lines were comparable for future analyses.

Additionally, an HCT116 cell line that over-expresses cyclin C was established in order to determine the influence of increasing the level of a CDK8-activating cyclin. Figure 2.6 shows RV-cyclin (Fig 2.6 A) and cyclin C levels (Fig 2.6 B) in all of the HCT116 clonal lines. All RV-cyclin-expressing clones had levels of RV-cyclin expression, and were not statistically different, although the wt RV-cyclin appeared to be expressing more RV-cyclin than the two mutants. RV-cyclin expression does not up-regulate cyclin C, and the HCT116 cyclin C-over-expressing clone has about 2.5 times greater cyclin C mRNA expression than any of the RV-cyclin expressing clones or the control cells.

Sample collection and analysis of *EGR1* expression in the RV-cyclin mutant cell lines was done with a longer time course (0 to 150 minutes post serum stimulation) in order to assess effects on the duration of the serum response (Fig 2.7). *EGR1* was chosen, because it had the greatest activation by RV-cyclin in both the HeLa cell transient transfection (Fig 2.2) and the HCT116 serum stimulation experiment (Fig 2.5).

Similar to the previous time courses, wt RV-cyclin (Fig. 2.7 purple bars) enhanced the serum response of *EGR1* 2-fold above the control activation (Fig. 2.7 green bars) beginning at 60 minutes post serum stimulation (Fig 2.7). This enhancement continued to be statistically significant to 120 minutes post serum stimulation. The RV-cyclin K80A/E111A mutant, which does not bind CDK8 but can still interact with TAF9, did not show any enhancement of *EGR1* expression above the control cells at any time point (light blue bars Fig. 2.7). In fact, serum activation of *EGR1* expression was reduced by the K80A/E111A mutant RV-cyclin when compared to the control at 60 minutes post serum stimulation, pointing to a strong role for CDK8-binding in RV-cyclin's ability to enhance *EGR1* gene expression.

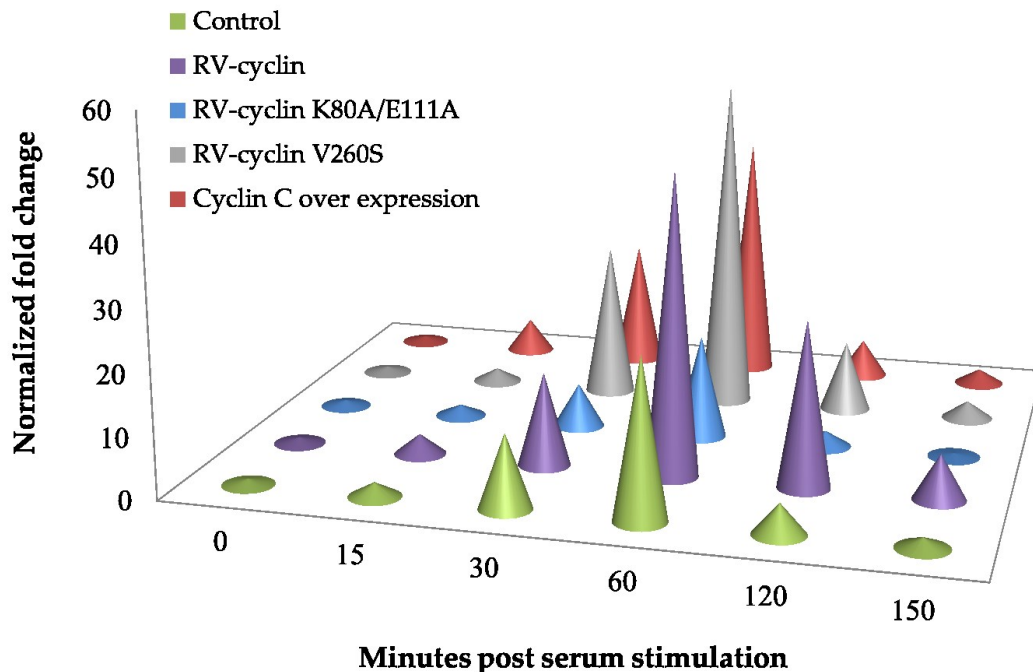


Figure 2.7 Normalized fold change in *EGR1* expression over time post serum stimulation in HCT116 cells, as calculated by qRT-PCR analysis and normalization to *GAPDH*. Relative expression was calculated using *GAPDH* as a reference gene. Control HCT116 cells are shown in green, and wt RV-cyclin expressing cells are shown in purple. The RV-cyclin K80A/E111A mutant, which binds TAF9 but does not bind CDK8, is shown in blue, and the RV-cyclin V260S mutant which binds CDK8 but not TAF9 is shown in grey. The HCT116 cells that are expressing 2.6 times the amount of cyclin C as control cells are shown in red. This data is a mean of three independent biological replicates.

The RV-cyclin V260S mutant, which maintains an interaction with CDK8 while not binding to TAF9, activated *EGR1* 12-fold significantly above control cells at 30 minutes and at 60 minutes post serum stimulation (Fig. 2.7 gray bars). However, unlike wt RV-cyclin, this mutant was unable to maintain *EGR1* activation above control levels out to 120 minutes post serum stimulation. This was very similar to the results in HCT116 cells over expressing cyclin C (Fig 2.7 red bars). These cells enhanced *EGR1* activation above the control at 30 min and at 60 min. The inability of the RV-cyclin K80A/E111A mutant to activate *EGR1* expression above control levels upon serum stimulation suggests CDK8 binding is absolutely required for RV-cyclin to enhance *EGR1* expression. Additionally the RV-cyclin-TAF9 interaction is important

in controlling the timing of the activation, and is required to extend the activation by RV-cyclin. The V260S mutant enhanced the *EGR1* serum response in a manner similar to cyclin C over-expression. This analysis shows that a functional interaction with both CDK8 and TAF9 is needed for wt RV-cyclin's regulation of *EGR1* transcription, and that the RV-cyclin is essentially functioning as an alternate CDK8-activating cyclin with an additional transcription AD. However, the AD only functions after transcription has been initiated in response to serum.

None of the RV-cyclin or cyclin C expressing clones had activated *EGR1* expression under starved conditions, and this was demonstrated for *FOS* and *JUN* as well (Fig 2.5). Therefore, we analyzed *EGR1* expression in wt RV-cyclin-expressing and control HCT116 cells under normal growing conditions without synchronization by serum deprivation. RV-cyclin was unable to increase *EGR1* expression without serum stimulation, as shown in Figure 2.8.

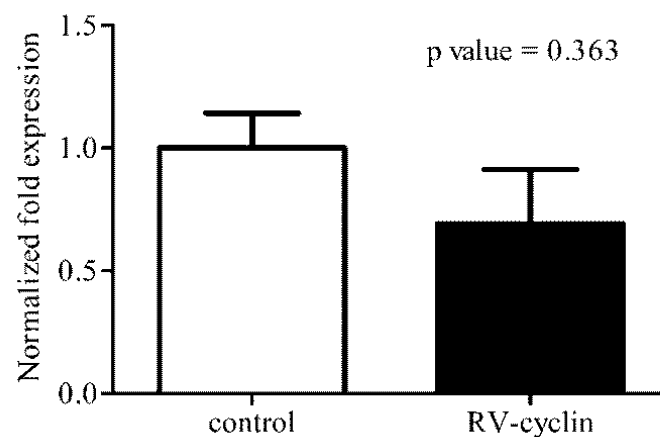


Figure 2.8 Normalized fold expression of *EGR1* in un-synchronized HCT116 cells grown in DMEM with 10% FBS. Statistical analysis was done using a student's T-test on three biological replicates.

The lack of enhanced expression in normal growing conditions (Fig. 2.8), and the time that it takes for RV-cyclin to enhance expression in response to serum (Fig. 2.5 and 2.7) suggests

that RV-cyclin requires functional transcription initiation before it can up-regulate serum-response gene expression.

### **Discussion Aim 1**

All three cell systems used to analyze gene expression in response to the presence of RV-cyclin gave valuable information. The transient transfection experiments in HeLa cells showed that the two selected genes from the 32-hour post-transfection gene array, *CCND1* and *CDKN2D*, were up-regulated at 10 hours post transfection as well. This was soon after RV-cyclin's arrival in the nucleus. Consistent with the gene array, *CDKN2D* activation was greater than *CCND1* activation.

The three chosen serum response genes were up-regulated at 8 hours and 10 hours post transfection. This activation occurred to a much greater extent than *CCND1* and *CDKN2D* activation by RV-cyclin. Due to the large difference between the two sets of genes, and how quickly RV-cyclin was translated and delivered to the nucleus, it is possible that the *CCND1* and *CDKN2D* up-regulation might be a downstream result of RV-cyclin's function on the serum-response-gene products [152, 158]. A way to test this hypothesis in the future would be to shut off translation and see if RV-cyclin is still able to activate *CDKN2D* expression. Alternatively, this difference could be due to intrinsic differences within each gene's promoter, and this will be discussed in the following chapter. Even though the regulation of *CCND1* and *CDKN2D* expression by RV-cyclin might not be direct, the cell cycle gene array and qRTPCR confirmation demonstrates that these genes can be used as markers of RV-cyclin functionality.

The HeLa inducible system was chosen for analysis of mutant RV-cyclin on *CDKN2D* activation, but before this was done, wt RV-cyclin's function on *CDKN2D* activation was characterized. This process uncovered interesting data. RV-cyclin was unable to activate

*CDKN2D* in cells growing in normal conditions either when it was stably-induced, or transiently induced for 48 hours. When the stably induced cells were deprived of serum, RV-cyclin was able to active *CDKN2D* gene expression, and this activation increased as serum levels were reduced. These data suggest that RV-cyclin requires environmental queues to turn on genes before it can enhance expression. The serum concentration reduction might mimic stress induced by transient transfection, and that is why RV-cyclin activated *CDKN2D* expression in both the transient transfection and in inducible cells at low serum concentrations. This is similar to the serum-starvation/restoration experiments in the HCT116 cells. The mutation analysis revealed that both interaction with CDK8 and TAF9 is required for RV-cyclin to fully enhance *CDKN2D* expression.

RV-cyclin's presence in the HCT116 cells under normal growing conditions and under serum starvation did not yield a change in serum-response gene expression, similar to *CDKN2D* expression. Serum starvation and subsequent serum stimulation were required to see a change in *FOS*, *EGRI*, and *JUN* by RV-cyclin, suggesting that RV-cyclin alone is not able to activate serum response gene expression in HCT116 cells. This poses the question as to how real the activation might be in WDS tumor development, and the Orf b protein might be the answer to this question. Orf b constitutively activates the AKT pathway [55], which can cross-talk with the MAPK pathway, and regulate serum response gene expression [162, 163]. This interaction may stimulate RNA Pol II initiation, and then RV-cyclin might specifically enhance expression of certain genes turned on by the pathways the Orf b protein stimulated.

The control cells had consistent timing of *FOS*, *EGRI*, and *JUN* activation with what has been previously published in the literature. *FOS* typically is activated before *EGRI* and *JUN*, with the peak transcript levels at 30 min. *EGRI* and *JUN* transcript levels peak between 30 min

and 60 minutes post serum stimulation, and are beginning to level off or decrease at 60 minutes [153, 164-166].

*EGR1* was chosen for further analysis, as its expression was the most responsive to RV-cyclin in the transient transfection and in the initial serum starvation/stimulation time course. RV-cyclin maintains the *EGR1* serum response well after the control cells are shutting down *EGR1* transcription. The interaction with CDK8 is completely necessary for the enhancement, and the K80A/E111A mutant actually reduces *EGR1* activation at 60 min when compared to control cells. Furthermore, the K80A/E111A mutant RV-cyclin was a very difficult clone to produce, suggesting that expression of this mutant was negative for growth selection in HCT116 cells. Many clones were produced that had integrated RV-cyclin K80A/E111A DNA, but only one out of the 300 or more clones screened actually expressed the mutant protein. This effect may be due to the apparent down-regulation of these genes that are necessary for proliferation.

Previous work has shown that the isolated RV-cyclin AD can block TAF9-dependent transcription activation and this block can be overcome by the over-expression of exogenous TAF9 [61]. The possible sequestration of TAF9 by the RV-cyclin K80A/E111A mutant may mimic this interference with TAF9 contact by cellular transcription factors, or may lead to incomplete formation of TFIID at important loci. However, more experimental evidence is needed to make this conclusion.

Consistent with cyclin C over-expression, the RV-cyclin V260S mutant enhanced *EGR1* expression significantly above the control at 30 minutes; this was before the effects of wt RV-cyclin were apparent. In addition to dampening the *EGR1* response in the beginning, the TAF9 interaction also appears to be important for extending the serum response enhancement by wt

RV-cyclin. The wt RV-cyclin cells were able to double the time that *EGR1* was elevated above control, cyclin C, or V260S levels.

The interaction with CDK8 is necessary to enhance expression of both *EGR1* and *CDKN2D*, but the role of the RV-cyclin/TAF9 interaction is less clear. Although the TAF9 interaction is required to activate *CDKN2D* in stressed, inducible HeLa cells, this interaction only regulated the enhancement of *EGR1* in the serum response. An explanation for this might come from the inherent differences between the two cellular systems employed. For example, the experimental set up with serum stimulation in the HCT116 cells allowed an observable burst in *EGR1* gene expression, which could be measured in a relatively short time course. If we would have looked at one time point only, i.e. the 120 min time point, we would have come to the same conclusion as we did with *CDKN2D*, saying that both functional domains are needed for enhancement. Perhaps the TAF9 interaction does the same thing with *CDKN2D* gene expression as it does with *EGR1*, and the system that we used to measure *CDKN2D* expression didn't allow us to see the TAF9 regulation as clearly. The difference could also lie within the promoter elements required for *EGR1* and *CDKN2D* expression, and the components of TFIID that are recruited to each gene's promoter.

The timing and the nature of the serum-response have been well characterized in many different cell lines. Accordingly, the nature of *FOS*, *EGR1*, and *JUN* serum response in the control HCT116 cells correlates with what has been published. Activation of all three genes levels off and begins to diminish between 30 min and 60 min post serum stimulation [153, 164-167]. In light of this information RV-cyclin's ability to double the amount of time *EGR1* transcripts are present in cells is a significant deregulation of the serum response. All three serum response genes tested are well-characterized proto-oncogenes, and are up-regulated in

many tumors [151, 152, 154, 159]. RV-cyclin's up-regulation of these genes could contribute to development of WDS. Furthermore, no other known cyclin, either cellular or viral, contains an activation domain in addition to a cyclin box. Therefore the mechanism by which RV-cyclin enhances transcript levels needs to be investigated.

## CHAPTER 3—AIM 2: DETERMINE IF GENE ACTIVATION BY RV-CYCLIN IS DUE TO ENHANCED TRANSCRIPTIONAL PROCESSIVITY

### **Introduction Aim 2**

RV-cyclin's activation of the serum response genes, even though it involves both functional domains, could be due to a number of different reasons. First of all, RV-cyclin binds PP2A, an important phosphatase in the MAPK signaling pathways, which controls expression of these genes [168-171]. Due to PP2A's involvement in these pathways, it is possible RV-cyclin was interacting with PP2A to enhance transcription initiation. Although the timing of serum response gene activation did not suggest this was happening, it was still important to investigate this possibility.

The four mammalian mitogen-activated protein kinase pathways (MAPK pathways) control expression of the serum response genes, *FOS*, *EGR1* and *JUN* [172, 173]. A diagram of the pathway controlling *FOS* and *EGR1* transcription is shown in Figure 3.1. When these pathways are activated by growth factors at the cell surface, a kinase-cascade is initiated resulting in phosphorylation of transcription factors [173, 174]. These “activated” transcription factors bind to specific promoter elements to initiate RNA Pol II transcription [173]. For the immediate early genes *FOS* and *EGR1*, the activated MAPK pathway leads to phosphorylation of the extracellular signal-regulated kinases 1 and 2 (ERK1/2), and the p90RSK complex [172, 175-177]. Activated ERK1/2 phosphorylates the transcription factor Elk-1, and the p90RSK complex phosphorylates SRF. Together, these activated transcription factors bind to the promoter of *FOS* and *EGR1* to form the ternary complex factor (TCF) [172, 175]. The TCF promotes recruitment of components needed for RNA Pol II transcription initiation, like TFIID, and the mediator

complex [172]. It does this by promoting phosphorylation of p300, which results in acetylation of the surrounding histones and activation of transcription [172, 175].

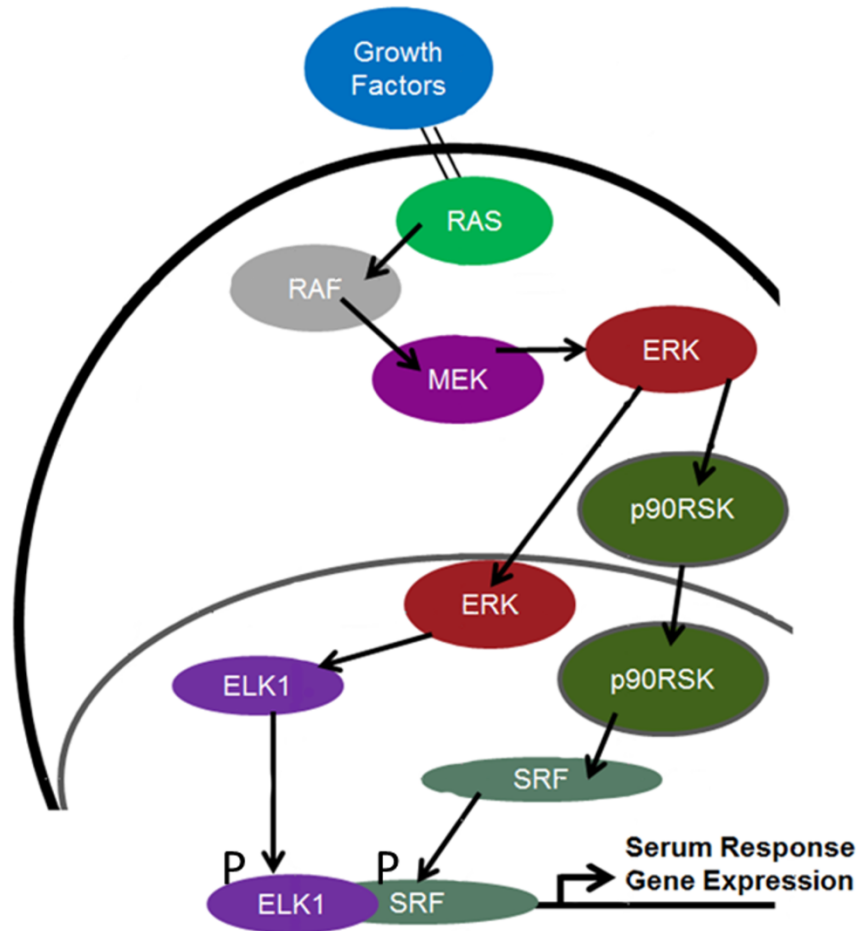


Figure 3.1 A diagram of the MAPK pathway stimulation by growth factors in serum. The end result of the pathway is phosphorylation of Elk-1 and SRF, which bind to the promoters of genes to initiate transcription.

In addition to possible activation of the MAPK pathway, RV-cyclin could also be affecting mRNA decay. Inhibition of XRN1-mediated mRNA decay is a common mechanism employed by a number of cytoplasmic viruses to modulate host-cell and viral transcription [178]. Due to the amount of time RV-cyclin was able to activate gene expression, an inhibition of mRNA decay of the serum response genes was a possibility. In order to explore this possibility,

an actinomycin D transcriptional shut-off assay was used to analyze serum response mRNA decay.

The timing of its function in the serum response and the nature of its binding partners suggested that RV-cyclin was acting directly at the gene locus, after transcription initiation. In order to test this possibility, two assays were employed: the nuclear run-on assay and chromatin-immunoprecipitation. The nuclear run-on assay was used to measure the rate of RNA Pol II transcription after 10 min of serum stimulation *in vivo*. This assay was used by Donner and others in 2010 to analyze the rate of RNA Pol II transcription elongation [121]. The nuclei were harvested after stimulation, and initiated Pol II was allowed to run-on *in vitro* in the presence of biotinylated UTP and with sarcosine to block initiation of new rounds of transcription. The biotinylated transcripts were collected with streptavidin beads and quantified with qRT-PCR. If more transcripts were produced from one cell type, say the RV-cyclin-expressing cells, there would be more biotinylated transcripts in the RV-cyclin-expressing cells than in the control cells during the linear phase of the run-on reaction. This technique allows the measure of the rate of RNA Pol II transcription elongation across the *EGR1* locus.

ChIP was used to measure the occupancy of tri-methyl histone H3 lysine 4 (tri-methyl H3K4), RNA Pol II, CDK8 and HA-tagged RV-cyclin across the *EGR1* gene locus. *EGR1* was chosen for the analysis because it was the most activated by RV-cyclin, and was used for characterization of the RV-cyclin mutants in the extended time course. The tri-methyl H3K4 mark is associated with open/active gene transcriptional start sites, and can be added to lysine 4 by any one of the following methyltransferases: MLL1, MLL2, MLL3, MLL4, MLL5, SET1a, SET1b, and ASH1 [87, 179]. This mark is associated with the transcriptional start site of active genes, and, although the exact timing of this mark's placement is under debate, it is thought that

it is required for early transcriptional events. These events include either transcription initiation and TFIID recruitment or recruitment of the Paf1 complex and capping enzymes necessary for elongation [87, 179].

The polyclonal RNA Pol II antibody used bound all of the RPB1 subunit of the holoenzyme, regardless of the phosphorylation state of the carboxy-terminal domain. RNA Pol II occupancy is generally greater at promoter regions of genes, indicating a paused polymerase waiting for the elongation signals [180]. Elongating RNA Pol II can be found in the open reading frames of genes, but to a much lower extent than when it is paused at the promoter, because the elongating polymerases are moving rapidly through this gene region [180]. Higher levels of RNA Pol II in the open reading frame correspond to greater elongation rates. CDK8 occupancy is also found across the entire gene locus of *p21*, *FOS*, *EGR1*, *EGR2*, and *EGR3* under the appropriate stimulation conditions. CDK8 is increased at the promoter, when compared to other gene regions [121, 122]. Finally, RV-cyclin had never been detected at the *EGR1* gene locus by ChIP before, so an anti-HA antibody was employed to detect HA-tagged RV-cyclin that might be bound to DNA.

### **Hypothesis Aim 2**

Due to the requirement of CDK8 kinase activity for efficient transcription elongation of the serum response genes, it was hypothesized that RV-cyclin's interaction with CDK8 enhances *EGR1* expression during the serum response by enhancing transcription elongation. For this reason, it was expected that RV-cyclin would not alter the phosphorylation state of Elk-1 or SRF, and would not inhibit mRNA decay. However, RV-cyclin would enhance RNA Pol II occupancy at the *EGR1* gene locus. Additionally, it was proposed that RV-cyclin would not alter

the amount of CDK8 at the locus and function by enhancing CDK8 kinase activity, and HA-RV-cyclin would be present at the locus and correlate with CDK8 occupancy.

## **Materials and Methods Aim 2**

### *Analysis of Elk-1 and SRF phosphorylation*

HCT116 cells were serum starved and stimulated as described in the materials and methods section for Aim 1. Nuclear extracts, SDS-PAGE and western blot analyses were also prepared as described in Aim 1.

### *Actinomycin D transcriptional shut off and mRNA decay analysis*

Sixty-minute serum-stimulated HCT116 cells were subjected to media containing 5 µg/ml of actinomycin D, and total RNA was collected at various time points post treatment. qRTPCR analysis was performed on *FOS*, *EGR1*, and *JUN* using the same protocol and primer sets described in Aim 1. The  $\frac{1}{2}$  life of each measured transcripts was calculated, and compared using a 2-way ANOVA analysis.

### *Nuclear Run-On*

Serum-deprived HCT116 cells were stimulated for 10 minutes or left un-treated prior to one wash in PBS, and subsequent lysis of the plasma membrane with 0.5% NP-40 in cold PBS. The isolated nuclei were washed with reaction buffer (20 mM Tris-HCL pH 7.5, 10mM MgCl<sub>2</sub>, 150 mM KCl), then re-suspended in cold reaction buffer with 50% glycerol to a final concentration of  $5 \times 10^8$  nuclei/ml. The final preparation was snap frozen in liquid nitrogen, and then stored at -80°C.

The *in vitro* run-on was carried out as follows:  $5 \times 10^6$  nuclei (10 µl of suspension) were placed in 30 µl of supplemented reaction buffer (reaction buffer plus 1 mM NTPs (ATP, CTP, and GTP), 0.4 mM Biotin-16-UTP (Epicenter), and 0.1% sarcosine), and pre-incubated on ice for

15 minutes. Run-on occurred at 37°C under constant shaking for 5 min and was terminated by snap freezing. Total RNA was extracted and biotinylated transcripts were collected using streptavidin Dynabeads (Invitrogen). cDNA was made from the entire quantity of biotinylated RNA obtained using the Verso kit described in Aim 1. Similarly, qPCR analysis was performed using the protocol and *EGR1* primer set described in Aim 1, which measures spliced transcripts. An *EGR1* primer set (ChIP primer set 907), which measured un-spliced *EGR1* transcripts was also used for analysis, but very little un-spliced, biotinylated, *EGR1* transcripts were obtained (Data not shown).

#### *Chromatin Immunoprecipitation (ChIP)*

A combination of two previously published ChIP protocols was used to produce the protocol for the assay [87, 181].  $1 \times 10^7$  serum-starved or appropriately serum-stimulated HCT116 cells, or transiently transfected HeLa cells were fixed by adding 37% formaldehyde to the media in the cell culture dish to a final concentration of 1%. Crosslinking was carried out for 15 minutes on a rocker at room temperature then quenched by adding 2 M glycine to a final concentration of 125 mM to the fix media in the plates. Fixed cells were scraped from the dishes in cold PBS containing 0.5% NP-40, and pelleted by centrifugation at  $1,500 \times g$ , 4° C for 15 minutes. The fixed cells were re-suspended in nuclei lysis buffer (50 mM Tris-HCl pH 8.0, 10 mM EDTA, and 1% SDS), using a volume of buffer that was 4 times the amount of the pellet size. The suspension was divided into 1ml aliquots, and each aliquot was subjected to sonication using the VirTis virsonic 600 ultrasonic cell disrupter and a microtip. Aliquots were sonicated at amplitude 4.5 for 12, 25 second pulses in a salt water: alcohol: ice bath, with a 30 second rest in between each pulse. This consistently gave an average fragment size between 200 and 500 b (Fig. 3.2). The aliquots for each sample were combined and frozen at -80°C to precipitate the

SDS, and a 25  $\mu$ l of the aliquot was saved for gel analysis to confirm the appropriate fragment size was achieved (Fig. 3.2).

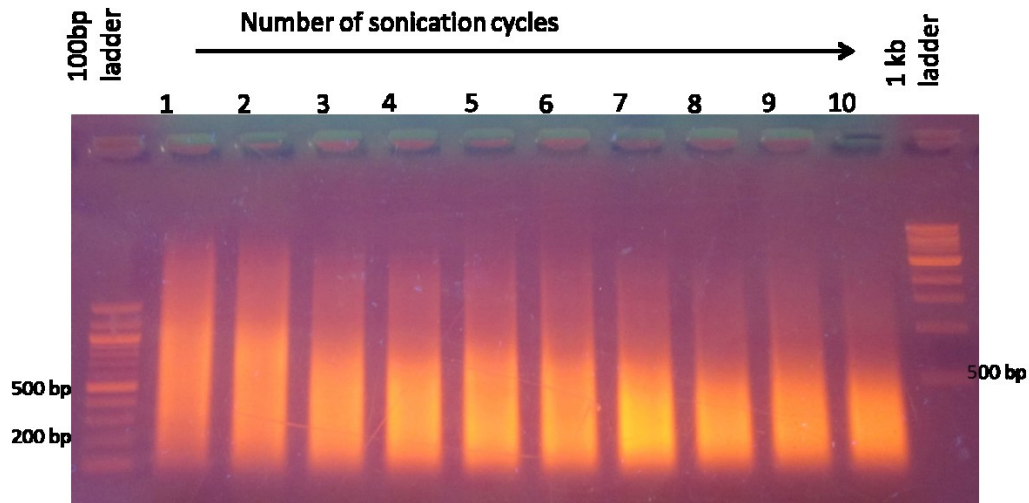


Figure 3.2 An example of the DNA fragmentation of cross-linked DNA used for subsequent ChIP analysis. The image of the agarose gel after electrophoresis of the purified, sonicated DNA shows an average DNA fragment size between 200 to 500 bases in length after 10 rounds of sonication. Fragmentation was carried out using the VirTis virsonic 600 ultrasonic cell disrupter and microtip. For this image, a 25  $\mu$ l aliquot was taken after each round of sonication on cross-linked HCT116 control cells. The material was reverse cross linked, and digested with proteinase K and RNase A. It was then subjected to phenol: chloroform extraction and ethanol precipitation before being run on a 1% agarose gel in Tris-acid EDTA buffer (TAE) at 90 volts for 60 minutes. The gel was stained with ethidium bromide and subjected to UV light for the detection of nucleic acids.

Fragment size analysis occurred by reverse cross-linking the sonicated DNA at 65° C for an overnight period in the presence of 20  $\mu$ g of proteinase K with a mineral oil overlay to prevent evaporation of the small sample size. Reverse cross-linked samples were digested with 20  $\mu$ g (UNITS?) of RNase A, and then centrifuged at 20,000 x g for 20 minutes at 4°C. DNA was extracted from the supernatant with phenol: chloroform (1:1) followed by a chloroform wash before precipitation with ethanol at -20° C for one hour. The DNA was washed once in 75% ethanol before re-suspension in 25  $\mu$ l of DEPC treated H<sub>2</sub>O. The DNA was mixed with 6x loading dye to a final concentration of 1x and loaded on a 1% agarose gel in TAE. The

fragments sizes were separated on the gel using electrophoresis at 70 volts for 55 minutes in TAE running buffer. The gel was pre-mixed with ethidium bromide allowing a picture to be taken with UV trans-illumination directly after the run was done. An example gel is shown in Figure 3.2 showing the fragment sizes achieved with increasing rounds of sonication.

For ChIP the sonicates were thawed, and the precipitated SDS was pelleted by centrifugation at 21,000 x g for 20 minutes at 4°C. The OD260/280 ratio was taken by diluting 2 µl of sonicate in 100 µl of 10 mM Tris buffer at pH8, and the DNA concentration calculated. The material was diluted to 0.2 mg/ml DNA in dilution buffer (16.7 mM Tris-HCl pH 8.0, 167 mM NaCl, 1.2 mM EDTA, 0.01% SDS, and 1.1% Triton X-100), and separated into 1 ml aliquots, which were frozen at -80°C or used directly for ChIP analysis.

Each aliquot was pre-cleared overnight using 2 µg of normal rabbit serum (Cell Signaling, Danvers MA), 2 µg of normal goat serum (collected from a goat) and 60 µl of protein G sepharose (GE Life Sciences). A 10 µl aliquot of the pre-cleared sonicate was taken at this time and frozen at -20° C as the 5% input sample. The remaining material (990 µl) of the pre-cleared sonicates was then incubated with one of the antibodies listed in table 3.1, and 25 µl of blocked, magnetic protein G Dynabeads (Invitrogen) with rotation overnight at 4°C. The beads were blocked using 1 mg of BSA and 500 µg of a sonicated calf thymus DNA.

Table 3.1 Antibodies used in ChIP

<b>Antibody</b>	<b>Amount used in ChIP with 0.2mg of chromatin</b>	<b>Manufacturer</b>
Anti-trimethyl histone 3 lysine 4 (C42D8)	2 µl of undiluted stock	Cell Signaling Technology
Anti-RNA Pol II (H-224) SC-9001	2 µg	Santa Cruz Biotechnology
Anti-CDK8 (C-19) SC-1521	3.6 µg	Santa Cruz Biotechnology
Anti-HA (HA.11 clone 16B12)	1:150 dilution suggested amount for IP	Biolegend/Covance
Normal Rabbit Serum	2-3.6 µg	Cell Signaling Technology

The bead-bound, immunoprecipitated complexes were washed once for 10 minutes on rotation at 4°C in each the following buffers: low salt wash (0.1 % SDS, 1 % Triton X-100, 1 mM PMSF, 20 mM Tris-HCl pH 8.0, 150 mM NaCl, 2 mM EDTA), high salt wash (0.1% SDS, 1% Triton X-100, 1 mM PMSF, 20 mM Tris-HCl pH 8.0, 500 mM NaCl, 2 mM EDTA), and LiCl wash (10 mM Tris-HCl pH 8.0, 0.25 M LiCl, 1% NP-40, 1% sodium deoxycholate, 1 mM EDTA, 1 mM PMSF). The beads were then washed twice with TE wash (10 mM Tris-HCl pH 8.0, 1 mM EDTA, 1 mM PMSF). Complexes were eluted from the beads using 500 µl of 50 mM Tris-HCl pH 8.0, 10 mM EDTA, 1% SDS at 65°C for 30 minutes.

The 5% input samples, taken before the immunoprecipitation, were defrosted during the elution, and supplemented with 500 µl of elution buffer. The 5% input samples were then treated the same way as the IP samples for the remaining procedure. 20 µl of 5M NaCl was added all samples, and then they were subjected to reverse cross-linking at 65°C for overnight. The reverse cross-linked material was digested with RNase A (20 µg) at room temperature and proteinase K (20 µg) at 45° C before phenol: chloroform extraction, and an additional chloroform wash.

DNA was precipitated with ethanol and sodium acetate (0.3 M final concentration) at -20° C overnight. Precipitated DNA was collected by centrifugation at 20,000 X g for 30 minutes at 4° C. The DNA pellet was washed once with 75% ethanol, and then dissolved in 200 µl of TE buffer. The DNA required one night at 4° C to dissolve completely. 1 µl of ChIP or 5% input DNA was then analyzed with qPCR analysis in triplicate reactions. Each reaction in a triplicate had a 25 µl final volume using Sybr Green (Bio Rad) and the primer sets indicated in Table 3.2. The master mix was prepared with 12.5 µl of Sybr green, 11 µl of DEPC treated H<sub>2</sub>O, 0.25 µl of 10mM forward primer, 0.25 µl of 10 mM reverse primer, and 1 µl of DNA.

Table 3.2 Primer sets used for ChIP analysis

<b><i>EGR1</i> primer set</b>	<b>Forward primer</b>	<b>Reverse Primer</b>
-811	5'-AGTGGCCGTGACTTCCTATCC-3'	5'-CTCGATCTATGGCACGGTGTC-3'
-109	5'-CGGGCGCTGTCGGAT-3'	5'-TCTGGAACGGCACGGGT-3'
-34	5'-ACCCGTGCCGTTCCAGA-3'	5'-ATCTCTCGCGACTCCCCG-3'
907	5'-AGGGCTTGTTTTGATGAGCG-3'	5'-GCTAGTGC GCGCCCC-3'
1374	5'-CTGCCCCCATCACCTATACT-3'	5'-CCACAAGGTGTTGCCACTGTT-3'
5247	5'-CAGAGGAACAATGAGGTATCCCC-3'	5'-CACTTCACTCAGGGCCTGATAAC-3'

These primer sets were previously used in ChIP analysis by Donner and others 2010 [121]

The same 3-step protocol described for amplifying cDNA in Aim 1 was used for qPCR analysis of the ChIP, but the annealing temperature was adjusted to the optimized temperature for each primer set. The optimum temperature was obtained by using a temperature gradient with HeLa DNA as a template. The *EGR1* -811 and -34 primer sets were amplified with an annealing temperature of 60° C, the 1374 and 5247 primer sets used an annealing temperature of 62° C, and the 907 and -109 primer sets used an annealing temperature of 64° C. % Input was calculated using c(t) values obtained in the qPCR analysis and the equation ( $\% \text{ Input} = 100 * 2^{(\text{adjusted input c(t) value} - \text{IP c(t) value})}$ ). The adjusted input c(t) value was obtained by subtracting 4.32 c(t) values from the average c(t) value obtained from the 5% input sample (following the log scale used in qPCR analysis). The primers used for analysis had been used previously in ChIP analysis of the *EGR1* locus, and the number designation of the primer set represents the *EGR1* position of the base in the middle of the amplicon relative to the *EGR1* transcription start site [121].

## **Results Aim 2**

### *Analysis of phosphorylated Elk-1 and SRF*

Cytoplasmic and nuclear extracts were prepared from serum starved or stimulated HCT116 cells to observe levels of SRF, phosphorylated SRF, and phosphorylated Elk-1 in

response to RV-cyclin expression. These extracts were analyzed by western blot with the appropriate antibodies (Fig 3.3).

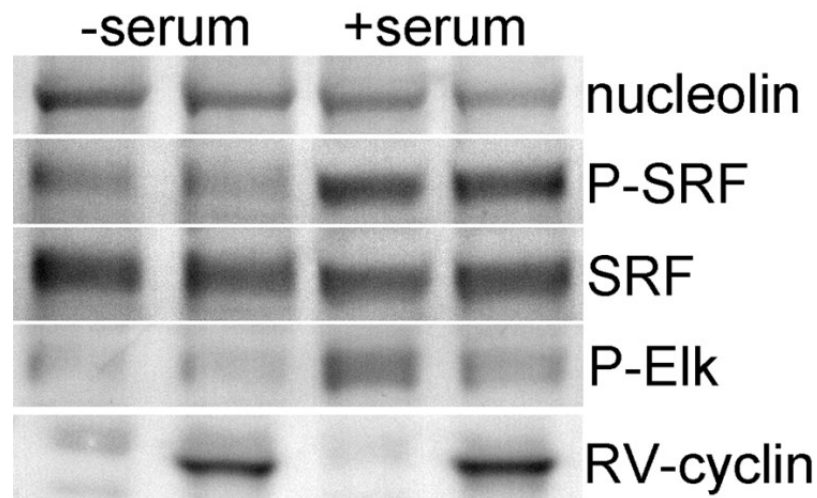


Figure 3.3 Western blot analysis of SRF, phosphorylated SRF, and phosphorylated Elk-1 in nuclear extracts from control and RV-cyclin expressing HCT116 cells in serum-starved or serum-stimulated conditions. Nucleolin was used as a loading control. This blot is a representative blot of six biological replicates, and demonstrates RV-cyclin does not cause aberrant phosphorylation of two transcription factors that control serum response gene expression. These data suggest RV-cyclin activates serum response gene expression in a manner outside of transcription factor phosphorylation.

As expected, control and RV-cyclin-expressing cells had similar levels of the unphosphorylated forms of Elk-1 and SRF under both serum-starved and serum-stimulated conditions, and Elk-1 and SRF were phosphorylated under serum-stimulation conditions (Fig 3.3). Levels of phosphorylation were equivalent or even diminished in RV-cyclin-expressing cells compared to control cells, and showed that RV-cyclin's enhancement of serum-response gene expression was not due to increases in these activated transcription factors. Enhancement occurs after transcription factor phosphorylation and initiation of serum-response gene expression. The depletion in ELK1 phosphorylation in RV-cyclin expressing cells could have been due to a loading error, as observed by the slight decrease in the intensity of the loading control, nucleolin.

*Actinomycin D transcriptional shutoff*

The half-life of all measured transcripts showed no significant difference between the HCT116 control and the HCT116 wt-RV-cyclin cells (Fig 3.4).

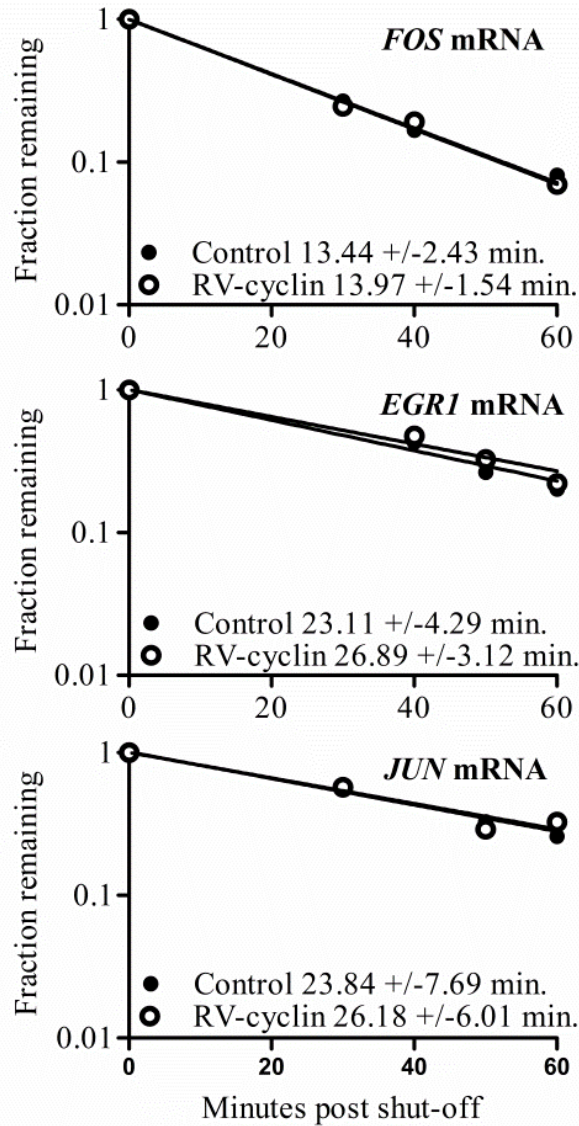


Figure 3.4 Actinomycin D shut-off, and mRNA decay analysis of *FOS*, *EGR1*, and *JUN* transcripts in HCT116 control and wt RV-cyclin expressing cells. The half-life of each transcript with corresponding standard deviation is indicated in the legend of each graph. The graphs represent one of three independent experiments used to calculate the half-life of each transcript, and these data suggest RV-cyclin does not alter the rate of serum response gene mRNA decay, eliminating another possible mechanism for RV-cyclin's activation of these transcripts.

The *FOS* half-life was 13.44 +/- 2.34 minutes in control cells and 13.97 +/- 1.54 min in RV-cyclin expressing cells. This was comparable to previously published values [146, 182, 183]. Similarly, in control cells *EGR1* had a half-life of 23.11 +/- 4.29 min and *JUN* had a half-life of 23.84 +/- 7.69 min. The half-life of *EGR1* in wt RV-cyclin expressing cells was 26.89 +/- 3.12, and *JUN* had a half-life of 26.18 +/- 6.01 minutes (Fig 3.4).

### Nuclear Run-on

Serum-starved or 10-minute serum-stimulated RV-cyclin-expressing cells were used for the nuclear run-on analysis (Fig. 3.5).

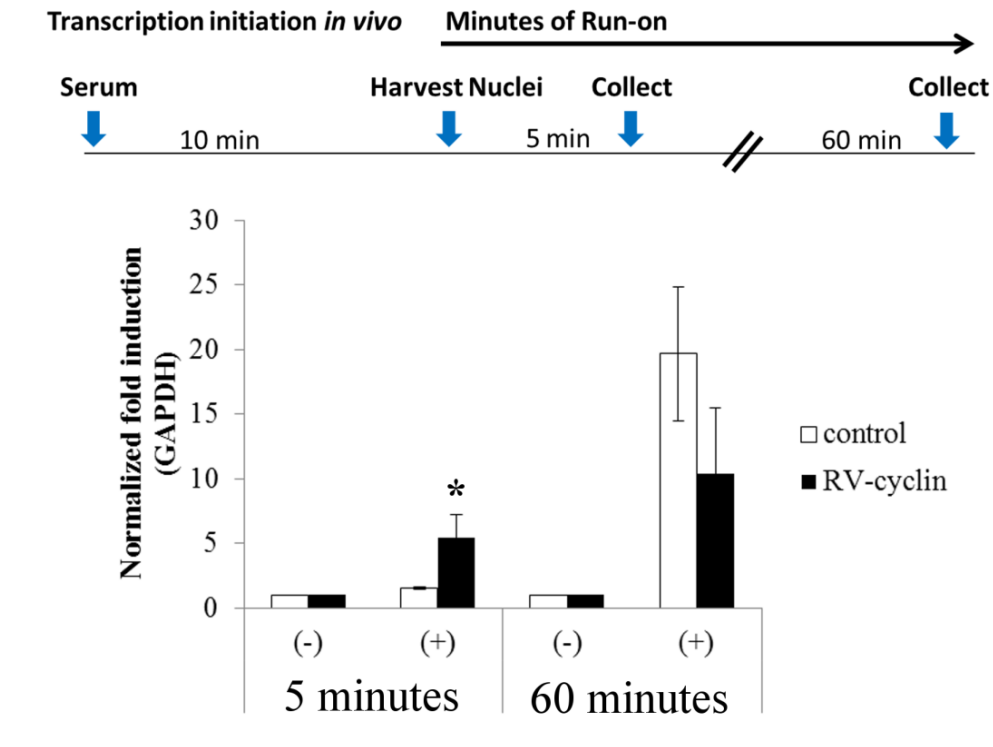


Figure 3.5 Nuclear run-on analysis of *EGR1* transcription elongation. A diagram of the analysis is found in the top panel. Nuclei were isolated from control HCT116 cells (white bars) and RV-cyclin-expressing HCT116 cells (black bars). The cells were exposed to either serum-starvation conditions (-) or serum-starvation conditions followed by a 10 minute serum-stimulation (+) before isolation of the nuclei and an in vitro run-on for either 5 minutes or 60 minutes. The \* indicates a p-value < 0.05, and this was calculated using a two-way ANOVA analysis of three independent experiments. These data demonstrate RV-cyclin enhances transcription elongation of the serum response genes.

The nuclei isolated from the serum-starved control and RV-cyclin expressing cells did not produce any spliced, biotinylated *EGR1* transcripts, and the serum-stimulated nuclei from both cell types produced biotinylated *EGR1* transcripts (Fig 3.5). However, the nuclei from the RV-cyclin-expressing cells produced significantly more biotinylated *EGR1* transcripts than control nuclei after 5 minutes of run-on *in vitro*. The control cells did not produce significant amounts of biotinylated *EGR1* transcripts above starvation levels until after the 5-minute time point (Fig 3.5).

At 60 minutes both control and RV-cyclin nuclei produced significant levels of biotinylated *EGR1* transcripts above starvation conditions (Fig 3.5), but there was no significant difference between serum-stimulated control and serum-stimulated RV-cyclin-expressing nuclei at this time. This was expected, as all polymerases loaded on the promoter during the *in vivo* 10-minute serum stimulation have run off, and additional rounds of transcription are blocked at initiation by excess sarcosine in the reaction. The fact that nuclei from RV-cyclin-expressing cells produced more biotinylated *EGR1* transcripts during the linear phase of the reaction (after 5 minutes) indicates that RV-cyclin is enhancing the rate of transcription elongation. This exact same assay was used by Donner et al to demonstrate that CDK8 was required for efficient transcription elongation of these genes [121]. ChIP experiments were then used to solidify this conclusion.

### *Chromatin Immunoprecipitation*

The *EGR1* gene locus was chosen as the target gene for the ChIP analysis, for the same reasons it was analyzed for the nuclear run-on, it was the gene most affected by RV-cyclin in both HeLa and HCT116 cells in Aim 1. The primers used for analysis of the ChIP material were designed and published by Donner and others in 2010 [121]. The first ChIP across the *EGR1*

gene locus was done using an antibody specific for the trimethyl mark on lysine 4 in the tail of histone H3.

The level of histone H3 tri-methyl lysine 4 occupancy across the *EGR1* locus was not altered by RV-cyclin after serum stimulation. The highest level of the mark occurred at position 907, near the 5' end of the gene with 21% of input recovered from RV-cyclin-expressing cells and 27% of input recovered from control cells (Fig. 3.6).

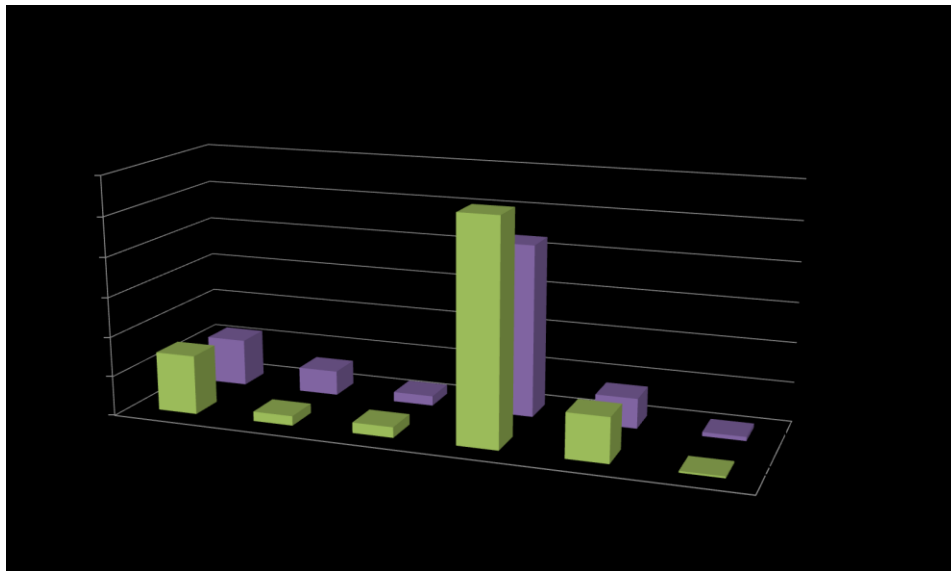


Figure 3.6 Chromatin immunoprecipitation of the *EGR1* locus using an antibody for tri-methyl histone h3 lysine 4 in control, serum-stimulated cells (green) and in serum-stimulated cells expressing RV-cyclin (purple). The qPCR analysis and determination of the % input recovered was performed using the primer sets for the *EGR1* gene locus, indicated in the top panel. These data show that RV-cyclin does not affect levels of tri-methyl histone H3 across the locus, suggesting RV-cyclin activates serum response gene expression independently of the COMPASS complex. This is one representative experiment of three biological replicates.

The histone H3 tri-methyl lysine 4 mark was also detected at positions -811 and 1374.

At -811, the RV-cyclin cells showed 5% of input and the control cells showed 7% of input, and at 1374 there was 3% and 5% of input from RV-cyclin and control cells, respectively (Fig 3.6).

The control cells showed greater H3K4 levels at two of the occupied positions, 907 and 1374, 6% greater at 907 and 2% greater at 1374. In general, these data suggest that RV-cyclin does not significantly alter levels of H3K4 trimethylation in the *EGR1* locus, and suggests that RV-cyclin

enhances serum-response gene expression using a mechanism to activate *EGR1* transcription that does not involve the COMPASS complex.

The next ChIP analysis focused on RNA Pol II's occupancy across the *EGR1* locus in control, wt RV-cyclin, mutant RV-cyclins (K80A/E111A and V260S) and cyclin C over-expressing HCT116 cells. Cells were fixed for ChIP analysis under serum-starvation conditions, and after 15, 30 and 60 minutes of serum stimulation (Fig 3.7). The percent input values that are graphed in Figure 3.7 are shown in Table 3.3. There were minimal levels of RNA Pol II at the *EGR1* gene locus under starvation conditions in all cell types. However, RV-cyclin-expressing cells did show increases of RNA Pol II occupancy at the *EGR1* enhancer region (-811) with 3 times over control and at the promoter region (-34) with 2 times over the control. The V260S RV-cyclin mutant and cyclin C over-expressing HCT116 cells also showed increased levels of RNA Pol II at the enhancer region, with an increase of 7-fold and 3-fold above the control, respectively (Fig 3.7). This increase continued into the promoter region at position -34; The V260S mutant increased RNA Pol II occupancy by 7 fold above the control and the cyclin C over-expressing cells had 6-fold more RNA Pol II. The RV-cyclin K80A/E111A mutant that does not bind CDK8 and inhibits *EGR1* gene expression after serum stimulation (Fig 2.7) did not increase the levels of RNA Pol II at the *EGR1* locus (Fig 3.7).

As expected, RNA Pol II was recruited to the *EGR1* gene locus after 15 minutes of serum stimulation in all cell types, however the level of recruitment in the K80A/E111A cells was not as robust as it was in the other HCT116 cell types (Fig 3.7). At 15 minutes post serum stimulation the wt RV-cyclin-expressing cells had 3 times greater input than control at position -811. This continued through the locus (4.82 x at -109, 2.34 x at -34, 2.15 x at 907, and 1.14 x at 1374).

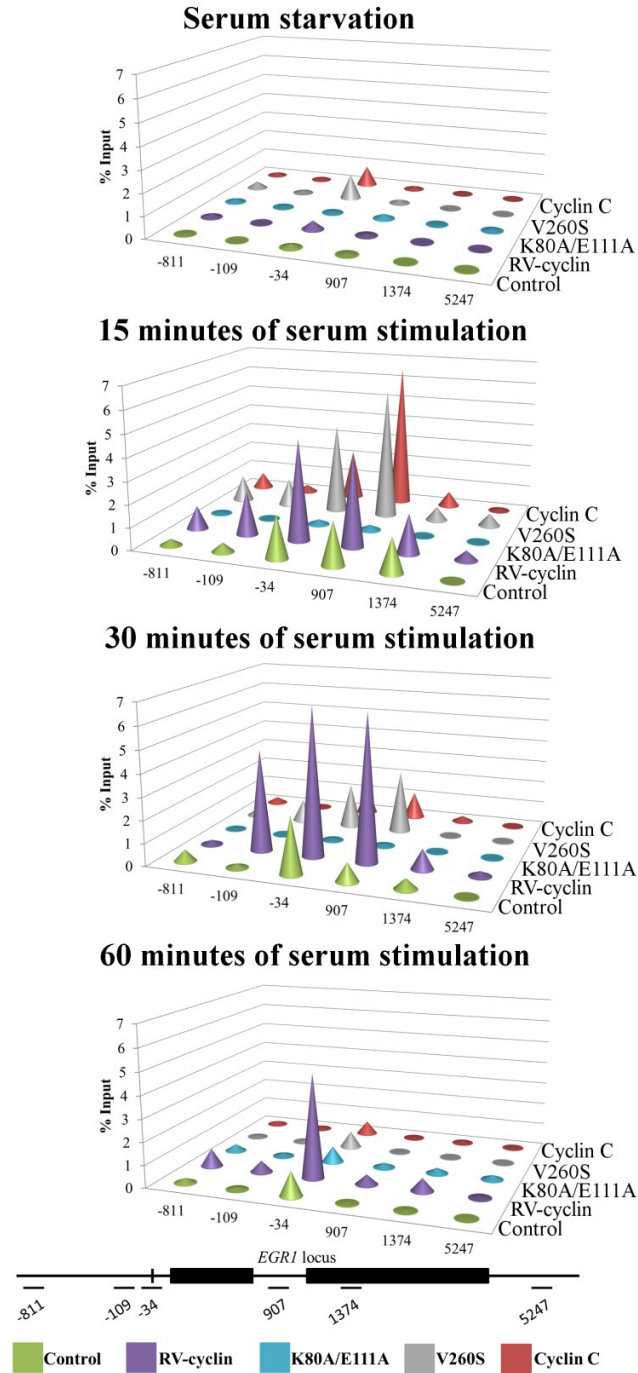


Figure 3.7 ChIP of the *EGR1* gene locus using the anti-RNA Pol II antibody from control (green) and RV-cyclin expressing HCT116 cells (wt in purple, K80A/E111A in blue, V260S in gray) and cyclin C over-expressing cells (red) fixed under serum starvation conditions, and after 15, 30 and 60 minutes of serum stimulation. Normal rabbit IgG was used as a negative control and gave a % input of around 0.01% (data not shown). This data is a representative graph of multiple experiments. The 60-minute serum stimulation ChIP particularly has been repeated with over 8 biological replicates. These data demonstrate RV-cyclin increases and changes the timing of RNA Pol II occupancy across the *EGR1* locus after serum stimulation.

Table 3.3 The percent input values obtained from the RNA Pol II ChIP of the *EGR1* locus through the time course

	% input at the <i>EGR1</i> locus under serum starvation					
	-811	-109	-34	907	1374	5247
<b>Control</b>	0.041633	0	0.149049	0.069534	0	0
<b>RV-cyclin</b>	0.142977	0	0.382586	0.09433	0	0
<b>V260S</b>	0.319493	0.107608	1.12807	0.158643	0	0
<b>K80A/E111A</b>	0.138107	0.060954	0.086201	0.213729	0.035252	0.10761
<b>Cyc C</b>	0.128858	0.083265	0.909948	0.145981	0.037005	0
	% input after 15 min of serum stimulation					
	-811	-109	-34	907	1374	5247
<b>Control</b>	0.291963	0.412898	1.923663	1.923663	1.519773	0
<b>RV-cyclin</b>	1.052526	1.991501	4.512279	4.152143	1.745761	0.430432
<b>V260S</b>	1.175974	1.23444	4.038603	5.831456	0.608722	0.55627
<b>K80A/E111A</b>	0.07662	0	0.225916	0.238797	0	0
<b>Cyc C</b>	0.723897	0.323953	2.256139	6.515411	0.680118	0.109869
	% input after 30 min of serum stimulation					
	-811	-109	-34	907	1374	5247
<b>Control</b>	0.526263	0.168855	2.538289	0.831539	0.464534	0
<b>RV-cyclin</b>	0.2022	4.543664	6.652314	6.560729	0.909948	0.222805
<b>V260S</b>	0.342424	0.99575	1.964083	2.796953	0	0
<b>K80A/E111A</b>	0.030266	0	0.082119	0.1011	0	0
<b>Cyc C</b>	0.276214	0	1.260378	1.19239	0.257716	0
	% input after 60 min of serum stimulation					
	-811	-109	-34	907	1374	5247
<b>Control</b>	0.209331	0.096982	1.097223	0.046194	0.051971	0.021254
<b>RV-cyclin</b>	0.797666	0.504825	4.671404	0.442533	0.567958	0.070504
<b>V260S</b>	0.06624	0.070504	0.744248	0.010336	0.020107	0
<b>K80A/E111A</b>	0.306478	0.142977	0.713931	0.212253	0.250669	0.200803
<b>Cyc C</b>	0.158643	0.082119	0.600342	0.043101	0.082119	0.048156

The control cells did not show any RNA Pol II occupancy at the 3' end of the *EGR1* locus, whereas the wt RV-cyclin cells had a reading of 0.4% input (Fig 3.7). The cells expressing the V260S RV-cyclin mutant had similar increases of RNA Pol II occupancy. However, positions -811 and 907 had 4 times and 3 times more RNA Pol II respectively than control cells. This was greater than wt RV-cyclin's RNA Pol II at these positions (Fig 3.7). The cyclin C over-expressing cells also showed increased RNA Pol II occupancy above control at all

positions except position -109 and had the greatest increase in RNA Pol II occupancy above control levels of any other clone at position 907 with a 6.5 % input. This position is in the open reading frame of the gene, which is occupied by elongating RNA Pol II (Fig 3.7).

At 30 minutes post serum stimulation, the RNA Pol II occupancy at the locus was reduced from levels seen at 15 minutes post serum stimulation in the control, the V260S mutant, and the cyclin C over-expressing cells (Fig 3.7). However, the wt RV-cyclin expressing cells show the greatest levels of RNA Pol II occupancy at the locus at this time point when compared to all other time points. This indicates that RNA Pol II transcription is still going strong at 30 minutes post serum stimulation in wt RV-cyclin expressing cells, and that it is shutting down in the other cell lines tested. There was an increase of RNA Pol II occupancy of 26 times above the control cells at the -109 position in RV-cyclin expressing cells (Fig 3.7). The trend continued down the locus with 2 times more at -34, 7 times more at 1374, and, unlike control cells, RNA Pol II was detected at *EGR1* position 5247. The V260S mutant and over-expressing cyclin C were similar to control RNA Pol II levels at 30 minutes. RNA Pol II occupancy in cells with K80A/E111A mutant RV-cyclin was drastically reduced (Fig 3.7).

The cells expressing the wt RV-cyclin maintained increased RNA Pol II levels at the *EGR1* locus at 60 minutes post serum stimulation (Fig 3.7). The fold increase of percent input above control was 3 times at -811, 5 times at -109, 4 times at -34, 9 times at 907, 10 times at 1374 and 3 times at 5247. In all the other HCT116 cells types, RNA Pol II was essentially returning to a pattern similar to serum starvation conditions (Fig 3.7). RV-cyclin's increase of RNA Pol II along the entire locus, suggests that *EGR1* is still being actively transcribed when transcription across the locus has shut down in the other HCT116 cell types.

The CDK8 ChIP of the *EGR1* gene locus in HCT116 cells revealed that RV-cyclin increases CDK8 occupancy at the *EGR1* gene locus under all serum conditions (Fig 3.8). The exact percent input values presented in the Figure can be found in Table 3.4. Upon serum stimulation CDK8 was recruited to the locus in all cell types tested. The wt RV-cyclin-expressing cells showed 5 times more CDK8 at -811, 2 times more at -34, 7 times more at 1374 and 4 times more at 5247 than control cells (Fig 3.8). The other cell types showed very little enhancement of CKD8 at the locus in starvation conditions.

At 15 minutes post serum stimulation, CDK8 was recruited to the *EGR1* promoter in control cells, similar to what has been published previously [121] (Fig 3.8). Cells expressing wt RV-cyclin showed increased levels of CDK8 at all positions when compared to the control ChIP. RV-cyclin-expressing cells had 2 times, 2 times, 1.5 times, 4 times, 14 times and 64 times more CDK8 at *EGR1* positions -811, -109, -34, 907, 1374, and 5247, respectively. The V260S mutant-expressing cells recruited even more CDK8 to the 3' end of the gene than the wt RV-cyclin-expressing cells after 15 minutes of serum stimulation, increasing CDK8 occupancy by 11 times over that of control at 907, 11 times more than the control at 1374, and 110 times more than control at 5247 (Fig 3.8). The cyclin C over-expressing cells showed moderate CDK8 increases above control levels at the 3' end of *EGR1*, with 3 times more CDK8 than control at 907, 6 times more at 1374, and 13 times more at 5247. These increases were similar to wt RV-cyclin enhancement at 907 and 1374, but these cells failed to increase CDK8 occupancy at position 5247.

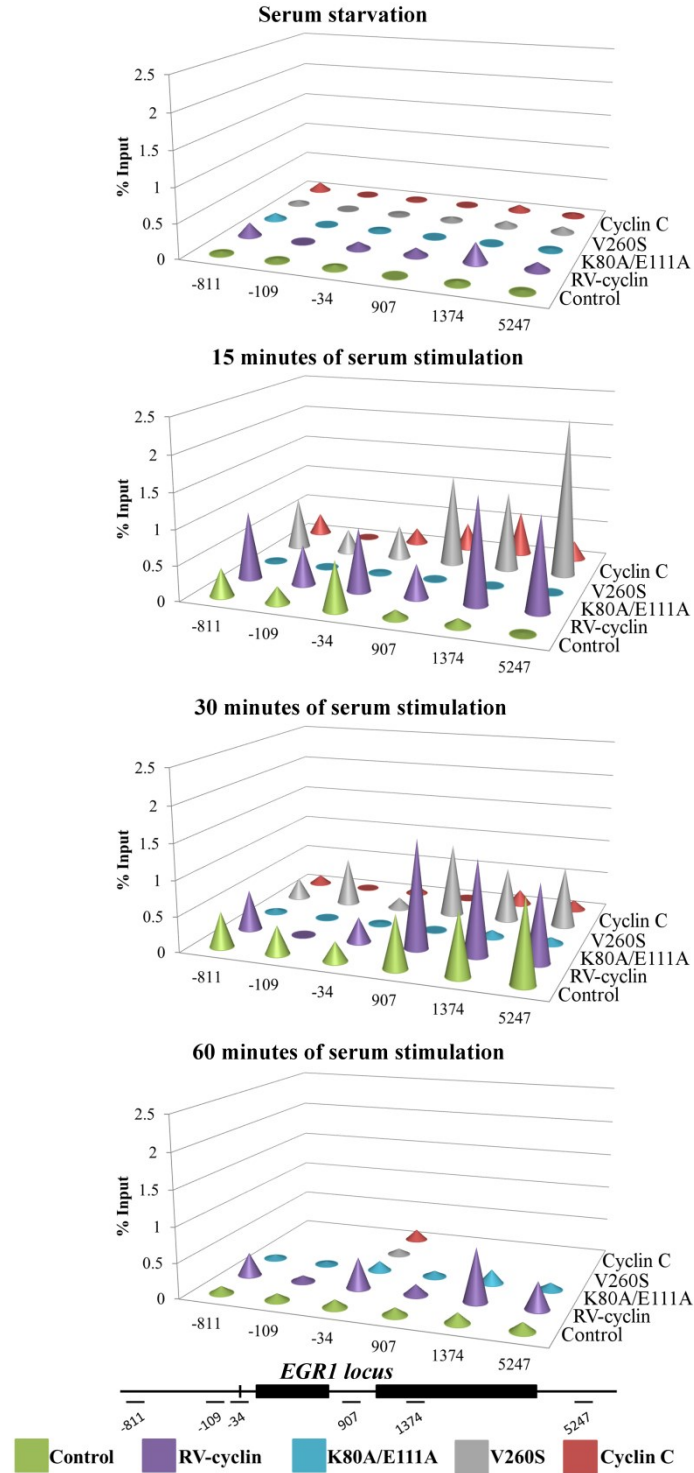


Figure 3.8 ChIP of the *EGR1* locus using the anti-CDK8 antibody and HCT116 control (green), wt (purple), K80A/E111A RV-cyclin (blue), V260S (gray), and cyclin C over-expressing (gray) cellular lysates fixed under serum starvation conditions and after 15, 30 and 60 minutes of serum stimulation. These data are representative of multiple biological replicates; the 60 minute and serum starvation ChIP have had 5 independent biological replicates.

Table 3.4 % Input values obtained from the presented CDK8 ChIP

	% input at the <i>EGRI</i> locus under serum starvation					
	-811	-109	-34	907	1374	5247
<b>Control</b>	0.0340	0.032891	0.046516	0	0.039387	0.026348
<b>RV-cyclin</b>	0.189972	0	0.099019	0.109869	0.287943	0.110633
<b>V260S</b>	0.060114	0	0.018502	0.05055	0.08269	0.086201
<b>K80A/E111A</b>	0.09175	0	0.025986	0	0	0.0251
<b>Cyclin C</b>	0.126206	0	0.019968	0	0.088625	0.043101
	% input after 15 min of serum stimulation					
	-811	-109	-34	907	1374	5247
<b>Control</b>	0.396078	0.233883	0.689612	0.113744	0.104665	0.02053
<b>RV-cyclin</b>	0.968522	0.567958	0.897421	0.477594	1.509276	1.32304
<b>V260S</b>	0.749425	0.344806	0.484261	1.313901	1.135916	2.271832
<b>K80A/E111A</b>	0.015559	0	0.019693	0	0	0
<b>Cyclin C</b>	0.310756	0	0.225916	0.385247	0.634572	0.264962
	% input after 30 min of serum stimulation					
	-811	-109	-34	907	1374	5247
<b>Control</b>	0.497875	0.396078	0.274306	0.739108	0.885066	1.151773
<b>RV-cyclin</b>	0.560139	0	0.347204	1.530344	1.332242	1.089643
<b>V260S</b>	0.296038	0.67542	0.156459	1.045256	0.765172	0.849012
<b>K80A/E111A</b>	0.052697	0	0.024927	0	0.09433	0.086201
<b>Cyclin C</b>	0.129754	0	0.121907	0	0.213729	0.138107
	% input after 60 min of serum stimulation					
	-811	-109	-34	907	1374	5247
<b>Control</b>	0.100402	0.096312	0.113744	0.106865	0.144973	0.127084
<b>RV-cyclin</b>	0.326206	0.085606	0.439476	0.152181	0.759887	0.387927
<b>K80A/E111A</b>	0.060114	0.042507	0.136205	0.08269	0.195313	0.099708
<b>V260S</b>	/	/	0.085015	/	/	/
<b>Cyclin C</b>	/	/	0.157547	/	/	/

After 30 minutes of serum stimulation, the control cells had more CDK8 at the locus than at any other time point. The CDK8 occupancy also increased across the locus in wt RV-cyclin-expressing cells, and at some points the occupancy was increased above control levels.

However, the fold increase of CDK8 occupancy by RV-cyclin was not as robust at 30 minutes as it was for the other time points. The wt RV-cyclin cells only increased CDK8 occupancy by 1.1 fold at -811, 1.5 fold at -34, 2 fold at 907, and 1.5 fold at 1374. CDK8 was still present at the

locus in V260S mutant-expressing and cyclin C over-expressing cells at 30 minutes, but the level of CDK8 was declining at the locus at this time point when compared to the 15-minute analysis. After 30 minutes of serum stimulation, the V260S cells had more CDK8 across the entire *EGR1* locus than the cyclin C over-expressing cells did, but the wt RV-cyclin cells had the most CDK8 at the locus out of any cell type. The cells expressing the K80A/E111A mutant were not able to recruit as much CDK8 as control cells, showing no increases of CDK8 occupancy at the locus.

At 60 minutes of serum stimulation, CDK8 levels are being depleted from the *EGR1* locus in all cell types, except wt RV-cyclin expressing cells. These cells maintained CDK8 at the locus with an increase of 3 times at -811, 3 times at -34, 1.5 times at 907, 5 times at 1374, and 3 times at 5247 in wt RV-cyclin cells. The analysis of the V260S mutant and the cyclin C over-expressing cells was only done at the -34 position, so comparisons between these cells at other positions across the locus are not possible at this time point. However, at the promoter, the CDK8 occupancy in these cells was similar to control levels, not showing the increase seen with wt RV-cyclin. The K80A/E111A RV-cyclin mutant at 60 minutes showed an overall reduction in CDK8 occupancy when compared to the control cells at this time point, continuing the trend that was observed for this clone at previous time points.

To confirm that RV-cyclin increases CDK8 occupancy across the entire *EGR1* locus, a CDK8 ChIP was performed with HeLa cells 8 hours post transfection with the pKH3 empty vector or with the pKH3A vector, encoding RV-cyclin (Fig 3.9). This time point was selected based on the results presented in Figures 2.1 and 2.2 in Aim 1. Indeed, the HeLa cells transfected with RV-cyclin had greater CDK8 occupancy across the *EGR1* gene locus at this time (Fig 3.9), which corresponds to the elevated levels of *EGR1* transcripts (Fig. 2.2). The percent inputs recovered from cells transfected with the empty vector for the *EGR1* positions -

811, -109, -34, 907, 1374, and 5247 were 0.19%, 0.08%, 0.08%, 0.25%, 0.11%, and 0.24% respectively. In cells transfected with wt RV-cyclin the same positions had percent input values of 0.47%, 0.60%, 0.48%, 1.51%, 0.69%, and 1.41%. This was a fold increase of 2.5 times at -811, 7 times at -109, 5 times at -34, 6 times at 907, 6 times at 1374, and 6 times at 5247. These data confirm increased CDK8 presence at target genes in association with RV-cyclin expression.

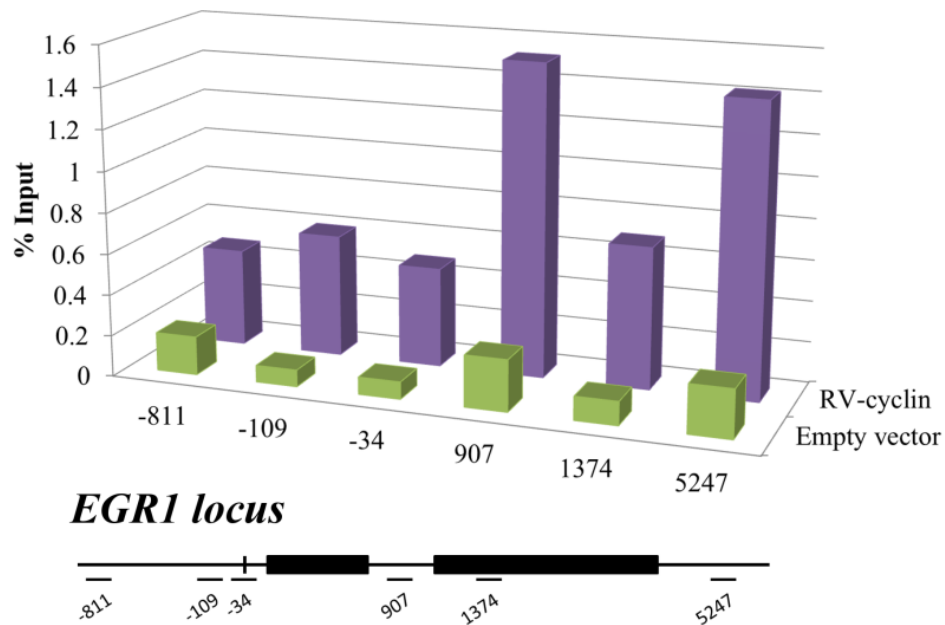


Figure 3.9 CDK8 ChIP analysis across the *EGR1* locus in HeLa cells transiently transfected with the pH3 empty vector (green), or the pH3A vector encoding RV-cyclin (purple).

ChIP using the HA antibody showed that RV-cyclin is present at the *EGR1* gene locus under all serum conditions (Fig 3.10). For this ChIP, the percent input was normalized to the background pull-down in the control cells, giving rise to the normalized fold increase in percent input above background presented in the y-axis. Under serum starvation conditions, RV-cyclin is mainly present at the *EGR1* promoter, with 4 and 9 times more HA signal than control at positions -811 and -34 respectively (Fig 3.10).

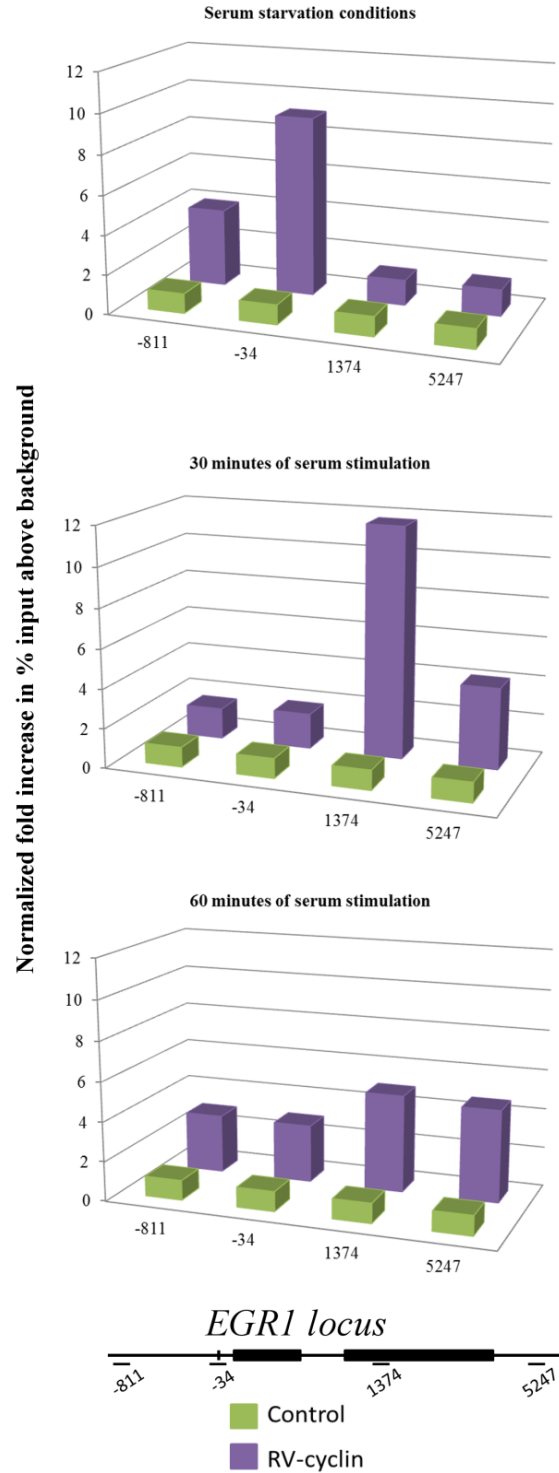


Figure 3.10 ChIP showing HA-tagged RV-cyclin occupancy along the *EGR1* gene locus in serum starvation conditions, and at 30 minutes and 60 minutes post serum stimulation in control (green) and wt RV-cyclin expressing (purple) HCT116 cells. The x-axis represents the different positions analyzed across the locus, and the y-axis represents the fold increase in % input above background, control levels.

After 30 minutes of serum stimulation, the RV-cyclin occupancy shifts to the 3' end of the gene. HA antibody pulled down 12 and 4 times more DNA from positions 1375 and 5247, respectively in HA-RV-cyclin expressing cells. There was minimal pull down of the *EGR1* enhancer and promoter with anti-HA antibody in RV-cyclin-expressing cells after 30 minutes. At 60 minutes of serum stimulation, more RV-cyclin was found at the promoter of *EGR1*, resulting in a pattern where RV-cyclin appears to be spread out across the *EGR1* locus. The HA antibody was able to pull down 3 times more of the *EGR1* promoter from RV-cyclin cells than from control cells at both -811 and -34 (Fig 3.10). Furthermore, RV-cyclin occupancy was still increased at the 1374 and 5247 positions. There was 5 fold more pull down from RV-cyclin expressing cells than control cells at these positions.

## **Discussion Aim 2**

The results presented demonstrate that RV-cyclin does not cause aberrant phosphorylation and activation of two key transcription factors controlling serum response gene expression, Elk-1 and SRF (Fig 3.3). Additionally, RV-cyclin does not reduce the rate of mRNA decay of the serum response genes tested (Fig 3.4), and the calculated  $\frac{1}{2}$  life of each transcript matches previously published values [146, 184, 185]. These data suggest RV-cyclin's activation of the serum response genes (Fig 2.2, Fig 2.6, and Fig 2.7) is due to a mechanism that lies after transcription factor phosphorylation and before the transcripts are degraded. The nuclear run-on experiments confirmed this conclusion and demonstrated that the presence of RV-cyclin enhances the rate of RNA Pol II transcription elongation across the *EGR1* gene locus (Fig 3.5).

The run-ons showed that more biotinylated *EGR1* transcripts were produced after 5 minutes of run-on *in vitro* using nuclear extracts from RV-cyclin cells than from control extracts in three independent experiments (Fig 3.5). The 60-minute run-ons show that RNA Pol II was

efficiently and equally initiated at the *EGR1* promoter in control and RV-cyclin cells (Fig 3.5). This supports a role for RV-cyclin in transcription elongation, because it took longer for the biotinylated *EGR1* transcripts to accumulate during the run-on in control cells than in RV-cyclin cells. This experiment was the exact same experiment utilized by Donner et al to demonstrate the requirement for CDK8 was required for transcription elongation of the serum response genes [121].

The ChIP experiments analyzing RNA Pol II occupancy on the *EGR1* locus (Fig 3.7) support the findings of the nuclear run-on experiments (Fig 3.5), and the inability of RV-cyclin to increase Elk-1 and SRF phosphorylation (Fig 3.3) or increase transcript levels of the serum response genes under serum-starvation conditions (Fig 2.6 and 2.7). The wt RV-cyclin cells were able to recruit more RNA Pol II to the *EGR1* locus in a manner that was independent of the tri-methyl histone H3K4 mark, and independent of transcription factor phosphorylation (Fig 3.6 and 3.7). These data suggest that increased RNA Pol II at the locus is a result of a mechanism that functions after transcription factor binding at the locus and requires signals from the activated pathway to enhance RNA Pol II transcription.

The time course analysis of *EGR1* transcript levels after serum stimulation (Fig 2.7) showed that both the cyclin C over-expressing cells and the V260S mutant cells had significantly greater *EGR1* transcript levels than control cells at 30 minutes. This could be a result of the large movement of RNA Pol II into the open reading frame (907) in these cells at 15 minutes (Fig 3.7). The RNA Pol II found at this position of the gene at this time point is elongating RNA Pol II. This suggests that cyclin C over-expression or expression of the V260S RV-cyclin mutant enhances RNA Pol II elongation. This coincides with the findings by Donner and others

in 2010 demonstrating a requirement for CDK8 kinase activity for efficient transcription elongation of *EGR1* [121].

The wt RV-cyclin-expressing cells had elevated levels of RNA Pol II at position 907 after 30 minutes of serum stimulation, but the level of elevation was not to the extent of those observed in the V260S or cyclin C cells. This corresponds to the lag in the ability of wt RV-cyclin cells to produce significantly more *EGR1* transcripts than control (Fig. 2.7). The RV-cyclin K80A/E111A mutant ChIP also corresponds to the *EGR1* transcription time course in Figure 2.7. This mutant RV-cyclin does not efficiently bind CDK8, and does not recruit RNA Pol II to the locus above control levels at any time (Fig 3.7). The levels of RNA Pol II at the locus in these cells are reduced from the control levels, and this coincides with the significantly reduced levels of *EGR1* transcripts produced from this clone at 60 minutes (Fig 2.7). These data suggest that CDK8 is, in part, responsible for the enhanced level of elongating RNA Pol II at the locus.

The 30 and 60 minute RNA Pol II ChIP (Fig 3.7) also corresponds to the *EGR1* gene expression data in Figure 2.7. The wt RV-cyclin cells were the only cell type able to extend the serum activation of *EGR1* out to 120 minutes, and these cells had elevated RNA Pol II levels above the control at both 30 and 60 minutes. Additionally, the extended presence of RNA Pol II in the open reading frame at 60 minutes suggests the RNA Pol II is still actively transcribing. In cyclin C over-expressing and V260S mutant cells RNA Pol II occupancy at the locus is steadily decreasing at 30 and 60 minutes when compared to 15 minute levels. The K80A/E111A RV-cyclin cells still had RNA Pol II levels that were reduced from the control at these time points, similar to the 15-minute time point. Taken together, the RNA Pol II ChIP data with the mutant and cyclin C cells suggest that RV-cyclin's interaction with CDK8 is necessary to enhance RNA

Pol II occupancy at the *EGR1* locus. Additionally, RV-cyclin's interaction with TAF9 is necessary to extend the presence of RNA Pol II (Fig 3.7) and increase the amount of time *EGR1* transcripts are elevated in cells after serum stimulation (Fig 2.7).

The wt RV-cyclin cells did not have as much RNA Pol II at position 907 as the V260S mutant or cyclin C over-expressing cells at 15 minutes post serum stimulation. However, comparison of the wt RV-cyclin and V260S mutant data in Figures 2.7 and 3.7 at the later time points suggests that wt RV-cyclin allows more RNA Pol II to re-initiate, which extends the burst of transcript levels. Therefore, in addition to enhancing RNA Pol II transcriptional elongation through the CDK8 interaction, wt RV-cyclin also increases the amount of RNA Pol II through re-initiation. The data presented in Figures 3.3 to 3.7 supports the initial statements of the hypothesis for aim 2, but demonstrate an additional function of the TAF9 interaction that was not expected. Increase occupancy of RNA Pol II in the open reading frames of genes is associated with an enhanced rate of transcription elongation, and these data are similar to previously published findings about enhanced transcription elongation [186].

An unexpected finding was observed in the CDK8 ChIP analysis. It was hypothesized that RV-cyclin would not increase the level of CDK8 at the gene locus when compared to the control, and instead enhance its kinase activity resulting in more elongating RNA Pol II. However, wt RV-cyclin clearly recruited more CDK8 to the locus under all serum conditions (Fig 3.8). This result was supported by ChIP analysis of the *EGR1* gene locus in HeLa cells transiently transfected with RV-cyclin (Fig 3.9). Furthermore, control cells recruited CDK8 to the promoter of *EGR1* at 15 minutes of serum stimulation, but the cyclin C over-expressing, the V260S mutant, and the wt RV-cyclin cells all had CDK8 at the promoter of *EGR1* at 15 minutes, but they had even more CDK8 in the open reading frame, unlike the control cells.

This result demonstrates that CDK8 is in the open reading frame of certain genes, a conclusion that has been made before by Donner and others in 2007 and in 2010 with ChIP analysis of the *p21*, *FOS*, *EGR1*, *EGR2*, and *EGR3* loci [121, 122]. It is possible that RV-cyclin is enhancing CDK8 phosphorylation of histone H3 Ser 10 in the open reading frame of these genes, as this is an important mark required for efficient transcription elongation during the serum response [102, 172]. A future ChIP analyzing this mark in wt and mutant RV-cyclin expressing cells will be very telling.

CDK8 occupancy at the *EGR1* locus correlated with HA-tagged RV-cyclin occupancy after 30 and 60 minutes of serum stimulation, supporting the hypothesis presented (Fig 3.10). Furthermore, RV-cyclin was present at the promoter of *EGR1* in serum starvation conditions. At this time it is possible RV-cyclin is interacting with TAF9 at the promoter, possibly regulating the initial events of transcription after serum starvation. This was an interesting observation, as the V260S mutant and cyclin C over-expressing cell lines had a more rapid burst of *EGR1* transcripts after serum stimulation than both the control and wt RV-cyclin expressing cell (Fig 2.7). A model was developed based on this data, and the fact that RV-cyclin contains a coiled-coiled domain, which could support trimerization of the protein. In this model RV-cyclin brings more CDK8 to the locus of certain genes in a trimer-complex, containing three CDK8 molecules instead of the monomers that would be present with cyclin C. Upon transcription activation, RV-cyclin enhances CDK8 kinase activity at certain targets like histone H3 and the CTD of RNA Pol II, because more CDK8 is physically present. It could then also employ an actual increase in the kinase activity of CDK8, compared to cyclin C, for a synergistic response. The result of this enhancement, no matter the mechanism, is more elongating RNA Pol II through the locus of the gene. In addition to CDK8 binding, RV-cyclin also interacts with TAF9 at the

promoter of the *EGR1* gene, to keep it open for future transcription re-initiation events in a gene-looping type of model.

CDK8's function in transcription elongation is widely disputed between many research groups. Some suggest that CDK8 functions as a transcriptional repressor [101, 187], where others have shown that CDK8 kinase activity is required for an efficient transcriptional response [100, 121, 122]. In transcription elongation, it has been proposed that CDK8 phosphorylates the CTD of RNA Pol II to recruit Brd4, which is required for pTefb recruitment to promote release of Pol II from the promoter. Many attempts were made to assess CDK9 occupancy at the *EGR1* gene locus in the cell lines used; however, the pull-downs were never successful even though multiple antibodies were employed. If this ChIP were to be optimized in the future, valuable information could be gained as to how CDK8 regulates CDK9 activity.

The *EGR1* gene locus was the only locus analyzed by nuclear run-on and ChIP analysis out of all the other genes activated by RV-cyclin in Figures 2.2 to 2.7. Transcription of other genes, like interferon, can be repressed by RV-cyclin [59], and it is likely that the function of RV-cyclin is not the same at all genes. However, there are similarities between the promoters of the genes activated by RV-cyclin: The *EGR1* promoter contains a TATA box (-34), two SP1 sites (-250 and -500), multiple serum-response elements (-100 and -300 to -400), an NF $\kappa$ B site (-200), two cAMP response elements (CRE) (-150 and -700), an AP1 binding site (-650), and an *EGR1* binding site (-600) [157, 188]. *FOS* and *JUN* also have TATA boxes in their promoters and contain AP-1 and SP-1 binding sites [189, 190]. The *FOS* promoter contains both a cAMP response element and a serum response element [189]. The *JUN* promoter instead of a CRE contains a TPA response element (TRE), an ATF-1 binding site and MEF2d site [189, 191]. The *CCND1* promoter is similar to the serum response genes, it has AP1, SP1, and EGR1 binding

sites, along with a serum response and CRE [192]. The similarities between these promoters are intriguing, and suggest a commonality between genes that are targeted by CDK8 and RV-cyclin. ChIP analysis of these genes, and other genes with different promoters with and without RV-cyclin could aid in determining RV-cyclin and CDK8's mechanism in RNA Pol II regulation.

Other future directions from this aim would be a more in depth ChIP analyses of the *EGR1* promoter, looking at levels of bound transcription factors and TAF9 under varying serum conditions. ChIPs analyzing the level of the phosphorylated histone 3 at serine 10 across the *EGR1* gene locus would also be very informative, and would perhaps pinpoint how RV-cyclin is modulating CDK8 phosphorylation and which CDK8 targets are important in RV-cyclin's activation of gene expression. Additionally, the role of PP2A in this process has not been explored, even though RV-cyclin binds to PP2A and possibly alters its cellular location. RV-cyclin might bring PP2A to the promoter of certain activated genes to dephosphorylate condensin during cell division, marking active genes and passing this information along to daughter cells [91]. This is something that needs to be explored further.

Finally the ChIP results indicate that RV-cyclin can only activate expression of *EGR1* genes when the MAPK pathway is activated, similar to the findings in the time course presented in Figure 2.7. This further suggests that RV-cyclin requires an outside signal to activate the MAPK pathway in order to enhance gene expression. The Orf b protein can activate the p90RSK complex [55], which would lead to SRF phosphorylation. This hypothesized mechanism could be easily explored with the ChIP assays using the HCT116 serum response, if Orf b was introduced into the HCT116 cells. In this aspect, a future study involving the co-expression of RV-cyclin and the Orf b protein would be very beneficial to further nail down the novel mechanism of retro-viral induced oncogenesis being proposed.

## CHAPTER 4—AIM 3: DETERMINE IF RV-CYCLIN ENHANCES THE KINETICS OF CDK8 PHOSPHORYLATION *IN VITRO*

### **Introduction-Aim 3**

The *in vitro* kinase assays shown in Figure 1.5 were performed with CDK8 immunoprecipitates from HeLa cells with or without induced RV-cyclin expression. These assays demonstrated that RV-cyclin enhances CDK8 phosphorylation of the substrates, but did not assess whether RV-cyclin enhances the actual rate of CDK8 phosphorylation or affected the components of the immunoprecipitates or modifications of CDK8 prior to isolation. The levels of CDK8 kinase, cyclin C and RV-cyclin could only be estimated through the protein concentration of the immunoprecipitates. Therefore, it was necessary to develop recombinant CDK8, cyclin C, and RV-cyclin, which could be purified and quantitated for analysis with Michaelis-Menten kinetics.

To do this, the baculovirus expression system was employed in a manner that His-tagged CDK8 could be co-expressed with either HA-tagged cyclin C or HA-tagged RV-cyclin using the Bac-to-Bac® expression system with the pFastBac® Dual donor plasmid (Invitrogen™/Life Technologies™). Previous studies analyzing the structure of cyclin C-bound CDK8 have suggested that co-expression of these proteins in the baculovirus system allows for efficient binding between the two recombinant proteins and successful co-purification [101]. Additionally, His-tagged CDK8 was produced alone in the baculovirus system, by Connie Brewster, and GST fusions of RV-cyclin and RV-cyclin mutants and cyclin C had been previously produced in *E. coli*.

Once produced, the recombinant proteins were slated for use in kinase assays where the level of the co-purified complexes could be controlled, along with the level of ATP and substrate (either histone H3 or RNA Pol II CTD). Two types of kinase assays were chosen for the analysis, one measuring the incorporation of radio-labeled phosphate ( $P^{32}$ ) into the CDK8 targets, and the second an ADP-glo kinase assay that measures the breakdown of ATP into ADP using a fluorescence-based assay.

This aim has been only partially completed to date. The recombinant proteins were produced and purified from the baculovirus infection, and preliminary kinase assays analyzing CDK8 autophosphorylation were carried out with both assay systems. However, the actual analysis of CDK8 enzyme kinetics with and without RV-cyclin was not performed. Therefore, the results presented in this chapter focus on those that have been accomplished.

### **Hypothesis-Aim 3**

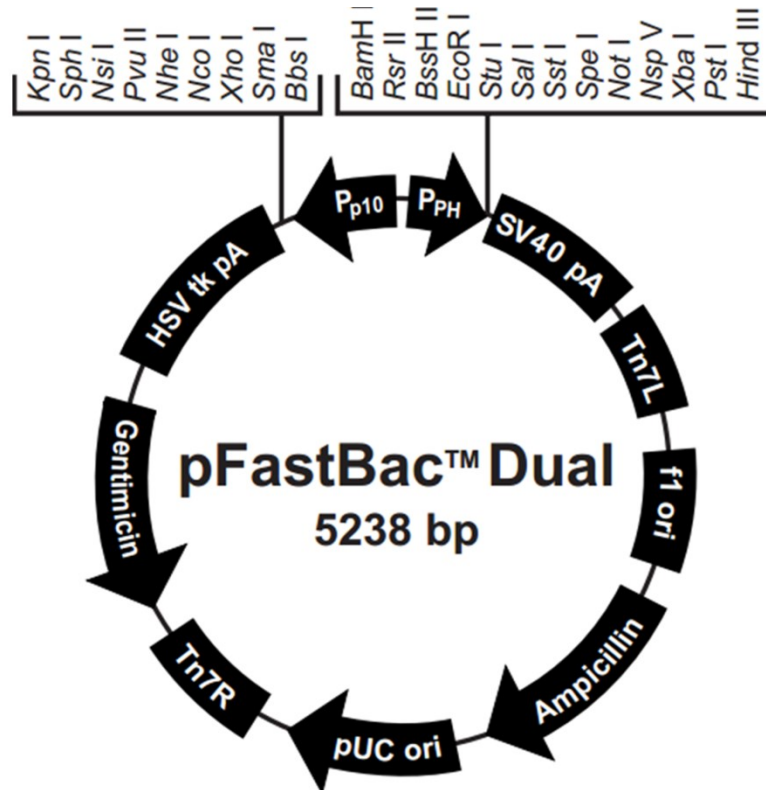
As RV-cyclin immunoprecipitates of CDK8 from RV-cyclin expressing cells are able to phosphorylate the CTD of RNA Pol II and histone H3 to a significantly greater extent than control immunoprecipitates (Fig 1.5), it is hypothesized that RV-cyclin increases the rate of CDK8 phosphorylation of both targets. This enhancement is in addition to RV-cyclin's ability to form trimers and bring more CDK8 to target genes *in vivo*. The end result is a combinatorial mechanism of gene activation by RV-cyclin—enhancement of CDK8 occupancy at target genes (Figs 3.8 and 3.9) and an increased rate of CDK8 kinase activity while there.

### **Materials and Methods-Aim 3**

#### *Production of recombinant baculovirus*

The Bac-to-Bac® baculovirus expression system from Invitrogen™/Life technologies™ was used to generate recombinant His-tagged CDK8, HA-tagged cyclin C, and HA-tagged RV-

cyclin following the manufacturer's instructions. Connie Brewster was responsible for cloning the His-tagged CDK8 and either the HA-tagged cyclin C or the HA-tagged RV-cyclin into the pFastBac Dual donor plasmid. A map of this donor plasmid can be found in Figure 4.1. A donor plasmid containing a His-tagged mCherry protein was graciously provided by Davin Henderson as a positive control for SF9 transfection.



[http://tools.lifetechnologies.com/content/sfs/vectors/pfastbacdual\\_map.pdf](http://tools.lifetechnologies.com/content/sfs/vectors/pfastbacdual_map.pdf)

Figure 4.1 Map of the pFastBac™ Dual donor plasmid used for the creation of the recombinant bacmid. The sequence of His-tagged CDK8 was placed under control of the polyhedron promoter (Pph) and HA-tagged cyclin C or HA-tagged RV-cyclin was cloned to be controlled by the p10 (Pp10) promoter. This image is a replication of the Figure found on page 67 of the Bac-to-Bac® Baculovirus expression system manual (MAN0000414) by Invitrogen™/Life Technologies™.

Once the donor plasmid was generated, it was transformed into DH10Bac™ *E. coli* cells.

These cells contain a baculovirus shuttle vector known as a bacmid. This vector is 136kb,

contains a kanamycin resistant gene, and has a mini-attTn7 target site. The mini-attTn7 sequence can be transposed with the mini-Tn7 element in the pFastBac Dual donor plasmid when the donor plasmid is present in the DH10Bac cells after transformation. The result of the transposition event is incorporation of donor plasmid into the bacmid. DH10Bac cells were transformed in S.O.C media, and colonies containing the recombinant bacmid were selected for on LB agar plates containing 50 µg/ml kanamycin, 7 µg/ml gentamicin, 10 µg/ml tetracycline, 100 µg/ml x-gal, and 40 µg/ml IPTG. White colonies were analyzed for recombinant bacmid production using PCR, and primer sets that amplified over the promoter region of the recombined bacmid. These primer sets contained a forward primer which was the reverse complement of the human CDK8 sequence, and a reverse primer that was the reverse complement of the human cyclin C sequence or the RV-cyclin sequence depending on which bacmid was being analyzed.

The recombinant bacmids were used for transfection of SF9 cells. This cell line was produced from fall armyworm ovarian cells, and is available commercially. The SF9 cells employed were a generous gift from Davin Henderson. SF9 cells were grown in SF-900 II SFM™ medium supplemented with penicillin and streptomycin at 28°C under constant shaking. They were maintained at a density between  $8 \times 10^5$  cells/ml and  $2.5 \times 10^6$  cells/ml. For each transfection,  $8 \times 10^5$  cells were plated in one well on a 6-well plate using un-supplemented Grace's insect cell culture medium. Cellfectin II was used for transfection of the cells with the recombinant bacmids, following the instructions from the Bac-to-Bac® manual. Transfected cells were maintained in the 6 well plates for 72 hours at 28 °C. The media was centrifuged at 300 x g and the supernatants were collected as the initial virus stock.

At this point there was too little virus to be detected by protein analysis, so the virus was propagated in SF9 cells. For each propagation,  $1 \times 10^7$  cells were plated in  $10 \text{ cm}^2$  cell culture dishes using SF900 medium and infected with  $\frac{1}{2}$  of the initial virus stock. The plates were incubated at  $28^\circ \text{C}$  for 72 hours and the medium was collected, centrifuged, and stored as the primary virus stock. At this point, SF9 cells infected with the mCherry + control virus turned a pink color. The infected SF9 cells collected during the purification of the virus stock were lysed with PBS containing 1% triton X-100 and two freeze-thaw cycles at  $-80^\circ \text{C}$ . The lysates were analyzed for His-CDK8 expression and HA-cyclin C or HA-RV-cyclin expression by separating 20  $\mu\text{g}$  of protein from the lysate with SDS-PAGE gel electrophoresis following the protocol described in chapter 3, and analyzed by western blot with either anti-His antibody from Sigma, or mouse anti-HA antibody (clone 12CA5) from Roche.

Selected primary virus stocks were used in a time course of SF9 infection to determine the optimum time for recombinant-protein collection, and to propagate enough virus for the large scale infection required for recombinant protein production. For each infection,  $2 \times 10^8$  cells were transferred to a 200 ml flask in SF900 medium to a final volume of 100 ml, and then  $\frac{1}{2}$  of the primary virus stock was added. Every 24 hours for 96 hours, 1 mL of culture was collected for protein analysis, and cells were analyzed for signs of cytopathic effect (CPE) from viral infection. At the end of the time course, when 70% of the initially infected cells had died, medium was collected and centrifuged for collection of the secondary virus stock. The samples collected during the time course were centrifuged at  $500 \times g$  and the cell pellets were lysed with RIPA buffer (150 mM NaCl, 1.0% IGEPAL® CA-630, 0.5% sodium deoxycholate, 0.1% SDS, and 50 mM Tris, pH 8.0). The lysates were analyzed for recombinant protein expression using SDS-PAGE gel electrophoresis and western blot analysis with anti-His and anti-HA antibodies.

### *Purification of recombinant proteins*

Infection of SF9 cells for the final collection of recombinant protein was done using a 300 ml culture of  $1.5 \times 10^6$  cells/ml and 10 ml of the secondary virus stock. Cells were incubated at 28°C for 18 hours and collected by centrifugation at 600 x g. Pellets were frozen at -80°C before the recombinant proteins were purified with Talon superflow metal affinity resin from Clontech. This resin employs a cobalt ion that binds to the His-tag on CDK8. The HA-tagged cyclin C and RV-cyclin co-purify with the His-tagged CDK8 as they interact with and bind to each other in the SF9 cells during baculovirus infection. Protein purification was carried out as directed by the manual, using a series of washes with 250 mM sodium phosphate, 1.5M sodium chloride pH 7, and stepwise washes and elution with 5 mM to 1 M imidazole under native protein conditions. Protein purity was analyzed with SDS-PAGE gel electrophoresis and Coomassie stain analysis of the eluents.

### *Kinase assays*

Two different kinase assays were employed to assess the activity of the purified recombinant CDK8 constructs. The ADP Glo kinase assay from Promega, and the  $P^{32}$  kinase assay described previously by Rovnak and others 2012 [82]. Each kinase assay measured the level of CDK8 autophosphorylation, with the intent of eventually introducing substrate and taking time points to measure the enzyme kinetics of each construct.

The kinase reactions for the ADP Glo kinase assay used 1  $\mu$ g of purified protein with 5  $\mu$ l of 1 mM ATP in a 50  $\mu$ l volume of kinase reaction buffer. The reaction was carried out for one hour at 30°C with constant shaking before addition of the ADP-glo reagent. The manufacturer instructions were followed, and the amount of ADP produced during each kinase reaction was detected with a luciferase read out. The greater the luciferase activity, the more ATP was

converted to ADP in the kinase reaction. The luciferase activity was compared to a standard curve, which used known concentrations of ADP. The kinase reactions for the P<sup>32</sup> kinase assays were done using recombinant protein complexes, with ATP and P<sup>32</sup> as described previously [82].

### **Results-Aim 3**

Four bacmid isolates from each set of PCR-positive DH10Bac clones (either the His-CDK8/HA-cyclin C clones or the His-CDK8/HA-RV-cyclin clones) were selected for initial virus stock production and carried into primary virus stock production. Two arbitrarily selected mCherry bacmid isolates were included for a positive control (Fig. 4.2). After two 72-hour passages, infected cells were analyzed for recombinant His-tagged CDK8 protein expression (Fig 4.2 A). All clones selected produced recombinant His-CDK8, so two positive clones (4 and 5 from the RV-cyclin recombinant group and 2 and 4 from the cyclin C recombinant group) were analyzed for HA-tagged cyclin C or HA-tagged RV-cyclin expression (Fig 4.2 B). In addition to CDK8 expression, all selected clones were expressing the appropriate recombinant HA-tagged cyclin.

The time course analysis of the secondary viral infection showed that His-CDK8 and the HA-cyclins were expressed at high levels by 24 hours post infection (Fig 4.3). The blot used for this analysis was developed with a mix of the His and HA primary antibodies. By 48 hours, the recombinant CDK8 produced is being degraded, as the faint, lower sized band just below the CDK8 band at 24 hours grows darker through the time course. Due to the production of the CDK8 degradation product, it was decided to collect the SF9 cells at 18 hours post infection, to minimize the amount of degraded His-CDK8 that was purified.

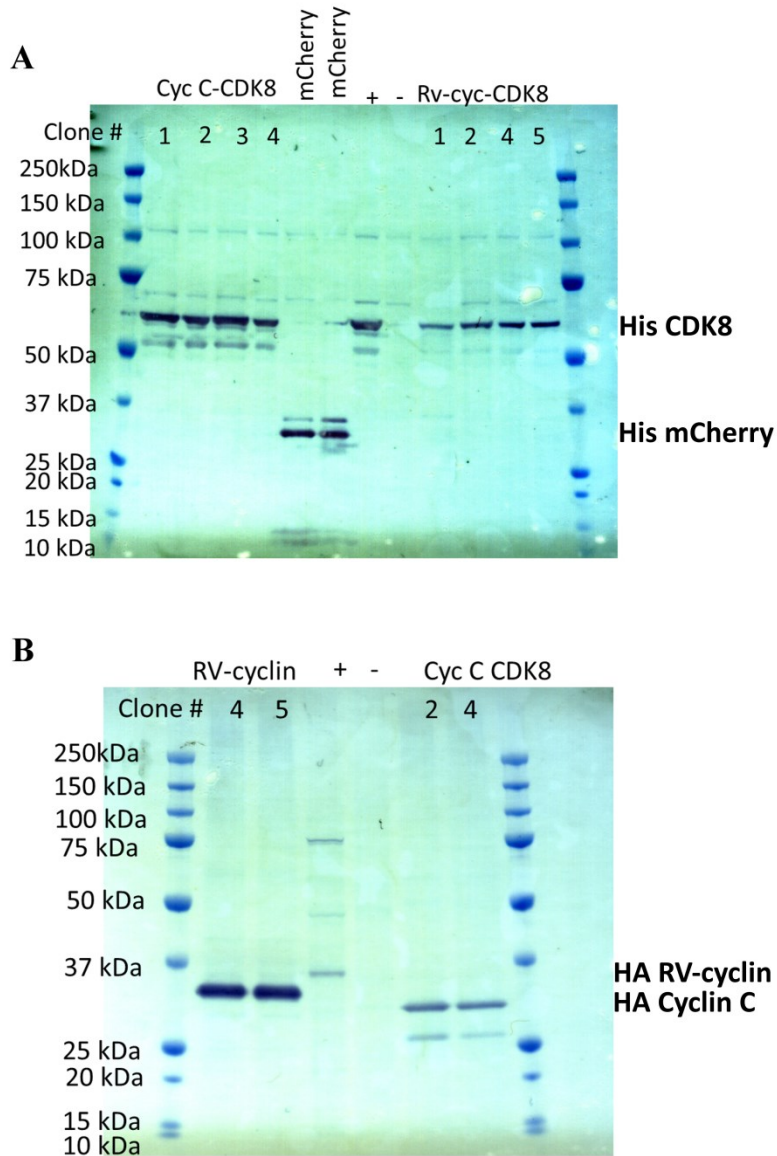


Figure 4.2 Western blot analyses of SF9 cell lysates after infection with the initial virus stock demonstrating the cells produced both recombinant proteins encoded for in the recombinant baculovirus. Blots were probed with a mouse anti-His primary IgG antibody (A). Selected clones were then analyzed for HA-cyclin expression using mouse anti-HA primary IgG antibody (B). Positive controls were His-tagged CDK8 without a co-purified cyclin (A), and protein lysate from the HCT116 cells stably expressing wt RV-cyclin with three HA-tags (B). The baculovirus produced, recombinant RV-cyclin has one HA tag, accounting for the size difference. The negative control for both blots was un-infected SF9 lysate.

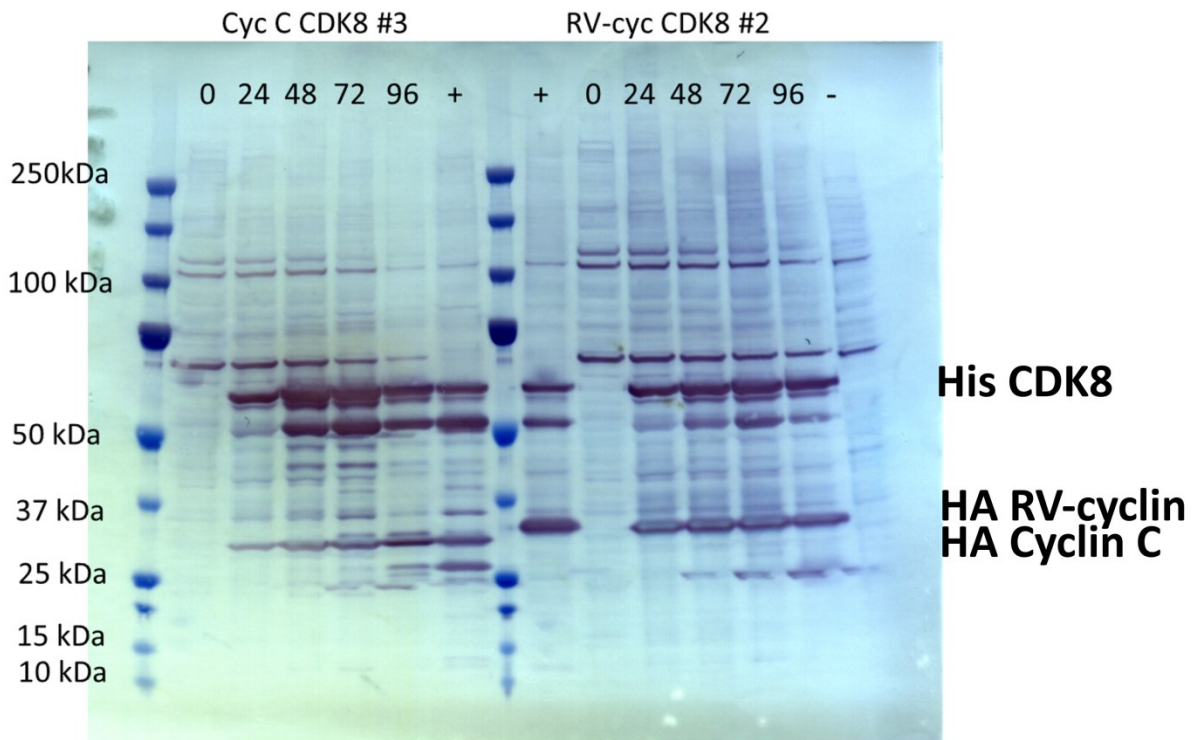


Figure 4.3 Western blot analysis of the cells collected during the production of the secondary baculovirus stock, demonstrating both recombinant proteins are produced by 24 hours post transfection, and continue to be produced during the course of infection observed. The blot was developed using a mix of the anti-His and anti-HA primary antibodies. The positive control was cell lysates from analysis of the primary infection presented in Figure 4.2. The negative controls were un-infected SF9 cell lysates.

The recombinant protein was isolated from SF9 cells infected with the secondary virus stock produced from the cells analyzed in Figure 4.3. These cells were collected at 18 hours post transfection and purified using the Talon resin from Clontech as described. The protein analysis using a Coomassie stained SDS-PAGE gel shown in Figure 4.4 revealed that both HA-tagged cyclins co-purified with the His-tagged CDK8 as expected. However, it proved to be very difficult to get the purified protein off of the beads, and only minimal soluble protein was recovered.

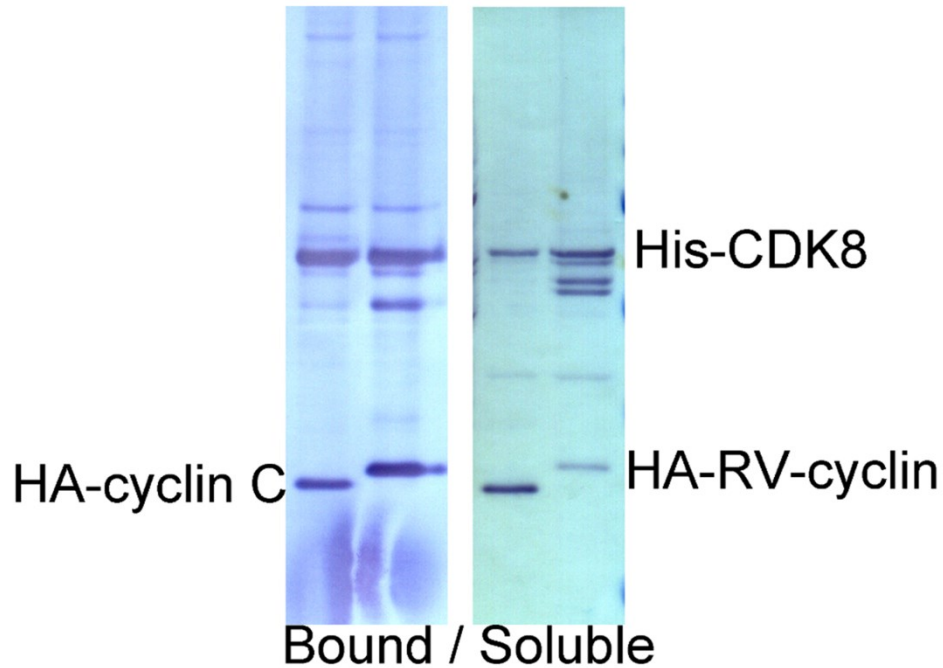


Figure 4.4 A Coomassie stained SDS-PAGE gel of bead-bound and soluble, purified protein. The analysis demonstrates that both HA-tagged cyclin C and HA-tagged RV-cyclin co-purify with His-tagged CDK8.

The recombinant co-purified proteins were used in ELISA assay to analyze cyclin CDK8 binding, and in an ADP-glo kinase assay as a preliminary analysis of CDK8 autophosphorylation.

Most recently, his-tagged, recombinant forms of CDK8 alone and co-produced with HA-tagged RV-cyclin or cyclin C have been produced in in Sf9 insect cells with a baculovirus infection, as well as separate preparations of GST fusions of RV-cyclin and cyclin C in *E. coli*. Binding of both HA-tagged cyclins to CDK8 in a 1:1 ratio was confirmed by western blot (Fig 1.7), and the binding of both cyclins to CDK8 withstood washing at high stringency, suggesting a high affinity between cyclin and CDK8 in both cases (unpublished data). Preliminary ELISA assays with bound, his-tagged CDK8 also demonstrated comparable binding of GST-cyclin C and GST-RV-cyclin (Fig 4.5).

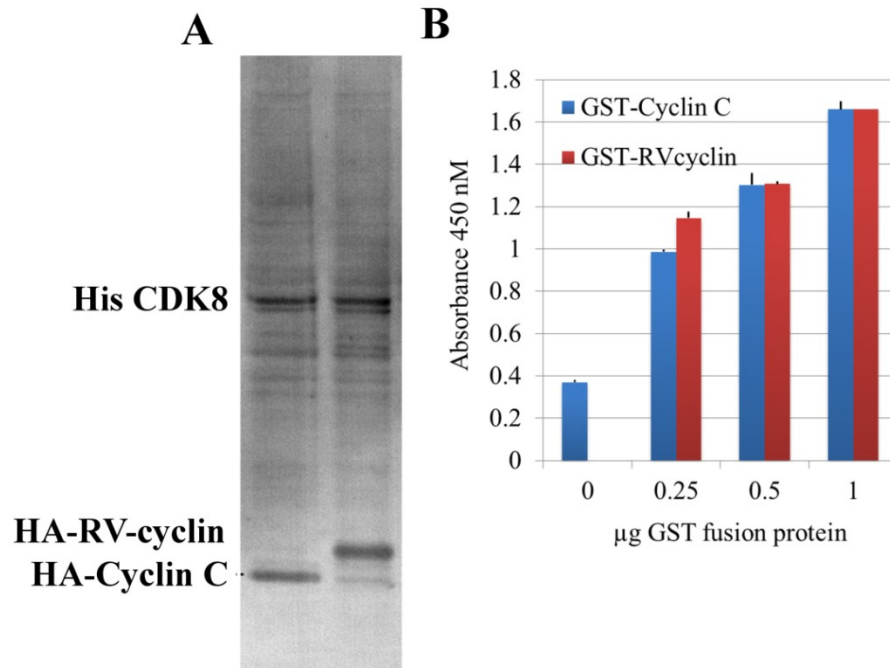


Figure 4.5 RV-cyclin binds CDK8 in a 1:1 ratio, similar to cyclin C and CDK8 binding. The recombinant his-CDK8 /HA-RV-cyclin or his-CDK8/HA-cyclin C were co-expressed and co-purified from the baculovirus expression system (A). An enzyme-linked immunosorbent assay (ELISA) was performed with the co-purified proteins in nickel-coated plates using anti-his and anti-HA antibodies (B), and binding was determined to occur in a 1:1 ratio between RV-cyclin and CDK8 and between cyclin C and CDK8 (Joel Rovnak Unpublished data).

The his-CDK8 from both co-purifications was able to autophosphorylate, and convert ATP to ADP to levels above kinase buffer alone (Fig 4.6). The P<sup>32</sup> kinase assays demonstrated that there was no apparent difference between the two his-CDK8 co-purifications in their ability to autophosphorylate (Fig 4.7). Some phosphorylation of cyclin C and RV-cyclin was also apparent. There was a band of phosphorylated cyclin C in the RV-cyclin/CDK8 co-purifications. This might be an indication that HA-RV-cyclin/His-CDK8 recombinant complexes may also contain cyclin C derived from SF9 cells during expression.

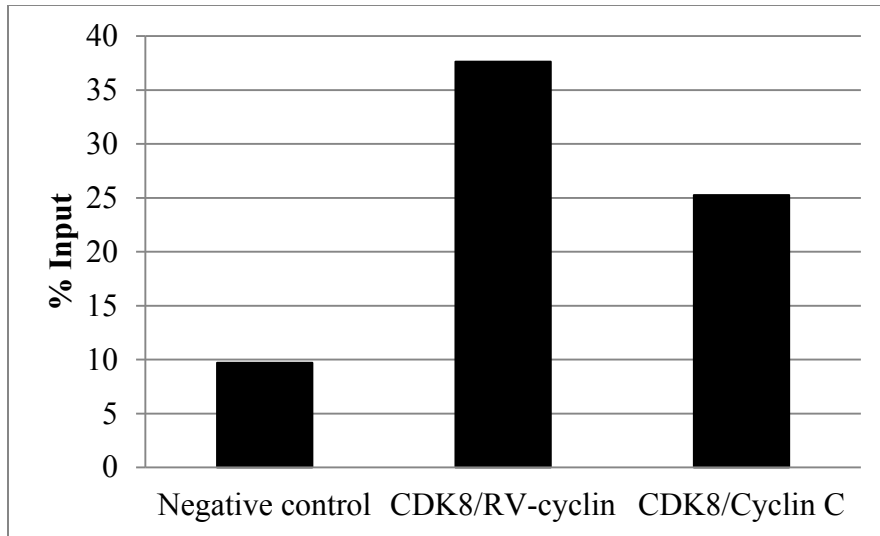


Figure 4.6 A preliminary ADP glo kinase assay demonstrating the ability of CDK8 to autophosphorylate in cyclin C or RV-cyclin co-purifications. The negative control was kinase buffer with ATP. This assay is a representative experiment of two independent biological replicates.

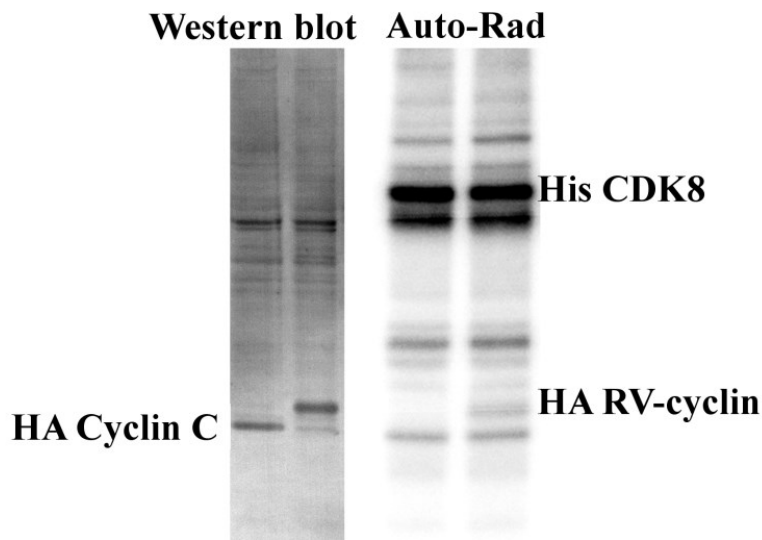


Figure 4.7 An example of an auto-rad image obtained from the  $P^{32}$  kinase analysis of autophosphorylation by the purified recombinant CDK8 in complex with either HA-tagged cyclin C or RV-cyclin. The corresponding western blot analysis of the purified proteins included in the kinase assay is shown on the right. All assays were done using bead-bound purified protein, and supported the conclusions gained with the ADP glo assay.

### **Discussion-Aim 3**

The SF9 cells were successfully transfected with the recombinant bacmids for both His-CDK8/cyclin C and His-CDK8/RV-cyclin, producing recombinant baculovirus (Fig 4.2 and 4.3). This virus was then used to produce co-purified complexes (Fig 4.4). It was difficult to get the complexes off of the beads, even at imidazole concentrations as high as 1 M. However, this served to demonstrate the continued 1:1 binding of both cyclin C and RV-cyclin to CDK8 under stringent salt concentrations and allowed a high degree of purification in a single step (Fig 1.7). That is why the RV-cyclin/CDK8 bead bound material was used in the kinase assays presented. The significance of the increased elution of cyclin C/his-CDK8 vs. RV-cyclin/hisCDK8 is not clear, but could result from the formation of RV-cyclin/His-CDK8 multimers prior to cobalt binding. It should be noted that His-CDK8 alone proved difficult to elute from metal affinity substrates. The ADP-glo and P<sup>32</sup> kinase assays do demonstrate that CDK8 in both co-purified complexes is capable of autophosphorylation. The bead-bound proteins did cause problems with the ADP-glo kinase assay. The talon beads without kinase would occasionally cause a large break down in ATP, leading to random, unexpected high background levels (data not shown). For this reason, the P<sup>32</sup> kinase assay should be used to assess bead-bound kinase activity in the future.

The auto-rad image in Figure 4.7 supports the preliminary findings obtained with the ADP-glo kinase assay. This assay showed that there was no apparent difference in CDK8's ability to autophosphorylate between the cyclin C and RV-cyclin containing co-purifications. Although the conditions likely reflect the maximum phosphorylation of substrate and not rate due to the extended incubation period with limited substrate. The results might suggest that if RV-cyclin does increase CDK8 kinase activity, it does so for substrates other than itself, like the

CTD of RNA Pol II or Histone H3 (Fig 1.5). Alternatively this data could suggest that RV-cyclin enhances CDK8 kinase activity on targets just by being able to form a homotrimer through the coiled-coil region (Fig 1.4) and binding 3 molecules of CDK8 instead of 1. However, the *in vitro* kinase assays presented in Figure 1.5 do not support this hypothesis, as equal amounts of CDK8 from the isolated nuclei were used for the analysis. In general, additional assays and complete calculation of the enzyme kinetics are needed before any conclusion can be made about the hypothesis presented.

There were low levels of HA-cyclin C and HA-RV-cyclin phosphorylation detected on the auto-rad image shown in the left panel of Figure 4.7. This data suggests endogenous cyclin C from SF9 cells bound His-CDK8, and was present in the CDK8/RV-cyclin preparation. This will be something to consider in the future, and shRNA-mediated knock down of endogenous SF9 cyclin C might be beneficial before the cells are used for the protein isolation.

GST-CTD substrates were not phosphorylated by purified preparations of cyclin C/CDK8 or RV-cyclin/CDK8, in the  $P^{32}$  assay, and GST-CTD phosphorylation could not be distinguished from autophosphorylation in the ADP-glo assay (data not shown). Assays testing GST-CTD phosphorylation were also performed with cyclin/CDK8 preparations that had been pre-incubated with cold ATP, also met with no success. Previous work identified a dephosphorylating event, catalyzed by PP2A, as necessary for full CDK8 activation [82]. The observed autophosphorylation may, in fact, be inhibitory.

Accounts of the kinase activity of purified, recombinant cyclin C/CDK8 from baculovirus preparations differ in the literature; several laboratories describe preparations that phosphorylate GST-CTD substrates with only cyclin C/CDK8, while other authors indicate a requirement for Med12 in the production of functional, recombinant kinase [101]. As cyclin C was

phosphorylated by CDK8 in the RV-cyclin preparations (Fig 4.7), it is possible that certain preparations may be complemented by mediator components or phosphatases derived from Sf9 cells, providing the Med12 needed for activation. It may be necessary to produce recombinant, human Med12 in order to fully activate CDK8 in the co-purified complexes for kinetic studies. When completed, these assays will shed more light into RV-cyclin's control of CDK8 function. They might show that RV-cyclin not only brings CDK8 to the locus, as presented in Figures 3.8 and Figures 3.9, but it might also have a synergistic function, where it enhances the rate of CDK8 kinase activity.

In any case, RV-cyclin will be a valuable probe of CDK8 function. With it, new discoveries about CDK8 regulation could have implications in multiple disciplines of cellular and molecular biology due to CDK8 involvement in cancer development, the immune response, and metabolism. The recombinant protein complexes produced could be used to analyze CDK8 phosphorylation on the other CDK8 targets not tested and could uncover important information of CDK8 enzyme kinetics.

## CHAPTER 5: CONCLUDING REMARKS AND FUTURE DIRECTIONS

The RV-cyclin is able to activate expression of *FOS*, *EGRI*, *JUN*, *CCND1*, and *CDKN2D* (Figs 2.2-2.7 and Figs 3.7 and 3.8). These are potent proto-oncogenes in a number of cancers, or in the case of *CDKN2D*, promote cell survival. RV-cyclin's activation of the serum response genes, *FOS*, *EGRI*, and *JUN*, requires the presence of serum stimulation, in serum-responsive HCT116 cells (Figs 2.6 and 2.7). In HeLa cells, RV-cyclin was able to activate the serum response genes without serum stimulation (Fig 2.2). This could be due to aberrant phosphorylation of Elk-1 and SRF in HeLa cells, as a mechanism of their transformation by papillomavirus.

RV-cyclin's activation of the *EGRI* gene in particular is due to its interaction with both TAF9 and CDK8 (Figs 2.7 3.7-10). The interaction with CDK8 is of utmost importance in this activation. The CDK8-binding deficient mutant (K80A/E111A) does not activate *EGRI* transcripts above control levels upon serum response (Fig 2.7), and did not elevate *CDKN2D* expression in the inducible HeLa cells (Fig 2.5). Expression of this mutant was selected against in HCT116 cells, and over 300 clones were screened in attempts to find one stably expressing the mutant (data not shown). Upon analysis this mutant had decreased ability to activate *EGRI* upon serum stimulation when compared to the control (Fig 2.7) and recruited very little RNA Pol II and CDK8 to the locus (Fig 3.7 and 3.8). One speculative hypothesis is that the K80A/E111A mutant sequesters TAF9 with its functional activation domain, and this inhibits RNA Pol II transcription. The isolated RV-cyclin AD, when provided with a nuclear localization signal, has been shown to interfere with transcription activation via TAF9, and this interference was overcome with excess TAF9 [60].

The TAF9 interaction appears to be important for regulating RV-cyclin's initial activation of *EGR1* and *CDKN2D* expression (Fig 2.5 and 2.7) and for extending RNA Pol II transcription of *EGR1* far past the time when transcription of this locus is being shut-down in control cells. Comparison of the V260S mutant with the cyclin C-over expressing HCT116 cells in ChIP analysis showed that expression of the RV-cyclin cyclin box motif mimicked cyclin C over-expression (Fig 3.7 and 3.8). In many aspects the dual function of CDK8 and TAF9 is expected. When considering the HA-ChIP of RV-cyclin's location at the locus (Fig 3.10) with the other data presented, it is possible that the cyclin box may, in a fashion similar to a DNA-binding domain, guide the activation domain to certain key loci through its interaction with CDK8, this function is in addition to RV-cyclin's ability to enhance levels of CDK8 at certain loci. Future *in vitro* transcription assays may help in elucidating these parts of the mechanism of activation.

Although the kinase analysis of the recombinant co-purified CDK8/RV-cyclin and cyclin C complexes has not yet been completed, the tools are prepared for completion (Figs 4.2-4.7). Both co-purifications of CDK8 cyclin complexes are functional, and were able to autophosphorylate as demonstrated by both kinase assays employed (Fig 4.6 and 4.7). Future enzyme kinetic analysis may conclude that RV-cyclin enhances CDK8 kinase activity by speeding up the rate of phosphorylation on specific CDK8 targets. This would be a significant effect in addition to bringing more CDK8 to the locus (Figs. 3.8 and 3.9).

The fact that RV-cyclin requires initiation of serum response suggests that RV-cyclin expression alone is not sufficient to activate oncogenic gene expression in a walleye cell, and that to generate the tumor necessary for efficient WDSV replication, another signal would be required. For this reason, the next big step in the analysis of RV-cyclin in WDS tumor formation

would be to analyze serum response gene expression in HCT116 serum starved cells with the presence of both RV-cyclin and the Orf b protein. The hypothesis would be that under serum starvation conditions, the combination of the two viral proteins would cause activation and expression of the serum response genes. This un-regulated, continued activation of the proto-oncogenes would result in WDS tumor development, and is an example of a novel *trans*-acting mechanism of retroviral tumor development.

In addition to the co-expression experiment, it would be required to show that the serum response genes are activated in the developing dermal sarcoma. Preliminary analysis of RNA from fall tumors suggests that walleye *EGRI* levels are elevated when compared to regressing spring tumors (unpublished data not shown). However, more tumors and sequences of other walleye serum response genes are needed for a complete analysis.

This study of RV-cyclin function has not only provided a greater understanding of the mechanism of WDS tumor formation, but it has also highlighted key cellular proteins that regulate tumor development. CDK8 in particular has been implicated in multiple cellular processes that contribute to disease states, like metabolism, proliferation, and immunity. In conclusion, RV-cyclin's use as a probe of CDK8 function will continue to advance our understanding of CDK8's role in basic cellular biological processes. This is similar to the contributions made to the field by other oncogenic, retroviral proteins like Tax from HTLV-1 and the ENV protein from JSRV.

## REFERENCES

1. **Rosenberg, N. and J. P.** Retrovirus Pathogenesis, in *Retroviruses*, J.M. Coffin, S.E. Hughes, and H.E. Varmus, Editors. 1997, Cold Spring Harbor Laboratory Press: Cold Spring Harbor, NY. p. 475-586.
2. **Weiss, R.A. and P.K. Vogt.** 2011. 100 years of Rous sarcoma virus. *The Journal of experimental medicine.* **208**:2351-5.
3. **Rosenberg, N.**, Overview of retrovirology, in *Retroviruses and insights into cancer*, J. Dudley, Editor 2011, Springer Science+Business Media, LLC: New York, NY. p. 1-30.
4. **Kurth, R. and N. Bannert.** 2010. *Retroviruses : molecular biology, genomics and pathogenesis*, Caister Academic, Norfolk, UK.
5. **Mothes, W. and P.D. Uchil,** Retroviral entry and uncoating, in *Retroviruses*, R. Kurth and N. Bannert, Editors. 2010, Caister Academic Press: Norfolk, UK. p. 107-128.
6. **Hunter, E.**, Viral entry and Receptors, in *Retroviruses*, J.M. Coffin, S.E. Hughes, and H.E. Varmus, Editors. 1997, Cold Spring Harbor Laboratory Press: Plainview, NY. p. 71-119.
7. **Telesnitsky, A. and S.P. Goff,** Reverse transcriptase and the generation of retroviral DNA, in *Retroviruses*, J.M. Coffin, S.E. Hughes, and H.E. Varmus, Editors. 1997, Cold Spring Harbor Laboratory Press: Plainview, NY. p. 121-160.
8. **Brown, P.O.**, Integration, in *Retroviruses*, J.M. Coffin, S.E. Hughes, and H.E. Varmus, Editors. 1997, Cold Spring Harbor Laboratory Press: Plainview, NY. p. 161-204.
9. **Rabson, A.B. and B.J. Graves,** Synthesis and processing of viral RNA, in *Retroviruses*, J.M. Coffin, S.E. Hughes, and H.E. Varmus, Editors. 1997, Cold Spring Harbor Laboratory Press: Plainview, NY. p. 205-262.
10. **Swanstrom, R. and J.W. Wills,** Synthesis, assembly, and processing of viral proteins, in *Retroviruses*, J.M. Coffin, S.E. Hughes, and H.E. Varmus, Editors. 1997, Cold Spring Harbor Laboratory Press: Plainview, NY. p. 263-334.
11. **Norkin, L.** 2010. *Virology: Molecular Biology and Pathogenesis*, ASM Press, Washington, DC.
12. **Martineau, D., P.R. Bowser, R.R. Renshaw, and J.W. Casey.** 1992. Molecular characterization of a unique retrovirus associated with a fish tumor. *J. Virol.* **66**:596-599.
13. **Martineau, D., R. Renshaw, J.R. Williams, J.W. Casey, and P.R. Bowser.** 1991. A Large Unintegrated Retrovirus DNA Species Present in a Dermal Tumor of Walleye *Stizostedion-Vitreum*. *Dis. Aquat. Organ.* **10**:153-158.
14. **Holzschu, D.L., D. Martineau, S.K. Fodor, V.M. Vogt, P.R. Bowser, and J.W. Casey.** 1995. Nucleotide sequence and protein analysis of a complex piscine retrovirus, walleye dermal sarcoma virus. *J. Virol.* **69**:5320-31.
15. **Quackenbush, S.L., D.L. Holzschu, P.R. Bowser, and J.W. Casey.** 1997. Transcriptional analysis of walleye dermal sarcoma virus (WDSV). *Virology.* **237**:107-112.
16. **Cavazza, A., A. Moiani, and F. Mavilio.** 2013. Mechanisms of retroviral integration and mutagenesis. *Human gene therapy.* **24**:119-31.
17. **Fan, H.**, Retroviruses and their role in cancer, in *The Retroviridae*, J. Levy, Editor 1994, Plenum Press: New York, NY. p. 313-362.

18. **Beemon, K.L. and M. Bolisetty**, Mechanisms of oncogenesis by retroviruses, in *Retroviruses and Insights into Cancer*, J. Dudley, Editor 2011, Springer Science+Business Media: New York, NY. p. 31-52.
19. **Fan, H., M. Palmarini, and J.C. DeMartini**. 2003. Transformation and oncogenesis by jaagsiekte sheep retrovirus. *Current Topics in Microbiology and Immunology*. **275**:139-77.
20. **Cook, L.B., M. Elemans, A.G. Rowan, and B. Asquith**. 2013. HTLV-1: persistence and pathogenesis. *Virology*. **435**:131-40.
21. **Zane, L. and K.T. Jeang**. 2014. HTLV-1 and leukemogenesis: virus-cell interactions in the development of adult T-cell leukemia. Recent results in cancer research. *Fortschritte der Krebsforschung. Progres dans les recherches sur le cancer*. **193**:191-210.
22. **Moules, V., C. Pomier, D. Sibon, A.S. Gabet, M. Reichert, P. Kerkhofs, L. Willems, F. Mortreux, and E. Wattel**. 2005. Fate of premalignant clones during the asymptomatic phase preceding lymphoid malignancy. *Cancer Res*. **65**:1234-43.
23. **Kim, Y.M., T.R. Geiger, D.I. Egan, N. Sharma, and J.K. Nyborg**. 2010. The HTLV-1 tax protein cooperates with phosphorylated CREB, TORC2 and p300 to activate CRE-dependent cyclin D1 transcription. *Oncogene*. **29**:2142-52.
24. **Grassmann, R., M. Aboud, and K.T. Jeang**. 2005. Molecular mechanisms of cellular transformation by HTLV-1 Tax. *Oncogene*. **24**:5976-85.
25. **Kimzey, A.L. and W.S. Dynan**. 1998. Specific regions of contact between human T-cell leukemia virus type I Tax protein and DNA identified by photocross-linking. *J Biol Chem*. **273**:13768-75.
26. **Nyborg, J.K., D. Egan, and N. Sharma**. 2010. The HTLV-1 Tax protein: revealing mechanisms of transcriptional activation through histone acetylation and nucleosome disassembly. *Biochim Biophys Acta*. **1799**:266-74.
27. **Geiger, T.R., N. Sharma, Y.M. Kim, and J.K. Nyborg**. 2008. The human T-cell leukemia virus type 1 tax protein confers CBP/p300 recruitment and transcriptional activation properties to phosphorylated CREB. *Mol Cell Biol*. **28**:1383-92.
28. **Verwoerd, D.W.** 1985. Biotechnology, viral oncogenesis and jaagsiekte. *The Onderstepoort Journal of Veterinary Research*. **52**:145-8.
29. **Demartini, J.C., R.H. Rosadio, and M.D. Lairmore**. 1988. The etiology and pathogenesis of ovine pulmonary carcinoma (sheep pulmonary adenomatosis). *Veterinary Microbiology*. **17**:219-36.
30. **Hofacre, A. and H. Fan**. 2010. Jaagsiekte sheep retrovirus biology and oncogenesis. *Viruses*. **2**:2618-48.
31. **Maeda, N., M. Palmarini, C. Murgia, and H. Fan**. 2001. Direct transformation of rodent fibroblasts by jaagsiekte sheep retrovirus DNA. *Proc Natl Acad Sci U S A*. **98**:4449-54.
32. **Palmarini, M., N. Maeda, C. Murgia, C. De-Fraja, A. Hofacre, and H. Fan**. 2001. A phosphatidylinositol 3-kinase docking site in the cytoplasmic tail of the Jaagsiekte sheep retrovirus transmembrane protein is essential for envelope-induced transformation of NIH 3T3 cells. *J Virol*. **75**:11002-9.
33. **Allen, T.E., K.J. Sherrill, S.M. Crispell, M.R. Perrott, J.O. Carlson, and J.C. DeMartini**. 2002. The jaagsiekte sheep retrovirus envelope gene induces transformation of the avian fibroblast cell line DF-1 but does not require a conserved SH2 binding domain. *J Gen Virol*. **83**:2733-42.

34. **Wootton, S.K., C.L. Halbert, and A.D. Miller.** 2005. Sheep retrovirus structural protein induces lung tumours. *Nature*. **434**:904-7.
35. **Caporale, M., C. Cousens, P. Centorame, C. Pinoni, M. De las Heras, and M. Palmarini.** 2006. Expression of the jaagsiekte sheep retrovirus envelope glycoprotein is sufficient to induce lung tumors in sheep. *J Virol*. **80**:8030-7.
36. **Maeda, N., W. Fu, A. Ortin, M. de las Heras, and H. Fan.** 2005. Roles of the Ras-MEK-mitogen-activated protein kinase and phosphatidylinositol 3-kinase-Akt-mTOR pathways in Jaagsiekte sheep retrovirus-induced transformation of rodent fibroblast and epithelial cell lines. *J Virol*. **79**:4440-50.
37. **Hull, S., J. Lim, A. Hamil, T. Nitta, and H. Fan.** 2012. Analysis of jaagsiekte sheep retrovirus (JSRV) envelope protein domains in transformation. *Virus Genes*. **45**:508-17.
38. **Walker, R.** 1969. Virus associated with epidermal hyperplasia in fish. National Cancer Institute monograph. **31**:195-207.
39. **Yamamoto, T., R.D. MacDonald, D.C. Gillespie, and R.K. Kelly.** 1976. Viruses associates with lymphocystis and dermal sarcoma of walleye (*Stizostedion vitreum vitreum*). *J. Fish. Res. Board Can.* **33**:2408-2419.
40. **Rovnak, J., R.N. Casey, C.D. Brewster, J.W. Casey, and S.L. Quackenbush.** 2007. Establishment of productively infected walleye dermal sarcoma explant cells. *J. Gen. Virol.* **88**:2583-9.
41. **Bowser, P.R., G.A. Wooster, S.L. Quackenbush, R.N. Casey, and J.W. Casey.** 1996. Communications: Comparison of Fall and Spring Tumors as Inocula for Experimental Transmission of Walleye Dermal Sarcoma. *J. Aquat. Anim. Health*. **8**:78-81.
42. **Rovnak, J. and S.L. Quackenbush.** 2010. Walleye dermal sarcoma virus: molecular biology and oncogenesis. *Viruses*. **2**:1984-1999.
43. **LaPierre, L.A., D.L. Holzschu, P.R. Bowser, and J.W. Casey.** 1999. Sequence and transcriptional analyses of the fish retroviruses walleye epidermal hyperplasia virus types 1 and 2: evidence for a gene duplication. *J Virol*. **73**:9393-403.
44. **Bowser, P., D. Martineau, and G. Wooster.** 1990. Effects of water temperature on experimental transmission of dermal sarcoma in fingerling walleyes (*Stizostedion vitreum*). *J. Aquat. Anim. Health*. **2**:157-161.
45. **Martineau, D., P.R. Bowser, G.A. Wooster, and L.D. Armstrong.** 1990. Experimental transmission of a dermal sarcoma in fingerling walleyes (*Stizostedion vitreum vitreum*). *Veterinary pathology*. **27**:230-4.
46. **Bowser, P.R., G. Wooster, and R.G. Getchell.** 1999. Transmission of walleye dermal sarcoma and lymphocystis via waterborne exposure. *J. Aquat. Anim. Health*. **11**:158-161.
47. **Bowser, P.R., M.J. Wolfe, J.L. Forney, and G.A. Wooster.** 1988. Seasonal prevalence of skin tumors from walleye (*Stizostedion vitreum*) from Oneida Lake, New York. *J. Wildl. Dis.* **24**:292-298.
48. **Bowser, P.R. and G.A. Wooster.** 1991. Regression of Dermal Sarcoma in Adult Walleyes. *J. Aquat. Anim. Health*. **3**:147-150.
49. **LaPierre, L.A., J.W. Casey, and D.L. Holzschu.** 1998. Walleye retroviruses associated with skin tumors and hyperplasias encode cyclin D homologs. *J. Virol*. **72**:8765-8771.
50. **Daniels, C.C., J. Rovnak, and S.L. Quackenbush.** 2008. Walleye dermal sarcoma virus Orf B functions through receptor for activated C kinase (RACK1) and protein kinase C. *Virology*. **375**:550-60.

51. **Nudson, W.A., J. Rovnak, M. Buechner, and S.L. Quackenbush.** 2003. Walleye dermal sarcoma virus Orf C is targeted to the mitochondria. *J Gen Virol.* **84**:375-81.
52. **Rovnak, J., J.W. Casey, and S.L. Quackenbush.** 2001. Intracellular targeting of walleye dermal sarcoma virus Orf A (rv-cyclin). *Virology.* **280**:31-40.
53. **Quackenbush, S.L., J. Rovnak, R.N. Casey, T.A. Paul, P.R. Bowser, C. Sutton, and J.W. Casey.** 2001. Genetic relationship of tumor-associated piscine retroviruses. *Mar Biotechnol (NY).* **3**:S88-99.
54. **Magden, E.,** Walleye dermal sarcoma virus orf C: a potential oncolytic therapy. The Department of Microbiology, Immunology, and Pathology 2011, Colorado State University.
55. **Daniels, C.C.,** Characterization of walleye dermal sarcoma virus orf b during tumor development. The Department of Microbiology, Immunology and Pathology 2008, Colorado State University.
56. **Lairmore, M.D., J.R. Stanley, S.A. Weber, and D.L. Holzschu.** 2000. Squamous epithelial proliferation induced by walleye dermal sarcoma retrovirus cyclin in transgenic mice. *Proc. Natl. Acad. Sci. U. S. A.* **97**:6114-9.
57. **Brewster, C.D., C.H. Birkenheuer, M.B. Vogt, S.L. Quackenbush, and J. Rovnak.** 2011. The retroviral cyclin of walleye dermal sarcoma virus binds cyclin-dependent kinases 3 and 8. *Virology.* **409**:299-307.
58. **Rovnak, J. and S.L. Quackenbush.** 2002. Walleye dermal sarcoma virus cyclin interacts with components of the mediator complex and the RNA polymerase II holoenzyme. *J. Virol.* **76**:8031-8039.
59. **Quackenbush, S.L., A. Linton, C.D. Brewster, and J. Rovnak.** 2009. Walleye dermal sarcoma virus rv-cyclin inhibits NF-kappaB-dependent transcription. *Virology.* **386**:55-60.
60. **Rovnak, J., B.W. Hronek, S.O. Ryan, S. Cai, and S.L. Quackenbush.** 2005. An activation domain within the walleye dermal sarcoma virus retroviral cyclin protein is essential for inhibition of the viral promoter. *Virology.* **342**:240-251.
61. **Rovnak, J. and S.L. Quackenbush.** 2006. Walleye dermal sarcoma virus retroviral cyclin directly contacts TAF9. *J. Virol.* **80**:12041-12048.
62. **Choi, Y.J. and L. Anders.** 2014. Signaling through cyclin D-dependent kinases. *Oncogene.* **33**:1890-903.
63. **Tsujimoto, Y., E. Jaffe, J. Cossman, J. Gorham, P.C. Nowell, and C.M. Croce.** 1985. Clustering of breakpoints on chromosome 11 in human B-cell neoplasms with the t(11;14) chromosome translocation. *Nature.* **315**:340-3.
64. **Tsujimoto, Y., J. Yunis, L. Onorato-Showe, J. Erikson, P.C. Nowell, and C.M. Croce.** 1984. Molecular cloning of the chromosomal breakpoint of B-cell lymphomas and leukemias with the t(11;14) chromosome translocation. *Science.* **224**:1403-6.
65. **Arnold, A., T. Motokura, T. Bloom, H. Kronenberg, J. Ruderman, H. Juppner, and H.G. Kim.** 1991. The putative oncogene PRAD1 encodes a novel cyclin. *Cold Spring Harbor Symposia on Quantitative Biology.* **56**:93-7.
66. **Motokura, T., T. Bloom, H.G. Kim, H. Juppner, J.V. Ruderman, H.M. Kronenberg, and A. Arnold.** 1991. A novel cyclin encoded by a bcl1-linked candidate oncogene. *Nature.* **350**:512-5.
67. **Kim, J.K. and J.A. Diehl.** 2009. Nuclear cyclin D1: an oncogenic driver in human cancer. *Journal of Cellular Physiology.* **220**:292-6.

68. **Sherr, C.J. and J.M. Roberts.** 1999. CDK inhibitors: positive and negative regulators of G1-phase progression. *Genes Dev.* **13**:1501-12.
69. **Alt, J.R., J.L. Cleveland, M. Hannink, and J.A. Diehl.** 2000. Phosphorylation-dependent regulation of cyclin D1 nuclear export and cyclin D1-dependent cellular transformation. *Genes Dev.* **14**:3102-14.
70. **Diehl, J.A., F. Zindy, and C.J. Sherr.** 1997. Inhibition of cyclin D1 phosphorylation on threonine-286 prevents its rapid degradation via the ubiquitin-proteasome pathway. *Genes Dev.* **11**:957-72.
71. **Musgrove, E.A., C.E. Caldon, J. Barraclough, A. Stone, and R.L. Sutherland.** 2011. Cyclin D as a therapeutic target in cancer. *Nat Rev Cancer.* **11**:558-72.
72. **Santarius, T., J. Shipley, D. Brewer, M.R. Stratton, and C.S. Cooper.** 2010. A census of amplified and overexpressed human cancer genes. *Nat Rev Cancer.* **10**:59-64.
73. **Guan, K.L., C.W. Jenkins, Y. Li, C.L. O'Keefe, S. Noh, X. Wu, M. Zariwala, A.G. Matera, and Y. Xiong.** 1996. Isolation and characterization of p19INK4d, a p16-related inhibitor specific to CDK6 and CDK4. *Molecular biology of the cell.* **7**:57-70.
74. **Hirai, H., M.F. Roussel, J.Y. Kato, R.A. Ashmun, and C.J. Sherr.** 1995. Novel INK4 proteins, p19 and p18, are specific inhibitors of the cyclin D-dependent kinases CDK4 and CDK6. *Mol Cell Biol.* **15**:2672-81.
75. **Thullberg, M., J. Bartkova, S. Khan, K. Hansen, L. Ronnstrand, J. Lukas, M. Strauss, and J. Bartek.** 2000. Distinct versus redundant properties among members of the INK4 family of cyclin-dependent kinase inhibitors. *FEBS letters.* **470**:161-6.
76. **Ogara, M.F., P.F. Sirkin, A.L. Carcagno, M.C. Marazita, S.V. Sonzogni, J.M. Ceruti, and E.T. Canepa.** 2013. Chromatin relaxation-mediated induction of p19INK4d increases the ability of cells to repair damaged DNA. *PloS one.* **8**:e61143.
77. **Zindy, F., J.J. Cunningham, C.J. Sherr, S. Jogle, R.J. Smeyne, and M.F. Roussel.** 1999. Postnatal neuronal proliferation in mice lacking Ink4d and Kip1 inhibitors of cyclin-dependent kinases. *Proc Natl Acad Sci U S A.* **96**:13462-7.
78. **Zindy, F., J. van Deursen, G. Grosveld, C.J. Sherr, and M.F. Roussel.** 2000. INK4d-deficient mice are fertile despite testicular atrophy. *Mol Cell Biol.* **20**:372-8.
79. **Ortega, S., M. Malumbres, and M. Barbacid.** 2002. Cyclin D-dependent kinases, INK4 inhibitors and cancer. *Biochim Biophys Acta.* **1602**:73-87.
80. **Ceruti, J.M., M.E. Scassa, J.M. Flo, C.L. Varone, and E.T. Canepa.** 2005. Induction of p19INK4d in response to ultraviolet light improves DNA repair and confers resistance to apoptosis in neuroblastoma cells. *Oncogene.* **24**:4065-80.
81. **Scassa, M.E., M.C. Marazita, J.M. Ceruti, A.L. Carcagno, P.F. Sirkin, M. Gonzalez-Cid, O.P. Pignataro, and E.T. Canepa.** 2007. Cell cycle inhibitor, p19INK4d, promotes cell survival and decreases chromosomal aberrations after genotoxic insult due to enhanced DNA repair. *DNA repair.* **6**:626-38.
82. **Rovnak, J., C.D. Brewster, and S.L. Quackenbush.** 2012. The Retroviral Cyclin Enhances Cyclin Dependent Kinase 8 Activity. *J. Virol.* **86**:5742-5751.
83. **Cler, E., G. Papai, P. Schultz, and I. Davidson.** 2009. Recent advances in understanding the structure and function of general transcription factor TFIID. *Cell Mol Life Sci.* **66**:2123-34.
84. **Baumann, M., J. Pontiller, and W. Ernst.** 2010. Structure and basal transcription complex of RNA polymerase II core promoters in the mammalian genome: an overview. *Molecular Biotechnology.* **45**:241-7.

85. **Bieniossek, C., G. Papai, C. Schaffitzel, F. Garzoni, M. Chaillet, E. Scheer, P. Papadopoulos, L. Tora, P. Schultz, and I. Berger.** 2013. The architecture of human general transcription factor TFIID core complex. *Nature*. **493**:699-702.
86. **Papai, G., P.A. Weil, and P. Schultz.** 2011. New insights into the function of transcription factor TFIID from recent structural studies. *Current Opinion in Genetics & Development*. **21**:219-24.
87. **Carey, M., C.L. Peterson, and S.T. Smale.** 2009. *Transcriptional regulation in eukaryotes : concepts, strategies, and techniques*. 2nd ed, Cold Spring Harbor Laboratory Press, Cold Spring Harbor, N.Y.
88. **Burke, T.W. and J.T. Kadonaga.** 1997. The downstream core promoter element, DPE, is conserved from *Drosophila* to humans and is recognized by TAFII60 of *Drosophila*. *Genes Dev*. **11**:3020-31.
89. **Chen, Z. and J.L. Manley.** 2003. Core promoter elements and TAFs contribute to the diversity of transcriptional activation in vertebrates. *Mol Cell Biol*. **23**:7350-62.
90. **Saint, M., S. Sawhney, I. Sinha, R.P. Singh, R. Dahiya, A. Thakur, R. Siddharthan, and K. Natarajan.** 2014. The TAF9 C-terminal conserved region domain is required for SAGA and TFIID promoter occupancy to promote transcriptional activation. *Mol Cell Biol*. **34**:1547-63.
91. **Xing, H., N.L. Vanderford, and K.D. Sarge.** 2008. The TBP-PP2A mitotic complex bookmarks genes by preventing condensin action. *Nature Cell Biology*. **10**:1318-23.
92. **Choi, Y., S. Asada, and M. Uesugi.** 2000. Divergent hTAFII31-binding motifs hidden in activation domains. *J Biol Chem*. **275**:15912-6.
93. **Uesugi, M., O. Nyanguile, H. Lu, A.J. Levine, and G.L. Verdine.** 1997. Induced alpha helix in the VP16 activation domain upon binding to a human TAF. *Science*. **277**:1310-3.
94. **Uesugi, M. and G.L. Verdine.** 1999. The alpha-helical FXXPhiPhi motif in p53: TAF interaction and discrimination by MDM2. *Proc Natl Acad Sci U S A*. **96**:14801-6.
95. **Blazek, E., G. Mittler, and M. Meisterernst.** 2005. The mediator of RNA polymerase II. *Chromosoma*. **113**:399-408.
96. **Kornberg, R.D.** 2005. Mediator and the mechanism of transcriptional activation. *Trends in Biochemical Sciences*. **30**:235-9.
97. **Galbraith, M.D., M.A. Allen, C.L. Bensard, X. Wang, M.K. Schwinn, B. Qin, H.W. Long, D.L. Daniels, W.C. Hahn, R.D. Dowell, and J.M. Espinosa.** 2013. HIF1A Employs CDK8-Mediator to Stimulate RNAPII Elongation in Response to Hypoxia. *Cell*. **153**:1327-1339.
98. **Tsutsui, T., H. Umemura, A. Tanaka, F. Mizuki, Y. Hirose, and Y. Ohkuma.** 2008. Human mediator kinase subunit CDK11 plays a negative role in viral activator VP16-dependent transcriptional regulation. *Genes to Cells : Devoted to Molecular & Cellular Mechanisms*. **13**:817-26.
99. **Belakavadi, M. and J.D. Fondell.** 2010. Cyclin-dependent kinase 8 positively cooperates with Mediator to promote thyroid hormone receptor-dependent transcriptional activation. *Mol. Cell. Biol*. **30**:2437-2448.
100. **Galbraith, M.D., A.J. Donner, and J.M. Espinosa.** 2010. CDK8: A positive regulator of transcription. *Transcription*. **1**:4-12.
101. **Knuesel, M.T., K.D. Meyer, C. Bernecky, and D.J. Taatjes.** 2009. The human CDK8 subcomplex is a molecular switch that controls Mediator coactivator function. *Genes. Dev*. **23**:439-451.

102. **Knuesel, M.T., K.D. Meyer, A.J. Donner, J.M. Espinosa, and D.J. Taatjes.** 2009. The human CDK8 subcomplex is a histone kinase that requires Med12 for activity and can function independently of mediator. *Mol. Cell. Biol.* **29**:650-661.
103. **Ramanathan, Y., S.M. Rajpara, S.M. Reza, E. Lees, S. Shuman, M.B. Mathews, and T. Pe'ery.** 2001. Three RNA polymerase II carboxyl-terminal domain kinases display distinct substrate preferences. *J Biol Chem.* **276**:10913-20.
104. **Dahmus, M.E.** 1994. The role of multisite phosphorylation in the regulation of RNA polymerase II activity. *Progress in Nucleic Acid Research and Molecular Biology.* **48**:143-79.
105. **Rickert, P., J.L. Corden, and E. Lees.** 1999. Cyclin C/CDK8 and cyclin H/CDK7/p36 are biochemically distinct CTD kinases. *Oncogene.* **18**:1093-1102.
106. **Rickert, P., W. Seghezzi, F. Shanahan, H. Cho, and E. Lees.** 1996. Cyclin C/CDK8 is a novel CTD kinase associated with RNA polymerase II. *Oncogene.* **12**:2631-2640.
107. **Marshall, N.F., J. Peng, Z. Xie, and D.H. Price.** 1996. Control of RNA polymerase II elongation potential by a novel carboxyl-terminal domain kinase. *J. Biol. Chem.* **271**:27176-27183.
108. **Buratowski, S.** 2009. Progression through the RNA polymerase II CTD cycle. *Mol Cell.* **36**:541-6.
109. **Feaver, W.J., J.Q. Svejstrup, N.L. Henry, and R.D. Kornberg.** 1994. Relationship of CDK-activating kinase and RNA polymerase II CTD kinase TFIIF/TFIIK. *Cell.* **79**:1103-1109.
110. **Glover-Cutter, K., S. Larochele, B. Erickson, C. Zhang, K. Shokat, R.P. Fisher, and D.L. Bentley.** 2009. TFIIF-associated Cdk7 kinase functions in phosphorylation of C-terminal domain Ser7 residues, promoter-proximal pausing, and termination by RNA polymerase II. *Mol Cell Biol.* **29**:5455-64.
111. **Peterlin, B.M. and D.H. Price.** 2006. Controlling the elongation phase of transcription with P-TEFb. *Mol Cell.* **23**:297-305.
112. **Ni, Z., A. Saunders, N.J. Fuda, J. Yao, J.R. Suarez, W.W. Webb, and J.T. Lis.** 2008. P-TEFb is critical for the maturation of RNA polymerase II into productive elongation in vivo. *Mol Cell Biol.* **28**:1161-70.
113. **Fabrega, C., V. Shen, S. Shuman, and C.D. Lima.** 2003. Structure of an mRNA capping enzyme bound to the phosphorylated carboxy-terminal domain of RNA polymerase II. *Mol Cell.* **11**:1549-61.
114. **Ng, H.H., F. Robert, R.A. Young, and K. Struhl.** 2003. Targeted recruitment of Set1 histone methylase by elongating Pol II provides a localized mark and memory of recent transcriptional activity. *Mol Cell.* **11**:709-19.
115. **Shandilya, J. and S.G. Roberts.** 2012. The transcription cycle in eukaryotes: from productive initiation to RNA polymerase II recycling. *Biochim Biophys Acta.* **1819**:391-400.
116. **Ahn, S.H., M. Kim, and S. Buratowski.** 2004. Phosphorylation of Serine 2 within the RNA Polymerase II C-Terminal Domain Couples Transcription and 3' End Processing. *Mol. Cell.* **13**:67-76.
117. **Liu, Y., C. Kung, J. Fishburn, A.Z. Ansari, K.M. Shokat, and S. Hahn.** 2004. Two cyclin-dependent kinases promote RNA polymerase II transcription and formation of the scaffold complex. *Mol Cell Biol.* **24**:1721-35.

118. **Hengartner, C.J., V.E. Myer, S.M. Liao, C.J. Wilson, S.S. Koh, and R.A. Young.** 1998. Temporal regulation of RNA polymerase II by Srb10 and Kin28 cyclin-dependent kinases. *Mol Cell.* **2**:43-53.
119. **Carlson, M.** 1997. Genetics of transcriptional regulation in yeast: connections to the RNA polymerase II CTD. *Annual Review of Cell and Developmental Biology.* **13**:1-23.
120. **Kuchin, S. and M. Carlson.** 1998. Functional relationships of Srb10-Srb11 kinase, carboxy-terminal domain kinase CTDK-I, and transcriptional corepressor Ssn6-Tup1. *Mol. Cell. Biol.* **18**:1163-1171.
121. **Donner, A.J., C.C. Ebmeier, D.J. Taatjes, and J.M. Espinosa.** 2010. CDK8 is a positive regulator of transcriptional elongation within the serum response network. *Nat. Struct. Mol. Biol.* **17**:194-201.
122. **Donner, A.J., S. Szostek, J.M. Hoover, and J.M. Espinosa.** 2007. CDK8 is a stimulus-specific positive coregulator of p53 target genes. *Mol. Cell.* **27**:121-133.
123. **Firestein, R., A.J. Bass, S.Y. Kim, I.F. Dunn, S.J. Silver, I. Guney, E. Freed, A.H. Ligon, N. Vena, S. Ogino, M.G. Chheda, P. Tamayo, S. Finn, Y. Shrestha, J.S. Boehm, S. Jain, E. Bojarski, C. Mermel, J. Barretina, J.A. Chan, J. Baselga, J. Tabernero, D.E. Root, C.S. Fuchs, M. Loda, R.A. Shivdasani, M. Meyerson, and W.C. Hahn.** 2008. CDK8 is a colorectal cancer oncogene that regulates beta-catenin activity. *Nature.* **455**:547-551.
124. **Tsutsui, T., R. Fukasawa, A. Tanaka, Y. Hirose, and Y. Ohkuma.** 2011. Identification of target genes for the CDK subunits of the Mediator complex. *Genes to cells : devoted to molecular & cellular mechanisms.*
125. **Porter, D.C., E. Farmaki, S. Altilia, G.P. Schools, D.K. West, M. Chen, B.D. Chang, A.T. Puzyrev, C.U. Lim, R. Rokow-Kittell, L.T. Friedhoff, A.G. Papavassiliou, S. Kalurupalle, G. Hurteau, J. Shi, P.S. Baran, B. Gyorffy, M.P. Wentland, E.V. Broude, H. Kiaris, and I.B. Roninson.** 2012. Cyclin-dependent kinase 8 mediates chemotherapy-induced tumor-promoting paracrine activities. *Proc. Natl. Acad. Sci. U. S. A.* **109**:13799-13804.
126. **Tsai, K.L., S. Sato, C. Tomomori-Sato, R.C. Conaway, J.W. Conaway, and F.J. Asturias.** 2013. A conserved Mediator-CDK8 kinase module association regulates Mediator-RNA polymerase II interaction. *Nat Struct Mol Biol.* **20**:611-9.
127. **Zhao, J., R. Ramos, and M. Demma.** 2012. CDK8 regulates E2F1 transcriptional activity through S375 phosphorylation. *Oncogene.* doi: 10.1038/onc.2012.364.
128. **Zhao, X., D. Feng, Q. Wang, A. Abdulla, X.J. Xie, J. Zhou, Y. Sun, E.S. Yang, L.P. Liu, B. Vaitheesvaran, L. Bridges, I.J. Kurland, R. Strich, J.Q. Ni, C. Wang, J. Ericsson, J.E. Pessin, J.Y. Ji, and F. Yang.** 2012. Regulation of lipogenesis by cyclin-dependent kinase 8-mediated control of SREBP-1. *J. Clin. Invest.* doi: 10.1172/JCI61462.
129. **Bancerek, J., Z.C. Poss, I. Steinparzer, V. Sedlyarov, T. Pfaffenwimmer, I. Mikulic, L. Dolken, B. Strobl, M. Muller, D.J. Taatjes, and P. Kovarik.** 2013. CDK8 kinase phosphorylates transcription factor STAT1 to selectively regulate the interferon response. *Immunity.* **38**:250-262.
130. **Akoulitchev, S., S. Chuikov, and D. Reinberg.** 2000. TFIID is negatively regulated by cdk8-containing mediator complexes. *Nature.* **407**:102-106.

131. **Fryer, C.J., J.B. White, and K.A. Jones.** 2004. Mastermind recruits CycC:CDK8 to phosphorylate the Notch ICD and coordinate activation with turnover. *Mol Cell.* **16**:509-20.
132. **Morris, E.J., J.Y. Ji, F. Yang, L. Di Stefano, A. Herr, N.S. Moon, E.J. Kwon, K.M. Haigis, A.M. Naar, and N.J. Dyson.** 2008. E2F1 represses beta-catenin transcription and is antagonized by both pRB and CDK8. *Nature.* **455**:552-556.
133. **Xu, W. and J.Y. Ji.** 2011. Dysregulation of CDK8 and Cyclin C in tumorigenesis. *J. Genet. Genomics.* **38**:439-452.
134. **Hsu, J.Y., Z.W. Sun, X. Li, M. Reuben, K. Tatchell, D.K. Bishop, J.M. Grushcow, C.J. Brame, J.A. Caldwell, D.F. Hunt, R. Lin, M.M. Smith, and C.D. Allis.** 2000. Mitotic phosphorylation of histone H3 is governed by Ipl1/aurora kinase and Glc7/PP1 phosphatase in budding yeast and nematodes. *Cell.* **102**:279-91.
135. **Soloaga, A., S. Thomson, G.R. Wiggin, N. Rampersaud, M.H. Dyson, C.A. Hazzalin, L.C. Mahadevan, and J.S. Arthur.** 2003. MSK2 and MSK1 mediate the mitogen- and stress-induced phosphorylation of histone H3 and HMG-14. *EMBO J.* **22**:2788-97.
136. **Choi, H.S., B.Y. Choi, Y.Y. Cho, H. Mizuno, B.S. Kang, A.M. Bode, and Z. Dong.** 2005. Phosphorylation of histone H3 at serine 10 is indispensable for neoplastic cell transformation. *Cancer Res.* **65**:5818-27.
137. **Suzuki, T., K. Kita, and T. Ochi.** 2013. Phosphorylation of histone H3 at serine 10 has an essential role in arsenite-induced expression of FOS, EGR1 and IL8 mRNA in cultured human cell lines. *J. Appl. Toxicol.* **33**:746-755.
138. **Ivaldi, M.S., C.S. Karam, and V.G. Corces.** 2007. Phosphorylation of histone H3 at Ser10 facilitates RNA polymerase II release from promoter-proximal pausing in *Drosophila*. *Genes Dev.* **21**:2818-31.
139. **Meyer, K.D., A.J. Donner, M.T. Knuesel, A.G. York, J.M. Espinosa, and D.J. Taatjes.** 2008. Cooperative activity of cdk8 and GCN5L within Mediator directs tandem phosphoacetylation of histone H3. *EMBO J.* **27**:1447-1457.
140. **Firestein, R. and W.C. Hahn.** 2009. Revving the Throttle on an oncogene: CDK8 takes the driver seat. *Cancer Res.* **69**:7899-7901.
141. **Firestein, R., K. Shima, K. Nosh, N. Irahara, Y. Baba, E. Bojarski, E.L. Giovannucci, W.C. Hahn, C.S. Fuchs, and S. Ogino.** 2010. CDK8 expression in 470 colorectal cancers in relation to beta-catenin activation, other molecular alterations and patient survival. *Int. J. Cancer.* **126**:2863-2873.
142. **Kapoor, A., M.S. Goldberg, L.K. Cumberland, K. Ratnakumar, M.F. Segura, P.O. Emanuel, S. Menendez, C. Vardabasso, G. Leroy, C.I. Vidal, D. Polsky, I. Osman, B.A. Garcia, E. Hernando, and E. Bernstein.** 2010. The histone variant macroH2A suppresses melanoma progression through regulation of CDK8. *Nature.* **468**:1105-1109.
143. **Ren, S. and B.J. Rollins.** 2004. Cyclin C/cdk3 promotes Rb-dependent G0 exit. *Cell.* **117**:239-51.
144. **Eferl, R. and E.F. Wagner.** 2003. AP-1: a double-edged sword in tumorigenesis. *Nature reviews. Cancer.* **3**:859-868.
145. **Vogt, P.K.** 1995. The story of Jun. *Archives of biochemistry and biophysics.* **316**:1-4.
146. **Sukhatme, V.P.** 1990. Early transcriptional events in cell growth: the Egr family. *J. Am. Soc. Nephrol.* **1**:859-866.
147. **Curran, T. and N.M. Teich.** 1982. Candidate product of the FBJ murine osteosarcoma virus oncogene: characterization of a 55,000-dalton phosphoprotein. *J. Virol.* **42**:114-22.

148. **Shaulian, E. and M. Karin.** 2002. AP-1 as a regulator of cell life and death. *Nature cell biology.* **4**:E131-6.
149. **Maki, Y., T.J. Bos, C. Davis, M. Starbuck, and P.K. Vogt.** 1987. Avian sarcoma virus 17 carries the jun oncogene. *Proc. Natl. Acad. Sci. U. S. A.* **84**:2848-52.
150. **Jochum, W., E. Passegue, and E.F. Wagner.** 2001. AP-1 in mouse development and tumorigenesis. *Oncogene.* **20**:2401-12.
151. **Angel, P. and M. Karin.** 1991. The role of Jun, Fos and the AP-1 complex in cell-proliferation and transformation. *Biochim Biophys Acta.* **1072**:129-57.
152. **Lopez-Bergami, P., C. Huang, J.S. Goydos, D. Yip, M. Bar-Eli, M. Herlyn, K.S. Smalley, A. Mahale, A. Eroshkin, S. Aaronson, and Z. Ronai.** 2007. Rewired ERK-JNK signaling pathways in melanoma. *Cancer Cell.* **11**:447-460.
153. **Sukhatme, V.P., S. Kartha, F.G. Toback, R. Taub, R.G. Hoover, and C.H. Tsai-Morris.** 1987. A novel early growth response gene rapidly induced by fibroblast, epithelial cell and lymphocyte mitogens. *Oncogene Res.* **1**:343-55.
154. **Sauer, L., D. Gitenay, C. Vo, and V.T. Baron.** 2010. Mutant p53 initiates a feedback loop that involves Egr-1/EGF receptor/ERK in prostate cancer cells. *Oncogene.* **29**:2628-2637.
155. **Riggs, P.K., O. Rho, and J. DiGiovanni.** 2000. Alteration of Egr-1 mRNA during multistage carcinogenesis in mouse skin. *Molecular carcinogenesis.* **27**:247-51.
156. **Baron, V., S. Duss, J. Rhim, and D. Mercola.** 2003. Antisense to the early growth response-1 gene (Egr-1) inhibits prostate tumor development in TRAMP mice. *Ann N Y Acad Sci.* **1002**:197-216.
157. **Thiel, G. and G. Cibelli.** 2002. Regulation of life and death by the zinc finger transcription factor Egr-1. *Journal of cellular physiology.* **193**:287-92.
158. **Virolle, T., A. Kronen-Herzig, V. Baron, G. De Gregorio, E.D. Adamson, and D. Mercola.** 2003. Egr1 promotes growth and survival of prostate cancer cells. Identification of novel Egr1 target genes. *J. Biol. Chem.* **278**:11802-11810.
159. **Ernst, A., M. Aigner, S. Nakata, F. Engel, M. Schlotter, M. Kloor, K. Brand, S. Schmitt, G. Steinert, N. Rahbari, M. Koch, B. Radlwimmer, J. Weitz, and P. Lichter.** 2011. A gene signature distinguishing CD133hi from CD133- colorectal cancer cells: essential role for EGR1 and downstream factors. *Pathology.* **43**:220-227.
160. **Qiu, Y.L., W. Wang, T. Wang, J. Liu, P. Sun, J. Qian, L. Jin, and Z.L. Xia.** 2008. Genetic polymorphisms, messenger RNA expression of p53, p21, and CCND1, and possible links with chromosomal aberrations in Chinese vinyl chloride-exposed workers. *Cancer epidemiology, biomarkers & prevention : a publication of the American Association for Cancer Research, cosponsored by the American Society of Preventive Oncology.* **17**:2578-84.
161. **Zhang, W., Z. Zeng, Y. Zhou, W. Xiong, S. Fan, L. Xiao, D. Huang, Z. Li, D. Li, M. Wu, X. Li, S. Shen, R. Wang, L. Cao, K. Tang, and G. Li.** 2009. Identification of aberrant cell cycle regulation in Epstein-Barr virus-associated nasopharyngeal carcinoma by cDNA microarray and gene set enrichment analysis. *Acta biochimica et biophysica Sinica.* **41**:414-28.
162. **De Luca, A., M.R. Maiello, A. D'Alessio, M. Pergameno, and N. Normanno.** 2012. The RAS/RAF/MEK/ERK and the PI3K/AKT signalling pathways: role in cancer pathogenesis and implications for therapeutic approaches. *Expert opinion on therapeutic targets.* **16 Suppl 2**:S17-27.

163. **Aksamitiene, E., A. Kiyatkin, and B.N. Kholodenko.** 2012. Cross-talk between mitogenic Ras/MAPK and survival PI3K/Akt pathways: a fine balance. *Biochem Soc Trans.* **40**:139-46.
164. **Tur, G., E.I. Georgieva, A. Gagete, G. Lopez-Rodas, J.L. Rodriguez, and L. Franco.** 2010. Factor binding and chromatin modification in the promoter of murine *Egr1* gene upon induction. *Cell. Mol. Life Sci.* **67**:4065-77.
165. **Verma, I.M. and W.R. Graham.** 1987. The *fos* oncogene. *Adv. Cancer Res.* **49**:29-52.
166. **Dunmon, P.M., K. Iwaki, S.A. Henderson, A. Sen, and K.R. Chien.** 1990. Phorbol esters induce immediate-early genes and activate cardiac gene transcription in neonatal rat myocardial cells. *Journal of Molecular and Cellular Cardiology.* **22**:901-10.
167. **Amit, I., A. Citri, T. Shay, Y. Lu, M. Katz, F. Zhang, G. Tarcic, D. Siwak, J. Lahad, J. Jacob-Hirsch, N. Amariglio, N. Vaisman, E. Segal, G. Rechavi, U. Alon, G.B. Mills, E. Domany, and Y. Yarden.** 2007. A module of negative feedback regulators defines growth factor signaling. *Nature Genetics.* **39**:503-12.
168. **Bae, D. and S. Ceryak.** 2009. Raf-independent, PP2A-dependent MEK activation in response to ERK silencing. *Biochemical and biophysical research communications.* **385**:523-7.
169. **Fey, D., D.R. Croucher, W. Kolch, and B.N. Kholodenko.** 2012. Crosstalk and signaling switches in mitogen-activated protein kinase cascades. *Frontiers in physiology.* **3**:355.
170. **Law, A.H., A.H. Tam, D.C. Lee, and A.S. Lau.** 2013. A Role for Protein Phosphatase 2A in Regulating p38 Mitogen Activated Protein Kinase Activation and Tumor Necrosis Factor-Alpha Expression during Influenza Virus Infection. *International Journal of Molecular Sciences.* **14**:7327-40.
171. **Liu, W.H., Y.J. Chen, T.L. Cheng, S.R. Lin, and L.S. Chang.** 2013. Cross talk between p38MAPK and ERK is mediated through MAPK-mediated protein phosphatase 2A catalytic subunit alpha and MAPK phosphatase-1 expression in human leukemia U937 cells. *Cellular Signalling.* **25**:1845-51.
172. **Galbraith, M.D. and J.M. Espinosa.** 2011. Lessons on transcriptional control from the serum response network. *Curr. Opin. Genet. Dev.* **21**:160-166.
173. **Whitmarsh, A.J.** 2007. Regulation of gene transcription by mitogen-activated protein kinase signaling pathways. *Biochim Biophys Acta.* **1773**:1285-98.
174. **Hodge, C., J. Liao, M. Stofega, K. Guan, C. Carter-Su, and J. Schwartz.** 1998. Growth hormone stimulates phosphorylation and activation of *elk-1* and expression of *c-fos*, *egr-1*, and *junB* through activation of extracellular signal-regulated kinases 1 and 2. *J Biol Chem.* **273**:31327-36.
175. **O'Donnell, A., Z. Odrowaz, and A.D. Sharrocks.** 2012. Immediate-early gene activation by the MAPK pathways: what do and don't we know? *Biochem. Soc. Trans.* **40**:58-66.
176. **Frodin, M. and S. Gammeltoft.** 1999. Role and regulation of 90 kDa ribosomal S6 kinase (RSK) in signal transduction. *Molecular and Cellular Endocrinology.* **151**:65-77.
177. **Dalby, K.N., N. Morrice, F.B. Caudwell, J. Avruch, and P. Cohen.** 1998. Identification of regulatory phosphorylation sites in mitogen-activated protein kinase (MAPK)-activated protein kinase-1a/p90rsk that are inducible by MAPK. *J Biol Chem.* **273**:1496-505.

178. **Moon, S.L. and J. Wilusz.** 2013. Cytoplasmic viruses: rage against the (cellular RNA decay) machine. *PLoS pathogens*. **9**:e1003762.
179. **Shilatifard, A.** 2006. Chromatin modifications by methylation and ubiquitination: implications in the regulation of gene expression. *Annu Rev Biochem*. **75**:243-69.
180. **Jonkers, I., H. Kwak, and J.T. Lis.** 2014. Genome-wide dynamics of Pol II elongation and its interplay with promoter proximal pausing, chromatin, and exons. *eLife*. **3**:e02407.
181. **Buro, L.J., S. Shah, and M.A. Henriksen.** 2010. Chromatin immunoprecipitation (ChIP) to assay dynamic histone modification in activated gene expression in human cells. *J. Vis. Exp.* **41**. doi: 10.3791/2053.
182. **Blattner, C., P. Kannouche, M. Litfin, K. Bender, H.J. Rahmsdorf, J.F. Angulo, and P. Herrlich.** 2000. UV-Induced stabilization of c-fos and other short-lived mRNAs. *Mol. Cell. Biol.* **20**:3616-3625.
183. **Gonzalez-Espinosa, C. and J.A. Garcia-Sainz.** 1996. Hormonal modulation of c-fos expression in isolated hepatocytes. Effects of angiotensin II and phorbol myristate acetate on transcription and mRNA degradation. *Biochim. Biophys. Acta.* **1310**:217-222.
184. **Gonzalez-Espinosa, C. and J.A. Garcia-Sainz.** 1996. Hormonal modulation of c-fos expression in isolated hepatocytes. Effects of angiotensin II and phorbol myristate acetate on transcription and mRNA degradation. *Biochim Biophys Acta.* **1310**:217-22.
185. **Blattner, C., P. Kannouche, M. Litfin, K. Bender, H.J. Rahmsdorf, J.F. Angulo, and P. Herrlich.** 2000. UV-Induced stabilization of c-fos and other short-lived mRNAs. *Mol Cell Biol.* **20**:3616-25.
186. **Danko, C.G., N. Hah, X. Luo, A.L. Martins, L. Core, J.T. Lis, A. Siepel, and W.L. Kraus.** 2013. Signaling pathways differentially affect RNA polymerase II initiation, pausing, and elongation rate in cells. *Mol Cell.* **50**:212-22.
187. **Taatjes, D.J.** 2010. The human Mediator complex: a versatile, genome-wide regulator of transcription. *Trends in Biochemical Sciences.* **35**:315-22.
188. **Pagel, J.I. and E. Deindl.** 2011. Early growth response 1--a transcription factor in the crossfire of signal transduction cascades. *Indian Journal of Biochemistry & Biophysics.* **48**:226-35.
189. **Karin, M.** 1995. The regulation of AP-1 activity by mitogen-activated protein kinases. *J. Biol. Chem.* **270**:16483-16486.
190. **Jiang, D., Y. Zhou, R.A. Moxley, and H.W. Jarrett.** 2008. Purification and identification of positive regulators binding to a novel element in the c-Jun promoter. *Biochemistry.* **47**:9318-34.
191. **Gupta, P. and R. Prywes.** 2002. ATF1 phosphorylation by the ERK MAPK pathway is required for epidermal growth factor-induced c-jun expression. *J Biol Chem.* **277**:50550-6.
192. **Klein, E.A. and R.K. Assoian.** 2008. Transcriptional regulation of the cyclin D1 gene at a glance. *Journal of Cell Science.* **121**:3853-7.